Imaging Life

Your resource for molecular imaging innovation

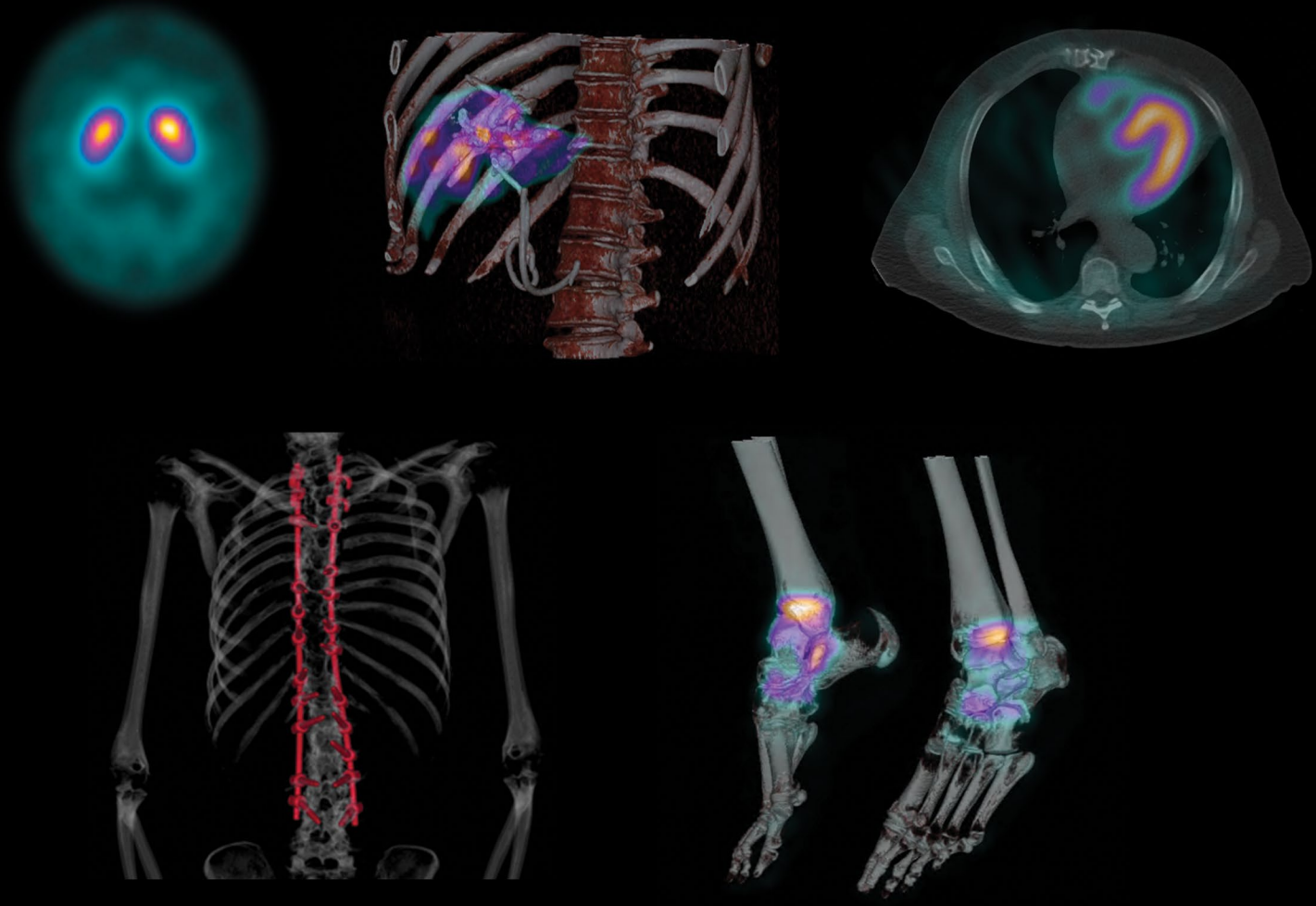

Expanding nuclear medicine's reach

International Edition · Issue 18

SIEMENS Healthineers

"When you can see everything at once—the brain, the heart, the liver, the abdomen, the pelvis—that to me is a game changer."

Professor Michael Fulham, MBBS
Royal Prince Alfred Hospital and the University of Sydney, Australia
Read the full story on p. 34.

Cover images: Data courtesy of Queen Elizabeth Hospital Birmingham, Birmingham, United Kingdom, and Baylor Scott & White Medical Center, Temple, Texas, USA.

Despite the continued challenges, we expand our reach.

While the pandemic continues to present challenges, one thing remains constant: the Molecular Imaging Business Line's continued commitment to increasing access to health care. Whether working from home, on location, or a blend of both, during the past year we have focused intently on developing new innovations, delivering upgrades on existing products, and investing in expanded research, all the while maintaining Siemens Healthineers' strategy of increasing access to care.

This issue of *Imaging Life* is dedicated to the power of reach. Our writers take you around the globe—from Australia to Switzerland to Texas, USA—to share with you examples of how the molecular imaging industry supports and expands research and clinical care, thereby increasing access to care to more people.

As one Research and Development team member points out, the goal of democratizing the abilities of SPECT/CT sparked efforts to develop Symbia Pro.Specta™—the latest in SPECT/CT, which modernizes workflow, reduces the footprint, and maximizes its functionality for patients. Read how experts expand the modality's reach on pages 4-11.

At Australia's Royal Prince Alfred Hospital, an early PET adopter now achieves an even higher level of patient care and research using Biograph Vision Quadra™. Using this whole-body system allows this pioneer to see everything at once, which benefits his research and clinical use.

With recent radiopharmaceutical developments, the timing could not be better for patients now that PETNET Solutions, Inc., is in the process of extending their reach. By opening new pharmacies and expanding the scope of production in existing facilities, tracers with short half-lives are more accessible to those in need. And speaking of new radiopharmaceuticals, we would be remiss if this issue did not explore the latest PSMA developments for those with advanced prostate cancer.

Parametric imaging is being utilized around the globe, across a range of clinical areas, and we cover how one Danish team is working to bring its capabilities to patients.

Artificial intelligence is providing prognostic value for cancer patients while potentially providing valuable data for assessing response to treatment. Measuring these parameters using AI has the potential to enable much broader use.

Enjoy these and other articles in this issue of *Imaging Life,* which highlight how the molecular imaging industry continues, even during this uncertain time, to expand its reach and provide increased care. I, along with the entire Molecular Imaging team, hope these stories will inspire you to consider ways you can expand your reach.

Matt Shah,
Vice President, Global Sales & Marketing
Molecular Imaging Business Line
Siemens Healthineers

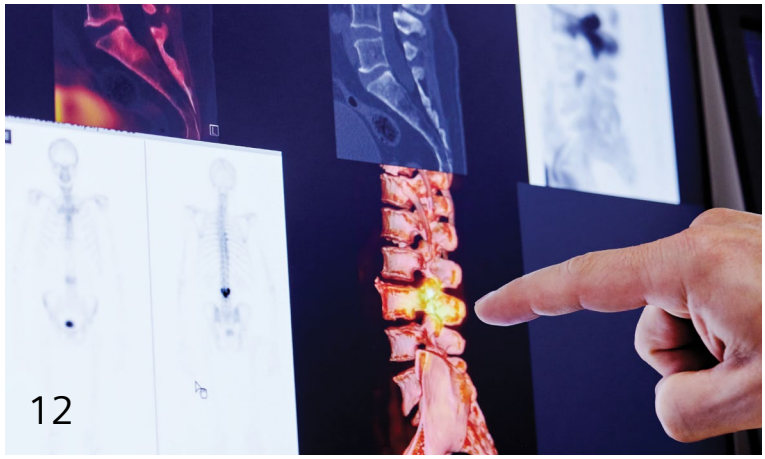

Spotlight

Advancing

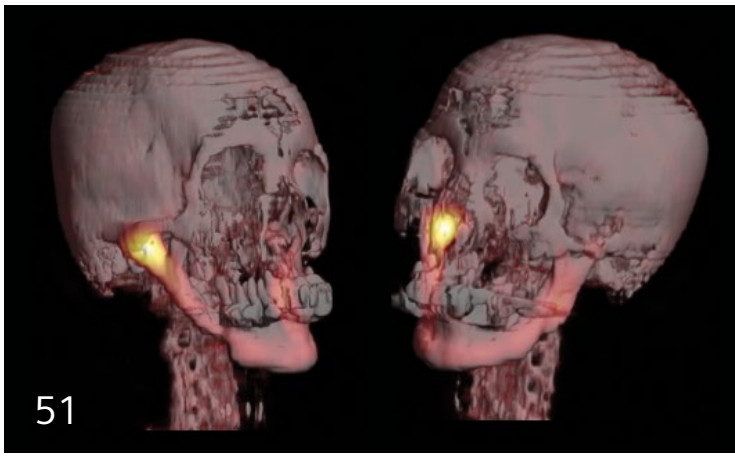

Expanding

Clinical results

Fully integrated SPECT/CT modernizes facilities to maximize abilities

Nuclear medicine experts on two continents describe how the new fully integrated SPECT/CT serves more patients and signals the beginning of a new era in nuclear imaging.

By Linda Brookes | Photography by Jonathan Browning and Scott van Osdol

Single-photon emission computed tomography (SPECT) combined with computed tomography (CT) was introduced as a hybrid SPECT/CT imaging modality almost two decades ago. Soon after the first commercially available diagnostic SPECT/CT system, Siemens' Symbia TruePoint™ system, was launched in 2004, researchers recognized the potential for improving image quality and incorporating quantitative image acquisition and reconstruction.

Alexander Hans Vija, PhD, who has been working in the field for more than 25 years and is currently head of SPECT research at Siemens Healthineers Molecular Imaging in Hoffman Estates, Illinois, USA, recalls that collaborative research led to Symbia Intevo™, which featured standardized quantification and the high-resolution xSPECT Bone™ reconstruction algorithm. "But from here, we wanted to have a more integrated solution and ultimately enable many more imaging departments to install a SPECT/CT system." This would allow more patients to access a wider range of services.

Symbia Pro.specta™ "brings closure to the era of the original Symbia TruePoint SPECT/CT," Vija says. For 20 years the aim has been to amalgamate the data and construct a system that is in reality "one system under the hood." Symbia Pro.specta is that system, he asserts. "It would be very exciting if it would motivate people who were holding on to their 15-year-old or older systems to upgrade. I believe this system moves the bar to a level where everybody can enter the SPECT/CT world," Vija says.

Transitioning from SPECT to SPECT/CT

Vija's hopes for Symbia Pro.specta have been realized at Baylor Scott & White (BSW) Medical Center-Temple in central Texas (USA), a part of the BSW Health, one of the largest not-for-profit healthcare systems in the US. "We had been wanting a SPECT/CT camera for many years," admits Michael L. Middleton, MD, director of the nuclear radiology division which employs three nuclear physicians and six technologists. Obtaining approval for purchase of a SPECT/CT system was challenging, however, due to reimbursement issues. "Approval of parathyroid SPECT/CT opened the door," he recalls, but even then, installation of a SPECT/CT system was delayed for years. "We were left with just two Symbia™ SPECT-only cameras. We desperately needed a third nuclear medicine camera just to keep up with demand. So, Symbia Pro.specta was a godsend," he says. The center has now been working with the new system for one year, and it has been providing more capabilities to a much wider variety of patients.

Expanded clinical applications

"The Symbia Pro.specta system has been most useful for parathyroid imaging, which we do once or twice a day," Middleton notes. "We also schedule our larger (BMI >35) cardiac patients on the camera because it improves attenuation correction on the myocardial perfusion scans in these patients who have issues due to soft tissue, large breasts, and fat."

Women with breast cancer who have had axillary breast surgery and cannot raise their arms, causing attenuation,

"I believe this system moves the bar to a level where everybody can enter the SPECT/CT world."

Alexander Hans Vija, PhD, Head of SPECT Research,
Siemens Healthineers Molecular Imaging, Illinois, USA

are also being moved to the Symbia Pro.specta system. Additionally, it is being used for octreotide scans where patients do not have access to PET, for MIBG scans, and imaging of ^{99m}Tc MAA particles and bremsstrahlung SPECT/CT for post-therapy imaging of ^{90}Y microsphere selective internal radiation therapy (SIRT) of liver cancer. Another advantage of the new camera and software is the improved visualization of lesions compared with planar imaging or SPECT alone, the BSW professionals add. "With Symbia Pro.specta, we have been able to start using the xSPECT Bone reconstruction algorithm, which helps us better localize and characterize bone disease," Middleton says.

Another noticeable effect after upgrading to SPECT/CT was the intelligent imaging experience that fully integrates SPECT and CT. Middleton noticed how the staff appreciates the automation of the workflow. "It reduces the time going from the control room to the camera room. They can basically run it from the control room." For lead nuclear medicine technologist Stephen Stoner, a big advantage of Symbia Pro.specta is streamlined design. "We don't have all the big computers that we used to have. That gives us more space within the control room itself," he says. "You just have the monitors and the keyboard on top of the table, with no big computer box underneath."

Middleton adds, "Any site acquiring one of these SPECT/CT cameras needs to schedule extra training time for the technologists to learn the new SPECT *syngo*® software platform. But then I think they will be happy with it." Middleton's team switched the software they used to read the scans to *syngo*.via™. "It wasn't a hard transition, and it's been an improvement, especially on the cardiac reading," he comments. "Overall, it's been a positive learning curve."

The Baylor Scott & White nuclear medicine team appreciates the automation of the workflow.

Dr. Middleton and lead nuclear medicine technologist Stephen Stoner examine scans on the Symbia Pro.specta SPECT/CT acquistion workstation.

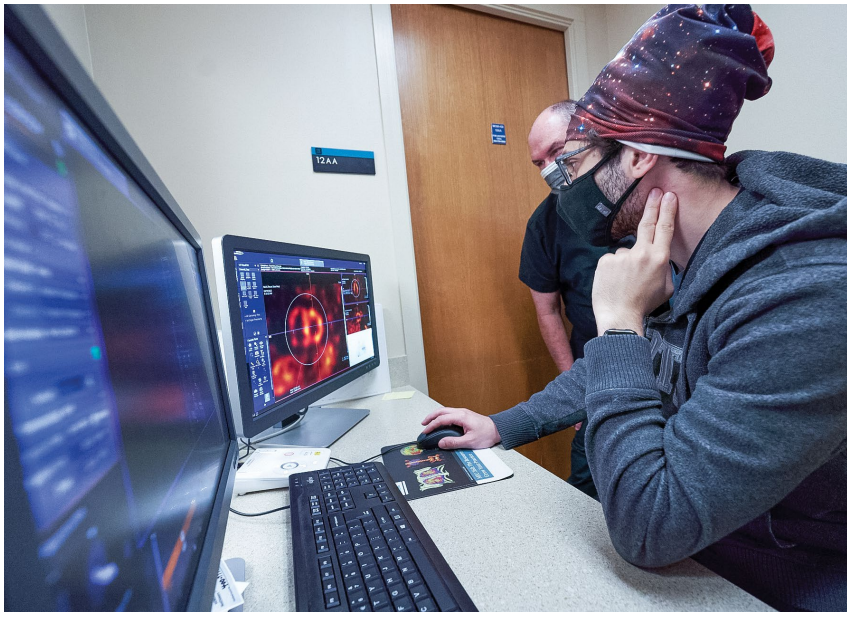

The streamlined design provides more space within the control room.

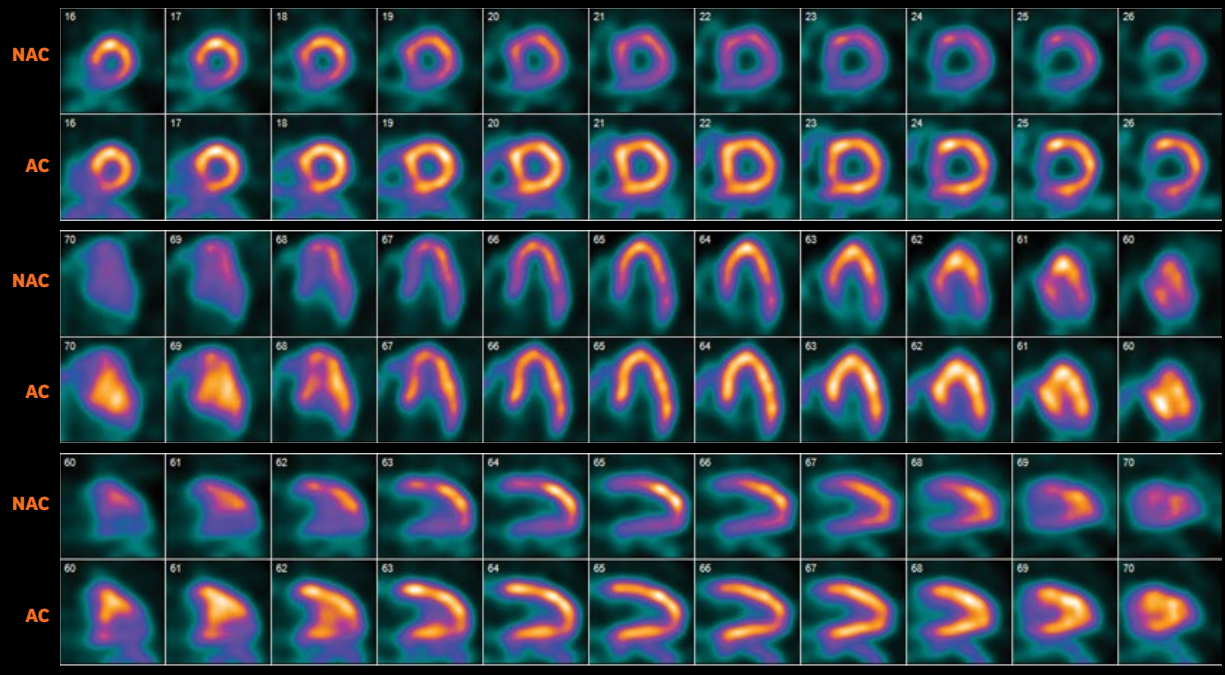

Improved inferior wall visualization by attenuation correction.
Courtesy of Queen Elizabeth Hospital, Birmingham, UK.

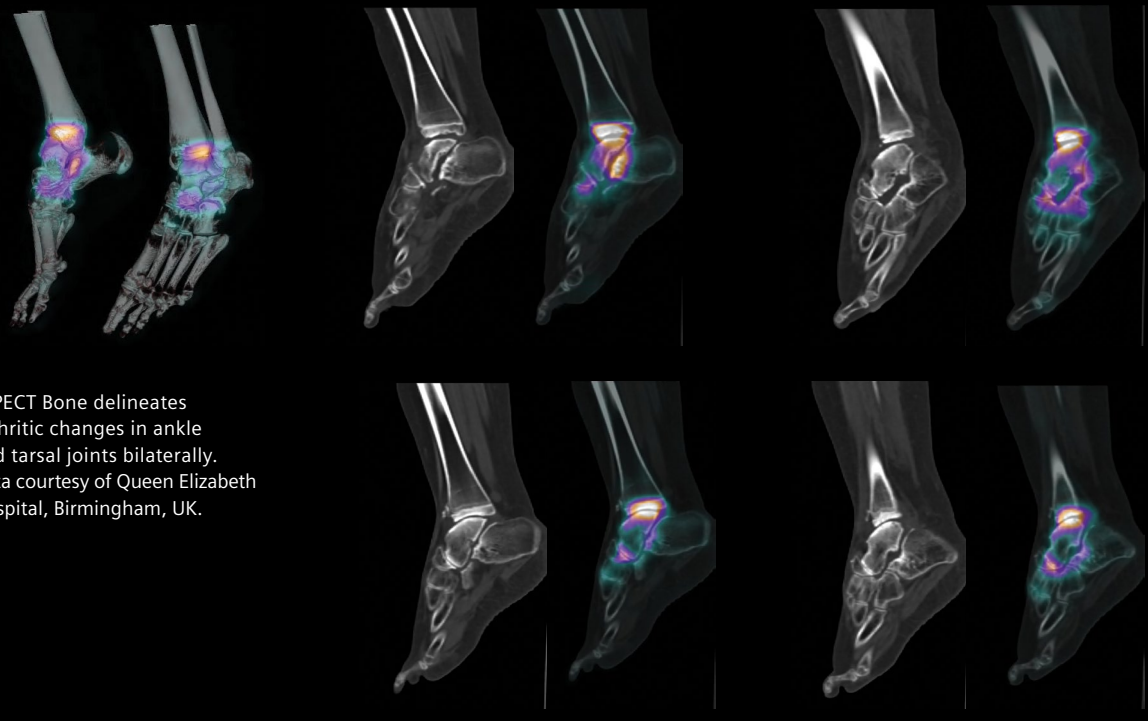

xSPECT Bone delineates arthritic changes in ankle and tarsal joints bilaterally.
Data courtesy of Queen Elizabeth Hospital, Birmingham, UK.

"With Symbia Pro.specta, we have been able to start using the xSPECT Bone reconstruction algorithm, which helps us better localize and characterize bone disease."

Michael L. Middleton, MD,
Baylor Scott & White-Temple, Texas, USA

Upgrading for practiced SPECT/CT users

Across the Atlantic, in the United Kingdom, staff in the department of nuclear medicine at the Queen Elizabeth Hospital Birmingham (QEHB) in the UK Midlands have been using SPECT/CT for over 10 years. When the hospital opened as part of the University Hospitals Birmingham NHS Foundation Trust in 2010, the department had a Symbia S SPECT, Symbia T SPECT/CT, and a Symbia T16 SPECT/CT. The Symbia T16 has since been replaced and the hospital now has a range of SPECT/CT scanners. In February 2020, a Symbia Pro.specta system was installed, which occupies the space where formerly a Symbia S SPECT camera was installed.

Erin Ross, PhD, consultant clinical scientist and deputy head of nuclear medicine at QEHB, recalls that when the hospital first opened, the radiologists had an open mind about using SPECT/CT. "As soon as they started using it, they embraced it and they kept putting everything onto the Symbia T16 due to the higher quality of CT." For many years since, Ross and her colleagues have been asking for "better CT, the best images in the quickest time, a diagnostic "one-stop shop" to overcome "a real blockage in efficiency," she says. "Now we've got such a high quality of SPECT/CT with Symbia Pro.specta." Khalid Hussain, MD, consultant radiologist at QEHB, confirms that "because of the high quality of the SPECT, we have been able to reduce the dose, which is excellent." He adds that "the quality

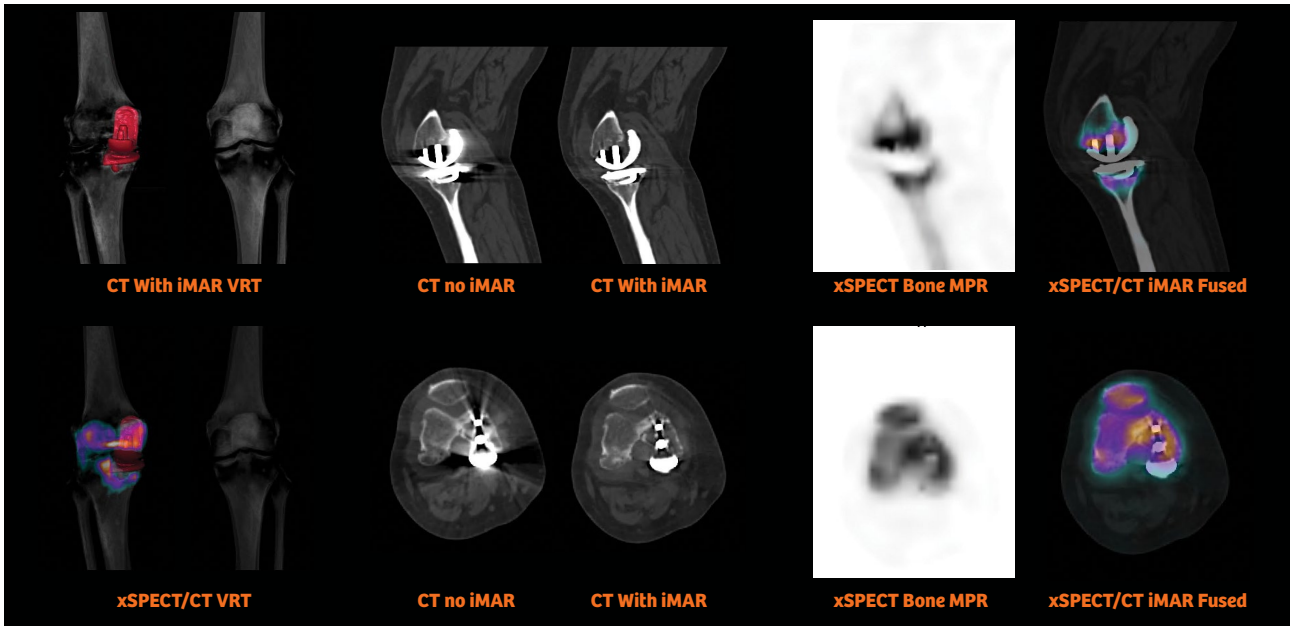

xSPECT Bone fused with CT with iMAR defines loosing of tibial component of knee hemi-arthoplasty.
Data courtesy of Queen Elizabeth Hospital, Birmingham, UK.

Laura Whitehouse, senior clinical technologist specializing in nuclear medicine, manages the Scan&GO touchscreen gantry display.

Symbia Pro.specta offers a short tunnel and open design with a focus on accommodating patients.

of the CT as part of the SPECT/CT is "much higher" than they have ever seen before.

A new SPECT/CT feature for the QEHB staff is iterative reconstruction on the CT. "The SAFIRE (sinogram affirmed iterative reconstruction) algorithm has also helped us lower doses in the CT examinations," Ross says. "Tin Filter has also significantly lowered CT doses as compared to the other machines." The technologists also appreciate the iMAR (iterative metal artifact reconstruction) technique, which they are using for the first time.

Providing a comfortable experience is important for technologists who engage with patients directly. During patient transfer, patients are less worried about falling off because the bed is wider. In the scanning room, the position of the handset on the gantry display is popular. Laura Whitehouse, senior clinical technologist specializing in nuclear medicine, appreciates that the camera is smaller, quieter, and less bulky when it's moving around the patient. "That's really important for patients who are nervous," she says. "They get a better experience, so they're more relaxed." She also praises the incorporation of the CT component. "It's all within the casing, and we don't have to bother

"Now we've got such a high quality of SPECT/CT with Symbia Pro.specta."

Erin Ross, PhD, Consultant Clinical Scientist and Deputy Head of Nuclear Medicine,
Queen Elizabeth Hospital, Birmingham, UK

With its smart workflow, the Symbia Pro.specta system allows a greater number of scans to fit in their schedule.

with turning the CT on and off. Everything's more compact, clean, smart, and user-friendly," she says. "I love that I'm not kicking the hardware box underneath the control room desk any longer," Ross adds.

For principal clinical technologist Yasmin Wahid, a welcome new feature on Symbia Pro.specta is the pre-recorded breathing instructions in different languages for the patients. Whitehouse also likes the appearance of the new, one-color interface, which she believes is important for patients when they first enter the room. "It's really appealing. It's smaller, and it doesn't look so bulky and scary," she comments. For Wahid, it's simpler and easier, "It's literally just one button and we're ready to go."

Intelligent imaging experience at QEHB

Everyday operations in the exam room are streamlined with smart workflows. Whitehouse likes that the workflows themselves are easier to set up. "When you're on the fly, you can chop and change whatever you want," she notes. "So, if the patient tells you they have pain elsewhere and if they've already had their injection, we can simply just add another scan. With the old system, we would have one set workflow, and if you wanted to add extra images, you would have to complete that workflow and reload another." She adds that with the Plan&GO, an intuitive bedside ruler for scan range planning ("We call it 'the magic ruler'"), it is easier to identify landmarks and position the patient.

As the lead of the nuclear cardiology service, Wahid appreciates that the gantry display (Scan&GO) is a new touchscreen, so that it is easy to focus the heart in the central field of view instead of having to click through a series of tabs to see different positions. "If we want to change the collimator, and we want to see the patient's ECG, now we have everything on one screen," she enthuses. She also highlights the reduction in time needed for cardiac scans with Symbia Pro.specta, especially for ECG-gated scans to measure left ventricular function. This is particularly useful for monitoring cardiac side effects of chemotherapy and greatly improves the patient experience. "With some patients, like those with an irregular heartbeat (arrhythmia), it would take us absolutely ages to acquire the

The pre-recorded breathing instructions for the patients are provided in different languages.

data," Wahid recalls. "Now we can do a quicker scan, so instead of being on the bed for about 35 minutes, it's now more like 15 minutes."

With Symbia Pro.specta and its smart workflow, QEHB nuclear medicine services can now be expanded, allowing greater numbers of SPECT/CT scans to be fitted into their schedule. These include post-therapy SPECT/CT for detection and characterization of radioactive ^{131}I focal uptake in patients with thyroid cancer. Octreotide scans have been restarted in support of the PET service. Significant expansion of SPECT/CT scans being done post ^{177}Lu DOTATATE therapy for neuroendocrine tumors. Increased numbers of FLR (future liver remnant) scans are being done for preoperative assessment, having been moved from the Symbia T2. The SIRT service for colorectal cancer and hepatocellular carcinoma has also been moved from the T2, because of the higher quality of the CT with Symbia Pro.specta.

Even for practiced SPECT/CT technicians, change can be challenging—but worth it. Whitehouse cautions that the Symbia Pro.specta interface is completely different from previous Symbia systems. "At first it can be a little daunting, but when you get used to it, everything is much more user-friendly," she says.

Reaching more patients through expanded use of Symbia Pro.specta SPECT/CT

The UK and USA medical facilities are looking forward to expanding their services with Symbia Pro.specta. "Our dream would be to get up and running with contrast-enhanced CT, for follow-up prostate or bone scans, and be able to go one-stop shop with that. That is our aim for next year," Ross says.

The positive experience of both the US and UK hospitals with the new Symbia Pro.specta reflects the culmination of Vija's vision of wider availability and easier use, but also demonstrates the potential for both nuclear medicine departments to expand their patient services even beyond those they envisaged when they first started using Symbia Pro.specta. ●

Linda Brookes is a freelance medical writer and editor. She divides her time between London and New York, working for a variety of clients in the healthcare and pharmaceutical fields.

Symbia Pro-specta™ SPECT/CT is not commercially available in all countries. Due to regulatory reasons, its future availability cannot be guaranteed. Please contact your local Siemens Healthineers organization for further details.

The statements by Siemens Healthineers customers described herein are based on results that were achieved in the customer's unique setting. Since there is no "typical" hospital and many variables exist (e.g., hospital size, case mix, level of IT adoption), there can be no guarantee that other customers will achieve the same results.

The amount of metal artifact reduction and corresponding improvement in image quality depends on a number of factors including: composition and size of the metal object, patient size, anatomical location and clinical practice. It is recommended to perform reconstructions withi iMAR enabled in addition to conventional reconstruction without iMAR.

In clinical practice, the use of SAFIRE may reduce CT patient dose depending on the clinical task, patient size, anatomical location, and clinical practice. A consultation with a radiologist and physicist should be made to determine the appropriate dose to obtain diagnostic image quality for the particular clinical task.

For More Information

siemens-healthineers.com/symbiaprospecta

Soaring to new heights with SPECT/CT

Since its introduction more than two decades ago, SPECT/CT imaging has seen significant technological advances that are expanding the modality's power and accuracy.

SPECT/CT expert Klaus Strobel from Lucerne Cantonal Hospital in Switzerland reveals how the method improves individual patient care and where he sees future clinical applications.

By Santina Russo | Photography by Raphael Zubler

Across the diagnostic imaging spectrum, SPECT and SPECT/CT have developed into staples that are depended upon to drive improved patient outcomes. With SPECT originating more than 50 years ago and evolving into SPECT/CT over two decades ago, these modalities continue to meet the challenges of today through the implementation of new features and methods of use, assisting physicians in the diagnosis and targeted care of each individual patient.

As a hybrid method, SPECT/CT combines single-photon emission computed tomography (SPECT), which provides metabolic information from injected radionuclides, with anatomical information of bones and organs obtained from computed tomography (CT). This unites the high sensitivity of SPECT with the specific physiological localization provided by CT. "This improves diagnostic accuracy for a wide range of clinical conditions compared to SPECT or CT imaging alone," confirms Prof. Dr. Klaus Strobel, head of the nuclear medicine department at the Lucerne Cantonal Hospital, Switzerland.

Broad range of clinical applications

Located in a large center for nuclear medicine in central Switzerland, Strobel's department is responsible for serving a population of around one million people. To enhance its diagnostic imaging capabilities, the department acquired two Symbia Intevo Bold™ SPECT/CT imaging scanners, one in 2019 and another in 2020, to replace its aging SPECT/CT scanners.

Strobel and his team—which includes three other physicians who are double board certified in radiology and nuclear medicine and 15 technologists who are also trained in both specialties—most frequently use SPECT/CT to investigate skeletal conditions like lesions of bone and joints. These experts also employ SPECT/CT for a broad range of other investigations, such as examinations of the thyroid and parathyroid glands, cardiac analysis to investigate perfusion and possible ischemia, and applications in the brain, for instance, on patients with suspected Parkinson's disease. The team also explores the modality's use for further clinical applications.

In fact, SPECT/CT has seen significant technological advances that have expanded the modality's scope. First, the quality of scans has increased due to better CT hardware, which is, according to Strobel, probably the most significant advancement in recent years. Modern machines feature more rapidly rotating radiation sources and detectors with a greater number of slices resulting in the ability to provide clear and high-resolution images while simultaneously reducing imaging time.

"When investigating possible metastatic growth in prostate or breast cancer patients, a SPECT/CT measurement can reveal information about metastases in bones, while a back-to-back contrast CT provides information on possible tumors in the lung or liver."

Klaus Strobel, MD, PhD, Lucerne Cantonal Hospital, Switzerland

Dr. Strobel's team prepares the contrast injector that is utilized for CT examinations with their Symbia Intevo Bold.

One-stop imaging

To harness the SPECT/CT to its full capabilities, Strobel and his team are using Symbia Intevo Bold to provide what he refers to as "one-stop imaging." His team routinely utilizes a contrast injector in conjunction with the CT. "When investigating possible metastatic growth in prostate or breast cancer patients, a SPECT/CT measurement can reveal information about metastases in bones, while a back-to-back contrast CT provides information on possible tumors in the lung or liver," Strobel explains. He goes on to emphasize the importance of providing fused 3D images to the referring physicians and to patients, as it promotes the power of the imaging modalities.

In addition, the CT capabilities combined with image processing software allow Strobel and his co-workers to perform measurements they were unable to provide before. The experts can now add calcium scoring to cardiac perfusion SPECT/CT as an additional prognostic data point to assess the risk for relevant coronary artery disease and myocardial infarction.

Strobel's team also applies unique Siemens Healthineers CT technologies like iMAR, the iterative algorithm for metal artifact reduction along with their SPECT/CT imaging techniques. This helps the team apply diagnostic SPECT/CT for patients who underwent a knee or a hip replacement and therefore carry metal prostheses.

"Such metal components normally create hindering artifacts in CT images," explains Strobel. A tailored image processing algorithm like iMAR reduces such artifacts and provides high-quality images of the tissue around metal protheses without any information being obscured. The iMAR images can be applied for attenuation correction to the SPECT images providing a dual benefit by enhancing the reconstructed image quality for both modalities.

Additionally, along with iMAR, Strobel and his co-workers regularly use dual-energy CT in patients with knee prothesis to increase visibility of subtle osteolysis at the metal-bone interface as a sign for early loosening.

Software makes the difference for patients

A major part of the improved capabilities can be attributed to the software. In particular, new reconstruction algorithms for planar and SPECT/CT images have improved in recent years. Strobel's team has done studies comparing planar whole-body imaging times and image quality for the same patient and has determined that "with the half-time image reconstruction technique, patients' comfort and throughput can be improved without impaired detectability of diagnostically relevant findings." Heart and bone scans that used to take 12 to 15 minutes are now done in only 6 to 7 minutes. "Of course, this is beneficial for the patients' comfort, especially if they are in pain," stresses Strobel. He adds, "I think half-time imaging is clearly the way to go."

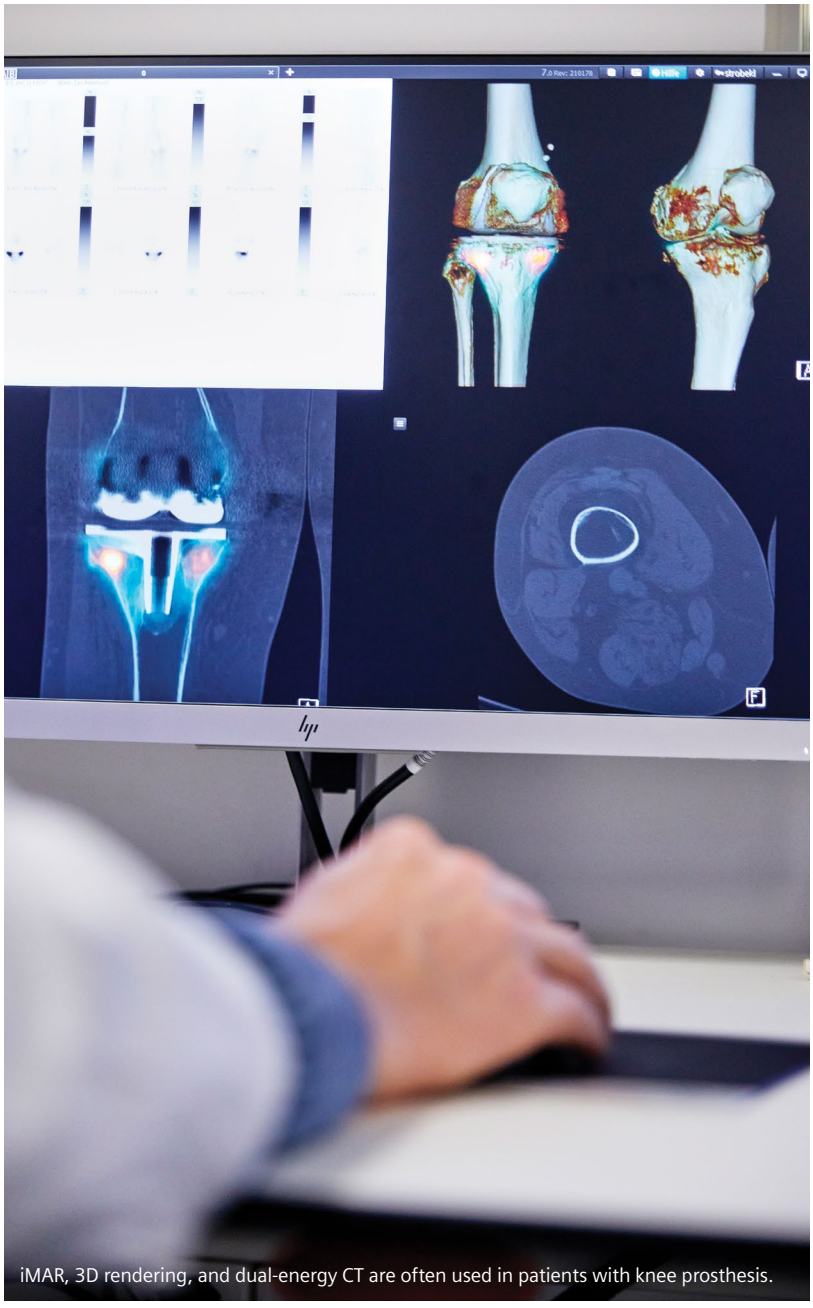

iMAR, 3D rendering, and dual-energy CT are often used in patients with knee prosthesis.

Strobel's team has explored further how far they can decrease imaging time of whole body SPECT/CT in cancer patients by obtaining images with variable whole-body acquisition parameters. The team completed a whole-body scan in 20 minutes using parameters of 3 seconds per view with 60 projections in continuous acquisition mode, forgoing the traditional step-and-shoot approach, for a 113-kg/249-lb patient. "I think it has all the information you need about the bone." Strobel goes on to say, "In this situation, you could imagine skipping the traditional planar images and doing the whole-body SPECT/CT only."

xSPECT Bone™ is another unique software capability that Strobel regularly uses. He states, "If we do bone SPECT/CT, we always use xSPECT Bone. This provides, of course, better image quality, better visualization, and anatomic resolution, compared to the conventional techniques." This observation is evident when Prof. Strobel compares images reconstructed with xSPECT Bone to conventionally reconstructed images.

Expanding the scope of SPECT/CT imaging

"Thanks to these technical advancements, we have certainly been able to improve diagnosis and patient care," Strobel concludes. It's no surprise that the use of SPECT/CT is steadily moving towards new clinical indications. Recently, Strobel's team has begun working together with lymphatic surgeons to explore imaging of the lymphatic nodes and vessels. These experts are also investigating specialized applications with available tracers, such as imaging cardiac amyloidosis (a severe disease of the heart) using a tracer currently used for bone imaging. "I can imagine that more diagnosable indications will come up when researchers further investigate the scope of bone and joint SPECT/CT scans," says Strobel. "We are still limited in imaging of soft tissues, and I see potential to improve in this area." The Lucerne team invented "SPECT/CT arthrography," a combination of CT arthrography with intraarticular contrast and SPECT as a new technique allowing the assessment of metabolic bone changes and cartilage or ligament lesions in one investigation in knee, ankle, or wrist disorders.

According to Strobel, a promising perspective is the quantification of tracer uptake in the images, providing standard uptake values (SUV)—already being done in PET/CT measurements. Strobel appreciates the solution for quantification referred to as xSPECT Quant™. "I think it is important that tracer quantification can be done in SPECT/CT as easily as in PET/CT; that one can place a volume of interest (VOI) in the lesion and immediately obtain the SUV to compare with older images, such as

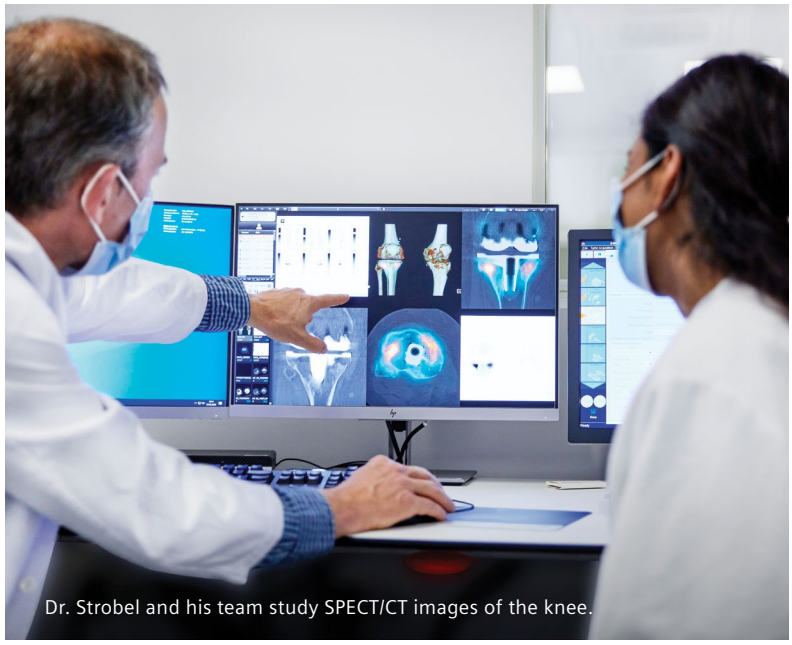

Dr. Strobel and his team study SPECT/CT images of the knee.

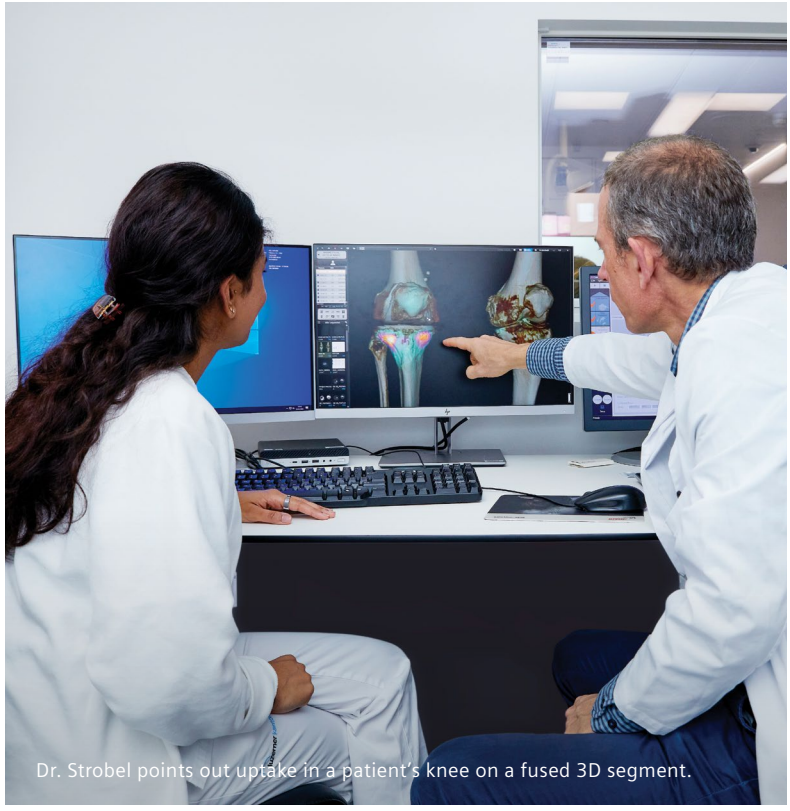

Dr. Strobel points out uptake in a patient's knee on a fused 3D segment.

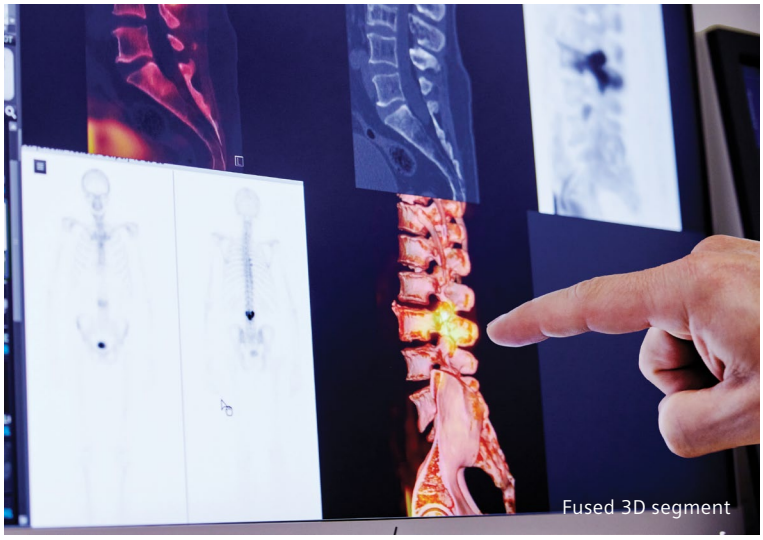
Fused 3D segment

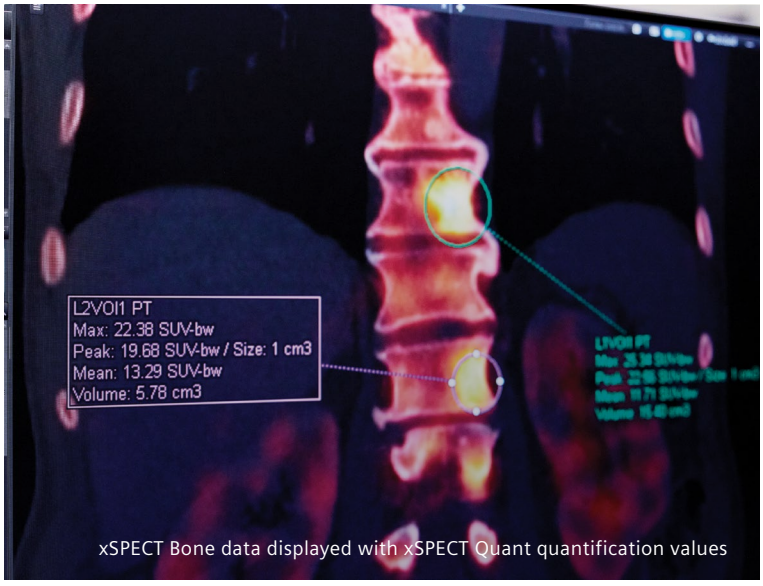

xSPECT Bone data displayed with xSPECT Quant quantification values

for therapy response assessment." Strobel also states, "This easy-to-use and precise tracer quantification tool was actually one of the main reasons for us to choose Symbia Intevo Bold, since it's unique on the market."

In fact, initial research results in the field indicate that tracer quantification may be used to guide treatment decisions or response to a given therapy.[1, 2] "There is still much research to be done," says Strobel, "but I think quantification in SPECT/CT will be an especially interesting application to explore in the future."

Broader applications for the original features of SPECT/CT have continuously been revealed throughout the life cycle. With the addition of new imaging tools, medical professionals are discovering innovative ways to utilize SPECT/CT to deliver cutting-edge service for patients. The modality continues to advance, and the coming years promise to reveal new uses that will keep it at the forefront of nuclear medicine for decades to come. ●

Santina Russo is a freelance science journalist in Zurich, Switzerland.

For More Information

siemens-healthineers.com/SymbiaIntevoBold

siemens-healthineers.com/xspectbone

siemens-healthineers.com/xspect-quant

References

1 Thuillier P, Maajem M, Schick U, et al. Clinical Assessment of 177Lu-DOTATATE Quantification by Comparison of SUV-Based Parameters Measured on Both Post-PRRT SPECT/CT and 68Ga-DOTATOC PET/CT in Patients With Neuroendocrine Tumors: A Feasibility Study. *Clin Nucl Med.* 2021;46(2):111-118. doi:10.1097/RLU.0000000000003412

2 Braun, M., Cachovan, M., Kaul, F. et al. Accuracy comparison of various quantitative [99mTc]Tc-DPD SPECT/CT reconstruction techniques in patients with symptomatic hip and knee joint prostheses. *EJNMMI Res 11*, 60 (2021). https://doi.org/10.1186/s13550-021-00794-7

The statements by Siemens Healthineers customers described herein are based on results that were achieved in the customer's unique setting. Since there is no "typical" hospital and many variables exist (e.g., hospital size, case mix, level of IT adoption), there can be no guarantee that other customers will achieve the same results.

The amount of metal artifact reduction and corresponding improvement in image quality depends on a number of factors including: composition and size of the metal object, patient size, anatomical location and clinical practice. It is recommended to perform reconstructions with iMAR enabled in addition to conventional reconstruction without iMAR.

The interview and photo shoot took place under all necessary health and safety measures according to local COVID-19 regulations.

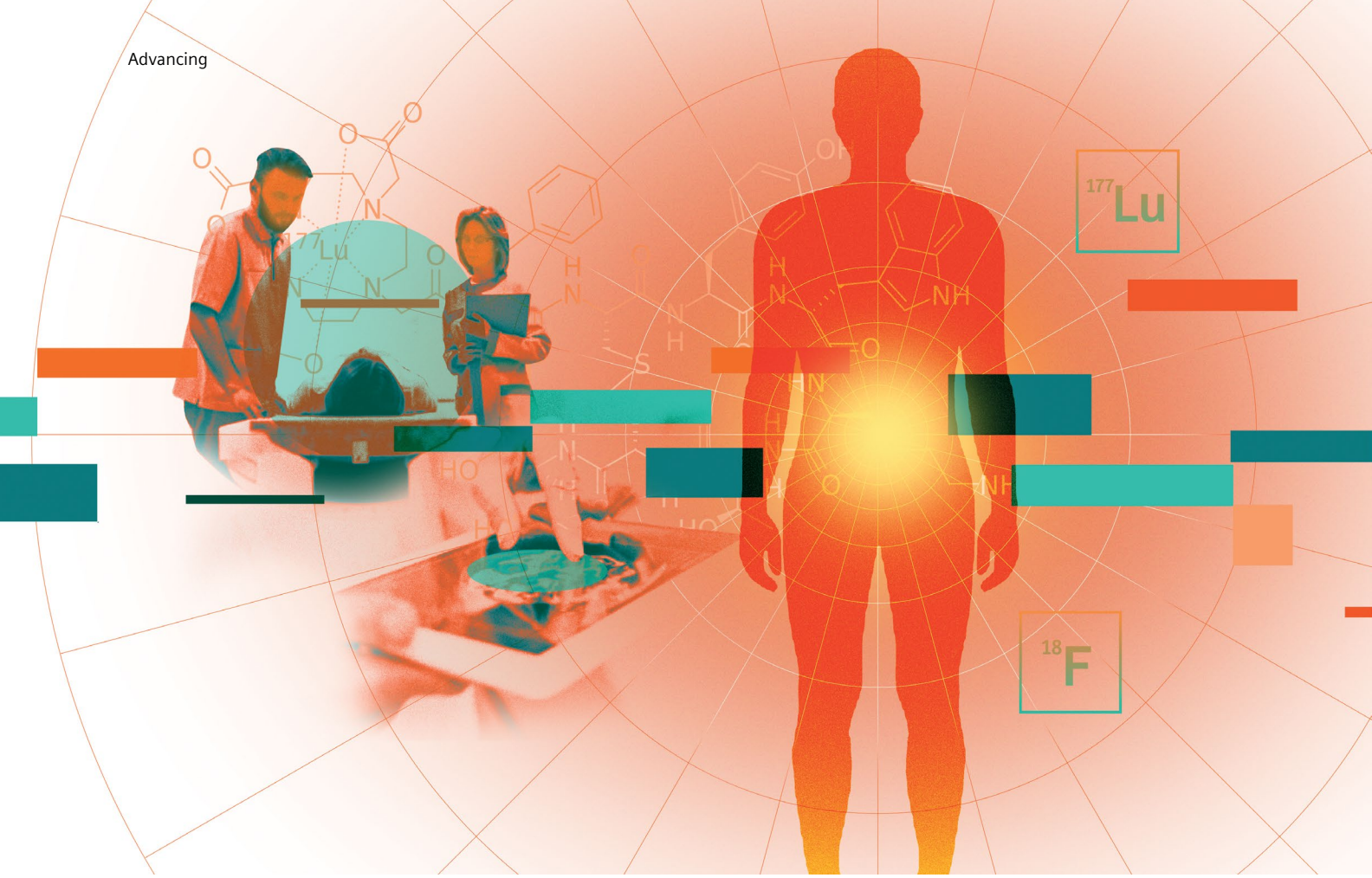

Advances in PSMA expand possibilities

A new PSMA-based approach that combines diagnosis and therapeutics could be a game-changer in the treatment of prostate cancer. We spoke to opinion leaders in nuclear medicine, urology, and biomedical engineering about how the new approach expands possibilities for patients and clinicians, as well as its implication for clinical management of prostate cancer.

By Florian Bayer | Illustration by David Hänggi
Data courtesy of Department of Nuclear Medicine, University Hospital Duesseldorf, Germany.

Prostate cancer is still one of the most common and most lethal cancers in men. While the exact reasons and risk factors are still not fully known, therapy options have made significant progress in recent years.

A revolutionary new technique holds out the prospect of even greater progress in the future: prostate-specific membrane antigen (PSMA)-ligand analysis using a combination of innovative radiopharmaceuticals for positron emission tomography (PET) imaging. First clinical results are encouraging, and the United States Food and Drug Administration (FDA) recently gave its approval for multiple PSMA products. FDA approval and the broad availability of PSMA PET diagnostic agents in the United States that have been incorporated into the National Comprehensive Cancer Network guidelines[1] will provide clinicians with options for improved understanding of the extent of disease—both at staging and in the case of a suspected recurrence of prostate cancer.

These developments provide the green light needed to promote the new diagnostic therapy for patients with prostate cancer. Retrospective and prospective PSMA studies confirm the superior diagnostic accuracy as well as the direct connection between PSMA-derived tumor burden and severity of disease.[2-5] Many more prospective multi-center studies on this new method are still ongoing. Numerous experts, however, already see this combination of imaging and theranostics as offering potential in cancer care. Siemens Healthineers' research and development efforts are being co-funded by the European Union's Horizon 2020 research and innovation program.

Taking PSMA to the next level

The basis of this entirely new approach is PSMA. Similar to but not to be confused with PSA (prostate-specific antigen), PSMA is a small peptide that targets prostate cancer cells for different imaging agents in nuclear medicine, namely PET.

Now, however, teams of researchers are taking PSMA imaging therapeutic applications to the next level. In several investigations in recent years, they found that PSMA-targeting molecules when combined with Lutetium-177 isotopes are effective in killing targeted cancer cells and tissue.[6] Due to its high precision and efficacy, this method has the potential to improve prostate cancer treatment in later stages of the disease.

What is new about the PSMA PET imaging that plays a decisive role here? To answer this question, it is essential to first look back in time. The focus in the past 20 years was on maximizing image resolution and on high detection rates of tumors and their structural changes, points out Professor Frederik Giesel, MD, MBA, an expert in nuclear medicine and head of the department for Nuclear Medicine at the University Hospital Düsseldorf, Germany. But this approach was akin to "searching for the needle in the haystack," as Giesel puts it. Therefore, instrumentation aside, the specificity of a targeted peptide, in the case of PSMA, opens the door for a target treatment—it moves PET squarely into precision medicine.

Brian Helfand, MD, PhD, a urologist based in Glenview, Illinois, USA, and an expert on prostate cancer, agrees with this position. "Prostate cancer is not very straightforward for clinicians. We need a lot of information to help us decide on the best treatment options that are correct for every patient," Helfand

"These radioligands guide us with very exact information about if and where any tumor tissue is left."

Frederik Giesel, MD, MBA, Director and Chairman of the Nuclear Medicine Department, University Hospital Duesseldorf, Germany, and visiting professor at Osaka University, Suita, Japan

says. Due to a lack of specificity and reliability of conventional tests, including PSA results, bone scan, and CT scans, these medical decisions were not as robust as they needed to be. What is more, these older imaging and lab results did not always fit together coherently, especially following seemingly successful treatment or a period with no tumor load, when one indicator would turn positive but the precise reason or location of the recurrent tumor was unknown.

Success in detecting earlier stage cancer tissues

The new radioligand therapies based on PSMA in combination with PET imaging are much more precise. "It feels like someone lit the Christmas tree," says Giesel referring to the much more precise identification of new cancer tissue with these new diagnostic agents. And he adds, "These radioligands guide us with very exact information about if and where any tumor tissue is left." This is a "major milestone" answering the previously unmet need of identification and treatment of prostate cancer recurrences, according to Giesel.

Just as with other radiotracer methods, PSMA is mainly used for already-diagnosed prostate cancers. "Currently, the diagnostic radiotracers are used in assessment of biochemical recurrence or high-risk primary prostate cancer where there is a significant chance of metastatic spread outside the pelvis," says Bruce Spottiswoode, PhD, director and senior biomedical engineer at Siemens Healthineers.

"A common problem with many of our standard therapies for prostate cancer is serious secondary effects. The new therapy, however, might improve that to a large extent," says Helfand. "It goes without saying that further research is still needed. But I am optimistic that this type of therapy, if successful, may even become an upfront therapy for many patients."

PSMA PET/CT imaging plays a special role in this new approach. Selecting patients and monitoring their response to therapy is now increasingly more effective. But in addition to the technological and medical progress, close cooperation of all sides of healthcare plays a crucial role.

Considerations for implementation in clinical practice

An important issue is the ultimate implementation and application in clinical practice. "What is meaningful in terms of a workflow? How can we save time and minimize errors? What sorts of measurements can we automate to make things easier? And ultimately: What degree of cancer staging support should we offer to enable clinical decision making?" asks Spottiswoode. He emphasizes Siemens Healthineers' close cooperation with many academic and clinical partners. "Not only to help us understand the bigger clinical picture, but also to improve the robustness of our research prototypes and to train our algorithms to recognize the subtleties of PSMA uptake."

Helfand says that some open questions remain, such as how to identify prostate cancer in earlier or even non-aggressive stages. In these cases, the PSMA expression might be too low for therapeutic purposes. "Nevertheless, this technique has the potential to become an absolute game-changer for being able to diagnose and treat with two very

"But I am optimistic that this type of therapy, if successful, may even become an upfront therapy for many patients."

Brian Helfand, MD, PhD, a urologist based in Glenview, Illinois, USA

MIP PSMA-PET

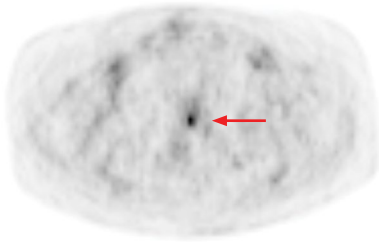

Axial PSMA-PET

Local recurrence

After radical prostatectomy, increase of PSA-level after 12 months up to 0.18 ng/ml. Recent MRI and bone scan negative. PSMA PET/CT presenting an intensive PSMA-uptake suspecting a local recurrence of prostate cancer. Data courtesy of Department of Nuclear Medicine, University Hospital Duesseldorf, Germany.

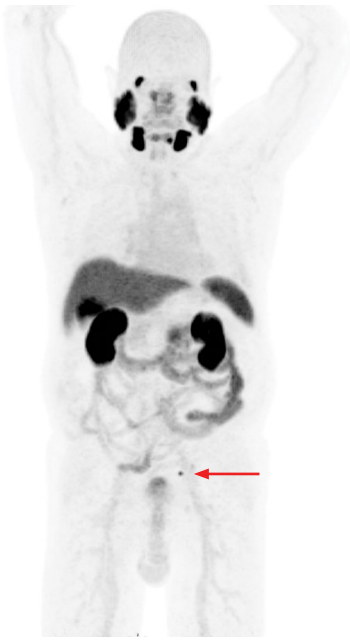

MIP PSMA-PET

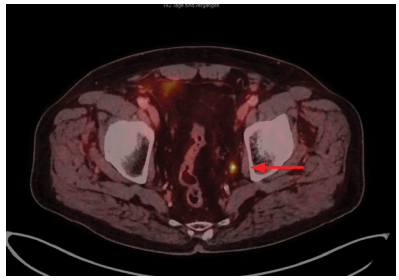

Axial PSMA-PET/CT

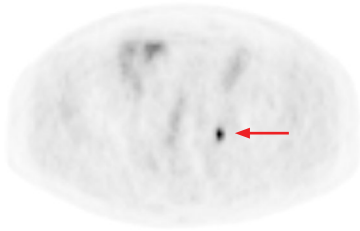

Axial PSMA-PET

Biomedical recurrence

After prostatectomy, recent PSA elevation up to 0.37 ng/ml. PSMA PET/CT presenting a focal PSMA uptake in a lymph node parailical left, indicating a lymph node metastasis (arrow). Data courtesy of Department of Nuclear Medicine, Universiy Hospital Duesseldorf, Germany.

"Not only to help us understand the bigger clinical picture, but also to improve the robustness of our research prototypes and to train our algorithms to recognize the subtleties of PSMA uptake."

Bruce Spottiswoode, PhD, director and senior biomedical engineer at Siemens Healthineers

similar molecules," says Helfand. In an ideal future, a different set of radiotracers and theranostic agents might even be able to ultimately target all prostate cancer cells in the entire body. "There is a lot of potential to continue from here."

The first major milestone was reached with FDA approval of PSMA products. Further large-scale clinical studies on Lutetium-177 and PSMA PET scans are being conducted. If the initial results are confirmed—and everything points to that—a new chapter in prostate cancer therapy is about to begin. And in a mere five to ten years, the new theranostics approach for this disease could become the new normal. ●

Florian Bayer is a journalist based in Vienna, Austria, who writes on healthcare topics. He worked as health editor at the newspaper *Standard* for four years.

The statements by Siemens Healthineers customers described herein are based on results that were achieved in the customer's unique setting. Since there is no "typical" hospital and many variables exist (e.g., hospital size, case mix, level of IT adoption) there can be no guarantee that other customers will achieve the same results.

Frederik Giesel, MD, MBA, is co-inventor of PSMA-1007.

For More Information

siemens-healthineers.com/molecular-imaging/news/mso-psma-variants-for-petct.html

siemens-healthineers.com/molecular-imaging/news/petnet-personalized-medicine

References

1 NCCN, SNMMI add piflufolastat F^{18} to guidelines for prostate cancer imaging (May 12, 2022): https://www.urologytimes.com/view/nccn-snmmi-add-piflufolastat-f18-to-guidelines-for-prostate-cancer-imaging

2 Afshar-Oromieh A, Zechmann CM, Malcher A, et al. Comparison of PET imaging with a ^{68}Ga-labelled PSMA ligand and ^{18}F-choline-based PET/CT for the diagnosis of recurrent prostate cancer. *Eur J Nucl Med Mol Imaging*. 2014;41(1):11-20. doi:10.1007/s00259-013-2525-5

3 Giesel FL, Hadaschik B, Cardinale J, et al. F-18 labelled PSMA-1007: biodistribution, radiation dosimetry and histopathological validation of tumor lesions in prostate cancer patients. *Eur J Nucl Med Mol Imaging*. 2017;44(4):678-688. doi:10.1007/s00259-016-3573-4

4 Voter, Werner, Pienta, Gorin, Pomper, Solnes et al. (2022): Piflufolastat F-18 (^{18}F-DCFPyL) for PSMA PET imaging in prostate cancer: https://www.tandfonline.com/doi/abs/10.1080/14737140.2022.2081155

5 Gaur, Mena, Harmon, Lindenberg, Pomper et al. (2020): Prospective Evaluation of ^{18}F-DCFPyL PET/CT in Detection of High-Risk Localized Prostate Cancer: Comparison With mpMRI https://www.ajronline.org/doi/10.2214/AJR.19.22042?mobileUi=0

6 Kratochwil C, Haberkorn U, Giesel FL. Radionuclide Therapy of Metastatic Prostate Cancer. *Semin Nucl Med*. 2019;49(4):313-325. doi:10.1053/j.semnuclmed.2019.02.003

Introducing Symbia Pro.specta SPECT/CT with myExam Companion

Modernize to MAXIMIZE

Take your nuclear medicine department into the future with intelligent SPECT/CT imaging. Symbia Pro.specta™ with myExam Companion gives you the power of more.

Redefine performance with new standards for SPECT/CT

Automatic SPECT motion correction and up to 64-slice CT enable faster scanning at the highest image quality.[1]

Reach your full potential with a smart workflow

An intuitive interface fully integrates SPECT and CT to help you consistently achieve high-quality, reproducible results.

Achieve optimized imaging from dedicated clinical tools

Transform your general SPECT/CT into a specialized camera that optimizes imaging for cardiology, neurology, oncology, and more.

[1] *Based on competitive literature at time of publication. Data on file.*

Symbia Pro.specta SPECT/CT is not commercially available in all countries. Due to regulatory reasons, its future availability cannot be guaranteed. Please contact your local Siemens Healthineers organization for further details.

Learn more at siemens-healthineers.com/symbiaprospecta

SIEMENS Healthineers

Whole-body parametric imaging expands clinical opportunities

Aarhus University Hospital in Denmark validates the clinical potential value of routine whole-body parametric imaging with PET/CT.

By Claudette Lew | Photography by Gorm Branderup | Data courtesy of Aarhus University Hospital, Denmark

(From left to right) Lars Gormsen, André Dias, and Ole Munk explore whole-body parametric imaging at Aarhus University Hospital, Denmark.

Dias and Gormsen next to Biograph Vision PET/CT used in the department to scan hundreds of patients with the new multiparametric imaging protocol.

PET imaging with fludeoxyglucose F 18 (FDG)[a] is an invaluable diagnostic tool that aids clinicians in making accurate diagnoses and evaluating treatment paths. As the current clinical standard, PET imaging currently utilizes a static image of the standardized uptake value (SUV), a semi-quantitative measurement of FDG uptake in tissue. With advances in PET/computed tomography (CT) technology hardware and software that make dynamic imaging acquisition achievable in routine clinical use, clinicians now have the ability to measure the true metabolic rate of tracer uptake (MRFDG). Parametric whole-body PET/CT imaging is an exciting new frontier in molecular imaging today.

Enabled on Siemens Healthineers Biograph Vision™ PET/CT scanner, whole-body parametric PET imaging is being utilized around the globe across a variety of clinical areas. Siemens Healthineers' customers are discussing and sharing the value it can bring to clinicians and identifying which patients might likely benefit.

Expanding diagnostic accuracy

Whole-body parametric PET/CT imaging can be utilized by clinicians for routine care because the acquisition parameters can be quickly assimilated into routine protocols with minimal additional scan time and without a steep learning curve. Clinician researchers at Aarhus University Hospital in Denmark are working on several new research projects using parametric imaging.

"This is the first time we can do whole-body parametric imaging" explains Ole Munk, physicist in the Department of Nuclear Medicine and PET-Centre in Aarhus. "So, this makes it possible to investigate new areas in oncology, where before dynamic imaging was limited to a single field of view."

One of the early users of this technology from Siemens Healthineers, the Aarhus team actively provides feedback on its usability and performance. They were able to acquire hundreds of whole-body FDG patient datasets using the new protocol in a relatively short time span using their three Biograph Vision™ 600 PET/CT scanners. To build these datasets, the team added the parametric imaging protocol to the first patient scan of the day on each system over a period of several months.[1]

Removing the limitations of static imaging

One of the reasons parametric imaging has so much potential for clinical use is due to its ability to

[a] Please see Indications and Important Safety Information for Fludeoxyglucose F 18 (^{18}F FDG) Injection on page 26. For full Prescribing Information, please see pages 77–79.

Fludeoxyglucose F 18 5-10mCi as an IV injection Indications and Usage

Fludeoxyglucose F 18 Injection is indicated for positron emission tomography (PET) imaging in the following settings:

- Oncology: For assessment of abnormal glucose metabolism to assist in the evaluation of malignancy in patients with known or suspected abnormalities found by other testing modalities, or in patients with an existing diagnosis of cancer.
- Cardiology: For the identification of left ventricular myocardium with residual glucose metabolism and reversible loss of systolic function in patients with coronary artery disease and left ventricular dysfunction, when used together with myocardial perfusion imaging.
- Neurology: For the identification of regions of abnormal glucose metabolism associated with foci of epileptic seizures.

Important Safety Information

- Radiation Risks: Radiation-emitting products, including Fludeoxyglucose F 18 Injection, may increase the risk for cancer, especially in pediatric patients. Use the smallest dose necessary for imaging and ensure safe handling to protect the patient and health care worker.
- Blood Glucose Abnormalities: In the oncology and neurology setting, suboptimal imaging may occur in patients with inadequately regulated blood glucose levels. In these patients, consider medical therapy and laboratory testing to assure at least two days of normoglycemia prior to Fludeoxyglucose F 18 Injection administration.
- Adverse Reactions: Hypersensitivity reactions with pruritus, edema and rash have been reported; have emergency resuscitation equipment and personnel immediately available. Full prescribing information for Fludeoxyglucose F 18 Injection can be found at the conclusion of this publication.

Dosage Forms and Strengths

Multiple-dose 30 mL and 50 mL glass vial containing 0.74 to 7.40 GBq/mL (20 to 200 mCi/mL) of Fludeoxyglucose F 18 injection and 4.5 mg of sodium chloride with 0.1 to 0.5% w/w ethanolas a stabilizer (approximately 15 to 50 mL volume) for intravenous administration. Fludeoxyglucose F 18 injection is manufactured by Siemens' PETNET Solutions, 810 Innovation Drive, Knoxville, TN 39732

---

differentiate between the actual tissue tracer uptake and "free" tracer in the blood pool. Thus, a typical image acquisition of parametric PET/CT using a Biograph Vision scanner will produce three different images: the MRFDG, which represents the real uptake of tracer into the cells, the distribution volume image (DVFDG) that shows the free component of FDG uptake in the background, and the third image is the standard SUV static image. Understanding the different quantifications in all three images is key to understanding how they can be successfully applied in certain oncology cases, for example.

"In certain cases where we may be in doubt as to whether an FDG-avid lesion on a static scan actually represents a true positive" says Lars Gormsen, MD, nuclear medicine physician, consultant and clinical professor at the Department of Nuclear Medicine and PET-Centre in Aarhus, "we may sometimes look into the quantitative MRFDG image and get a better idea. The point is that we're adding information from the MRFDG image to what we get from the static SUV image. At present, we don't see MRFDG as

"This makes it possible to investigate new areas in oncology, where before dynamic imaging was limited to a single field of view."

Ole Munk, physicist, Department of Nuclear Medicine and PET-Centre, Aarhus University Hospital, Denmark

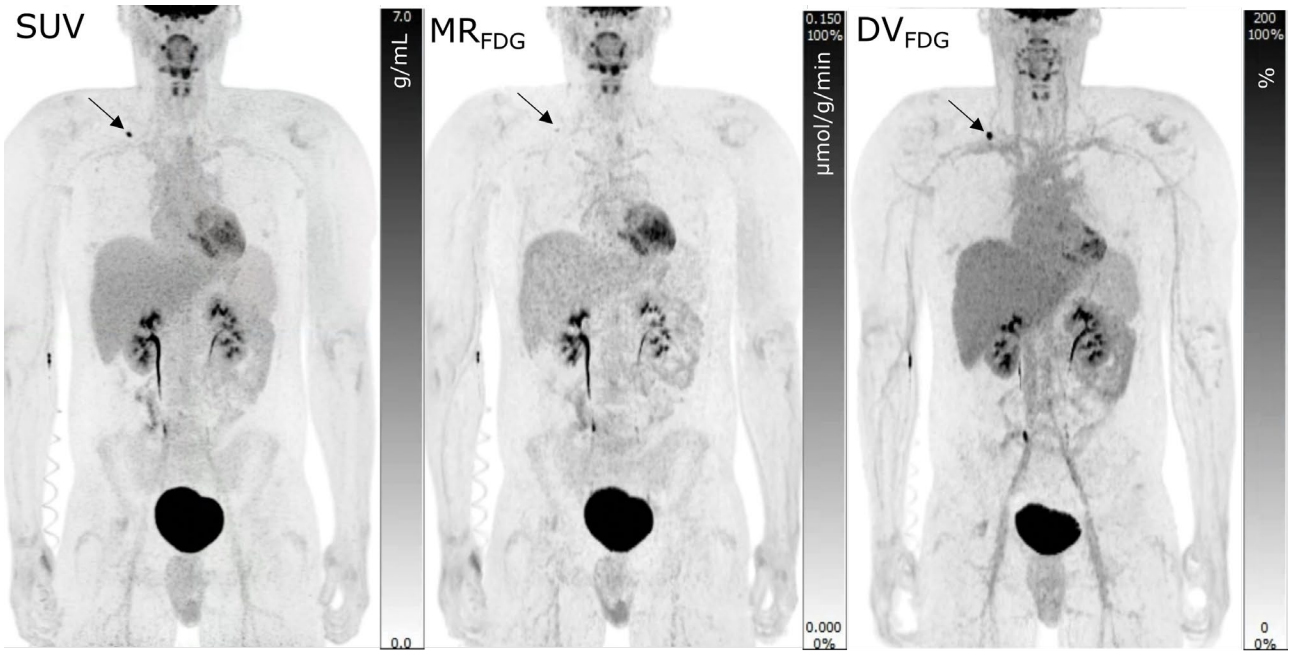

Example case of a multiparametric D-WB PET imaging. A 26-year-old male with Hodgkin's lymphoma, with previous bulk tumor in the mediastinum was referred for 3-month control after radiotherapy treatment. The PET scan showed no signs of residual disease in the mediastinum, but a new FDG hotspot was seen above the right clavicle (arrows). On static SUV images, such an FDG hotspot is suspicious for disease relapse. However, when analyzing the multiparametric images, it becomes clear that no actual FDG uptake was present in the lesion (MRFDG image representing FDG internalization) whereas the DVFDG images (representing "free FDG") showed unbound or "free" tracer. The finding was therefore dismissed as a false positive, and the report stated no signs of residual disease. Data courtesy of Aarhus University Hospital, Denmark.

something that will replace static PET scans."

Frequently on SUV, there is tracer uptake in lesions that would look like pathological uptake, but this uptake is actually a false positive finding. "We've seen examples in lymphoma cases after treatment," Gormsen continues, "where there might be a single lymph node still showing uptake, that sometimes will require you do consolidative radiotherapy on residual disease. We actually have an example of a patient where we could say that this is not residual lymphoma that should have consolidated radiotherapy because we could see it was "free" tracer. It was a clear false positive on the static FDG PET that was rooted out by looking at the MRFDG image."

Measuring tumor to background ratios

The Aarhus team reported that one of the things they are evaluating is the ability to measure tumor to background ratios in a different way. In theory, lesions that occur in very vascularized organs such as the liver, will be much easier to see on the MRFDG image due to the

"The point is that we're adding information from the MRFDG image to what we get from the static SUV image."

Lars Gormsen, MD, nuclear medicine physician, consultant, and clinical professor, Department of Nuclear Medicine and PET-Centre, Aarhus University Hospital, Denmark

André Dias and Lars Gormsen setting up the equipment used in this research. Gormsen (in the background) is preparing the Medrad Intego FDG injector used to administer the tracer and Dias (in the foreground) is preparing the Allogg ABSS automatic blood sampler used in one of the research papers where the population-based input function was calculated.

suppression of background signal. Patients with high blood sugar also are known to have altered background ratios because of the amount of glucose that is already in their system. It increases the background signal and reduces the signal in the lesions, which can impair the evaluation of lesions.

"On the MRFDG image, the measured level of tracer uptake in lesions remains the same, even with increased blood sugar as we are looking at the effective tracer internalization" reports André Dias, MD, nuclear medicine physician and staff specialist at Aarhus University Hospital. "This is previously known but nicely validated by the MRFDG images where we can see it very clearly—we're getting to visualize the uptake in a more precise fashion."

Making routine whole-body parametric PET imaging a reality

One of the barriers to whole-body parametric PET imaging in routine clinical use has been a complicated clinical workflow and long acquisition time. The development of new-generation PET/CT scanners like Biograph Vision with an extended field of view as well as more sophisticated evaluation software packages that offer automatic retrieval of the image-derived arterial input function, and automatic calculation of parametric imaging, in combination with dedicated shorter dynamic protocols, removes these barriers and can facilitate the wider use of whole-body parametric PET imaging.

The team at Aarhus University also worked on creating a population-based input function to allow for the reduction of scan time, but also to create a standard for industry-wide use. In collaboration with the Siemens Healthineers development team, the Aarhus team created a mathematical model to calculate the input function.

"The population-based input function works very well," explains Munk. "The original acquisition time of 70 minutes is now reduced to just 20 minutes, which is quite comparable to a standard clinical scan," Munk explains. "We take this population-based input function, which is standard shape, and we scale it. We scale it to the values that we derived from the last four

"We're getting to visualize the uptake in a more precise fashion."

André Dias, MD, nuclear medicine physician and staff specialist, Department of Nuclear Medicine and PET-Centre, Aarhus University Hospital, Denmark

passes [on the scanner]. So, this means that it's not the exact same input function for every patient, but it's actually individualized to each patient."

The Aarhus team has already published their clinical findings and typical MRFDG values for various tissue types.[2] They plan to continue research in this area, focusing on comparison studies, clinical applications, and validation studies of whole-body parametric PET imaging techniques for evaluating treatment response and kinetic modeling.

"PET imaging is really just maturing now," says Gormsen, "so we are refining the technique. We have spent the past 15 years looking at static PET images, and I think that we are ready to look into the finer details, which is really the kinetic analysis." ●

Claudette Lew is a freelance medical writer and editor.

The statements by Siemens Healthineers' customers described herein are based on results that were achieved in the customer's unique setting. Since there is no "typical" hospital and many variables exist (e.g., hospital size, case mix, level of IT adoption) there can be no guarantee that other customers will achieve the same results.

Biograph Vision is not commercially available in all countries. Due to regulatory reasons, its future availability cannot be guaranteed. Please contact your local Siemens Healthineers organization for further details.

For More Information

siemens-healthineers.com/vision

siemens-healthineers.com/molecular-imaging/news/mso-quantum-leap-biograph-vision-quadra

References

1 Dias AH, Pedersen MF, Danielsen H, Munk OL, Gormsen LC. Clinical feasibility and impact of fully automated multiparametric PET imaging using direct Patlak reconstruction: evaluation of 103 dynamic whole-body ^{18}F-FDG PET/CT scans. *Eur J Nucl Med Mol Imaging*. 2021 Mar;48(3):837-850. doi: 10.1007/s00259-020-05007-2. Epub 2020 Sep 7. Erratum in: Eur J Nucl Med Mol Imaging. 2021 Feb 13; PMID: 32894338.

2 Dias AH, Hansen AK, Munk OL, Gormsen LC. Normal values for ^{18}F-FDG uptake in organs and tissues measured by dynamic whole body multiparametric FDG PET in 126 patients. *EJNMMI Res*. 2022 Mar 7;12(1):15. doi: 10.1186/s13550-022-00884-0. PMID: 35254514; PMCID: PMC8901901.

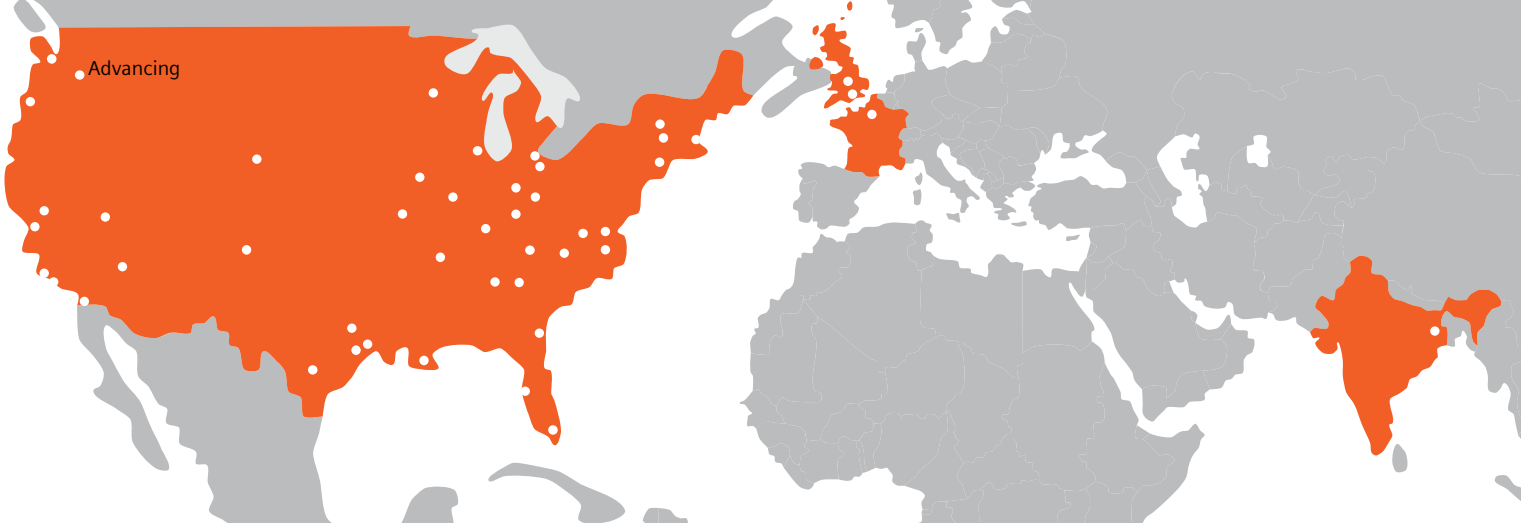

PETNET Solutions' global PET pharmacy network includes 47 radiopharamacies worldwide and serves over 2,800 imaging centers.

Fortifying the foundation for personalized medicine

PETNET Solutions invests in its network to increase patient access to PET biomarkers and support future biomarker development.

By Claudette Lew

As part of a commitment to support continued growth in the positron emission tomography (PET) and PET/Computed Tomography (CT) imaging industry that would enable more patients access to care, PETNET Solutions, Inc., a Siemens Healthineers company, is upgrading its network of cyclotron-equipped radiopharmacies for PET radiopharmaceuticals with new production facilities. PET imaging with fludeoxyglucose F 18 (FDG)[a] has gained increasing application as a highly valuable diagnostic and staging tool since it was initially approved for clinical use in oncology. Nearby production of the FDG biomarker is essential because of its short half-life of 110 minutes. As the trusted partner in PET imaging since 1996, PETNET's radiopharmacy capabilities will also serve the growing portfolio of novel radiopharmaceuticals beyond FDG that are continually being developed to target additional disease states.

PETNET's commercial production and distribution of FDG has to support the industry's growing demands and broader use of FDG PET imaging to target approved indications in cardiology, oncology, and neurology. PETNET's nationwide network of radiopharmacies enabled more patient access to PET imaging as initial utilization increased and then transitioned from research to standard of care. As additional tracers beyond FDG are developed targeting specific physiological processes to both diagnose and potentially deliver therapies, PETNET's operation as an expert, reliable partner to source, produce, and distribute high quality tracers will be more than ready to deliver as the industry advances.

"PETNET's expansion is really fueled by our goal for access of these very important PET tracers to more people," explains Barry Scott, CEO of PETNET Solutions. "The PET industry has grown tremendously over the last several years and we

[a] Please see Indications and Important Safety Information for Fludeoxyglucose F 18 (^{18}F FDG) Injection on page 31. For full Prescribing Information, please see pages 77–79.

Fludeoxyglucose F 18 5-10mCi as an IV injection Indications and Usage

Fludeoxyglucose F 18 Injection is indicated for positron emission tomography (PET) imaging in the following settings:

- Oncology: For assessment of abnormal glucose metabolism to assist in the evaluation of malignancy in patients with known or suspected abnormalities found by other testing modalities, or in patients with an existing diagnosis of cancer.
- Cardiology: For the identification of left ventricular myocardium with residual glucose metabolism and reversible loss of systolic function in patients with coronary artery disease and left ventricular dysfunction, when used together with myocardial perfusion imaging.
- Neurology: For the identification of regions of abnormal glucose metabolism associated with foci of epileptic seizures.

Important Safety Information

- Radiation Risks: Radiation-emitting products, including Fludeoxyglucose F 18 Injection, may increase the risk for cancer, especially in pediatric patients. Use the smallest dose necessary for imaging and ensure safe handling to protect the patient and health care worker.
- Blood Glucose Abnormalities: In the oncology and neurology setting, suboptimal imaging may occur in patients with inadequately regulated blood glucose levels. In these patients, consider medical therapy and laboratory testing to assure at least two days of normoglycemia prior to Fludeoxyglucose F 18 Injection administration.
- Adverse Reactions: Hypersensitivity reactions with pruritus, edema and rash have been reported; have emergency resuscitation equipment and personnel immediately available. Full prescribing information for Fludeoxyglucose F 18 Injection can be found at the conclusion of this publication.

Dosage Forms and Strengths

Multiple-dose 30 mL and 50 mL glass vial containing 0.74 to 7.40 GBq/mL (20 to 200 mCi/mL) of Fludeoxyglucose F 18 injection and 4.5 mg of sodium chloride with 0.1 to 0.5% w/w ethanolas a stabilizer (approximately 15 to 50 mL volume) for intravenous administration. Fludeoxyglucose F 18 injection is manufactured by Siemens' PETNET Solutions, 810 Innovation Drive, Knoxville, TN 39732

---

see no signs of it slowing down. We see only acceleration of not only the volume of PET biomarkers, but the number of different ones that are going to be developed in the near future."

Expanding access through production capability

With plans to upgrade several radiopharmacies in the coming years, PETNET selected South Florida and the Chicago, Illinois, areas in the United States to be the locations of the first two new sites. Both pharmacies will begin tracer production in 2022. Upgrades are in store not only for the sites themselves, but also for much of the tracer production equipment, such as high-capacity cyclotrons and chemical synthesis equipment. In addition to modernized lab space and increased production capacity, the South Florida location will also operate with a 30 percent increase in staffing to meet the market demands.

"In our new South Florida facility, we're installing two high-capacity cyclotrons," explains Josh Nutting, PETNET's Chief Operating Officer, "so we'll be able to offer other tracer products in parallel to FDG. It's really about access. We serve a lot of patients in Florida, and if we plan to enable more production capacity, that decision impacts things like an imaging center's decision to add another scanner, and subsequently a patient's ability to have more scheduling options for their scan. With the additional cyclotron capacity, FDG can be manufactured all day long,

South Florida location of new PETNET pharmacy

to meet the needs of our customers and ultimately give patients more flexibility in scheduling."

It is a considerable financial investment to build a new radiopharmacy or upgrade an existing one with high-powered equipment and additional staff, but PETNET is being proactive about its future and the future of the industry.

"PETNET's expansion is really fueled by our goal for access of these very important PET tracers to more people."

Barry Scott, CEO, PETNET Solutions, Inc.

"Opening a new facility in Chicago is an opportunity for us to modernize our operation from top to bottom. With a brand-new building and a high-capacity cyclotron that is replacing an older model," says Nutting, "we're able to significantly improve our capacity for today and into the future. We serve a lot of patients in the area and there's a fair amount of tracer development in the area as well."

"We're on track with a plan to put a lot of investment back into our network to make sure we can handle capacity for years to come," explains Scott. "Today we can reach about 98% of the US population with our pharmacies. To make sure we've got horsepower for five years from now, we've got to start investing now. It takes a lot of time, financial commitment, and very specialized resources to open new or upgraded facilities. There's a lengthy regulatory approval process between radiation safety, the Food and Drug Administration (FDA), and the Boards of Pharmacy. With the potential for many new tracers on the horizon, we want to make sure we stay well ahead of the wave, to where we can handle capacity and can always support access for more patients."

PETNET's new and upgraded facilities are not only able to offer quality, consistent tracers, but also the assurance that comes from knowing

PETNET Solutions, Inc., located near Chicago, Illinois.

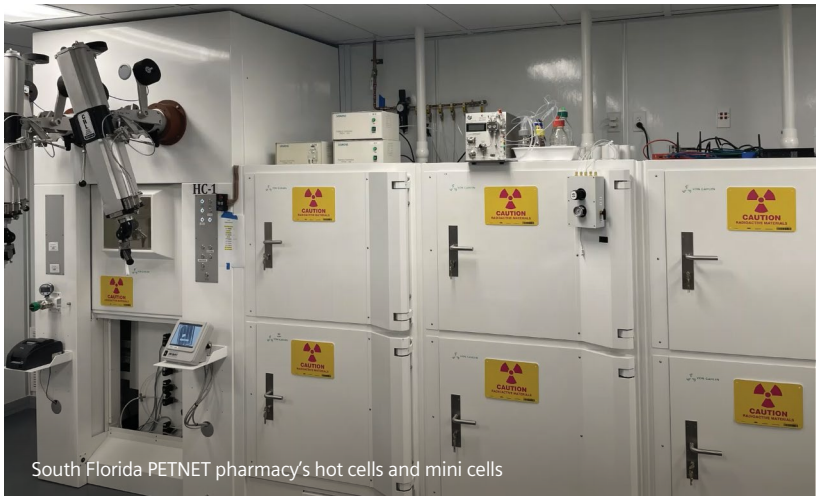

South Florida PETNET pharmacy's hot cells and mini cells

South Florida PETNET pharmacy's cyclotron room

"With the additional cyclotron capacity, FDG can be manufactured all day long, to meet the needs of our customers and ultimately give patients more flexibility in scheduling."

Josh Nutting, Chief Operating Officer, PETNET Solutions, Inc.

that everything that went into making that product has the high level of quality built into it.

"If you think about it," Nutting suggests, "there is an immunocompromised patient traveling to be injected with a sterile product that has been shipped right from a PETNET facility to an imaging facility. This requires confidence in the safety and quality of that product. Bringing that level of confidence to the patient as well as the caregiver is very important for us."

PETNET's investment into newer, state-of-the-art facilities in its network includes additional locations in the United States and expanding PETNET's pharmacies in Europe, specifically the United Kingdom and France. Nutting will be onsite in the UK to oversee the development, regulatory inspections, and opening of the new PETNET radiopharmacy there. When it's operational, the pharmacy will be able to service the entire country with imaging biomarkers.

New PET tracers take personalized medicine to the next level

PETNET's proactive investments into ramping up its production capabilities are based not only on the current utilization levels and clinical applications of PET imaging with FDG, but also on the early successes with new tracers that target specific diseases such as prostate cancer, where a patient's treatment can be more personalized and optimized for specific targets.

"FDG is wonderful for general imaging and does well in many areas, but when clinicians are looking for a very specific answer, it may not be quite as good in some cases. New biomarkers have had success in offering perspective on very specific disease cases within the body. Prostate cancer is one example," notes Scott. "Neurology is another. Imaging plaque in the brain can be very subtle and there are new tracers that offer clinicians more clarity than they can get using CT and MRI. As we get more precise with medicine, more diagnostic agents are being developed that can image disease with much more accuracy. That's why it's so important. That's what is really initiating the surge in growth we're anticipating."

As developers find successful new agents, they turn to PETNET as a partner and expert resource in commercial tracer production and to take advantage of PETNET's expansive tracer distribution footprint, as well as bringing new tracers in the market with a deeply experienced customer-facing team. "For PETNET," Scott emphasizes, "our vision is to be the provider and contract manufacturer of choice in PET radiopharmaceuticals because we believe in supporting the continued growth in PET/CT imaging with FDG and expanding the availability of novel PET imaging agents. We want to ensure new imaging agents are available to our customers, and ultimately for the benefit of more patients." ●

Claudette Lew is a freelance medical writer and editor.

For More Information

siemens-healthineers.com/petnet

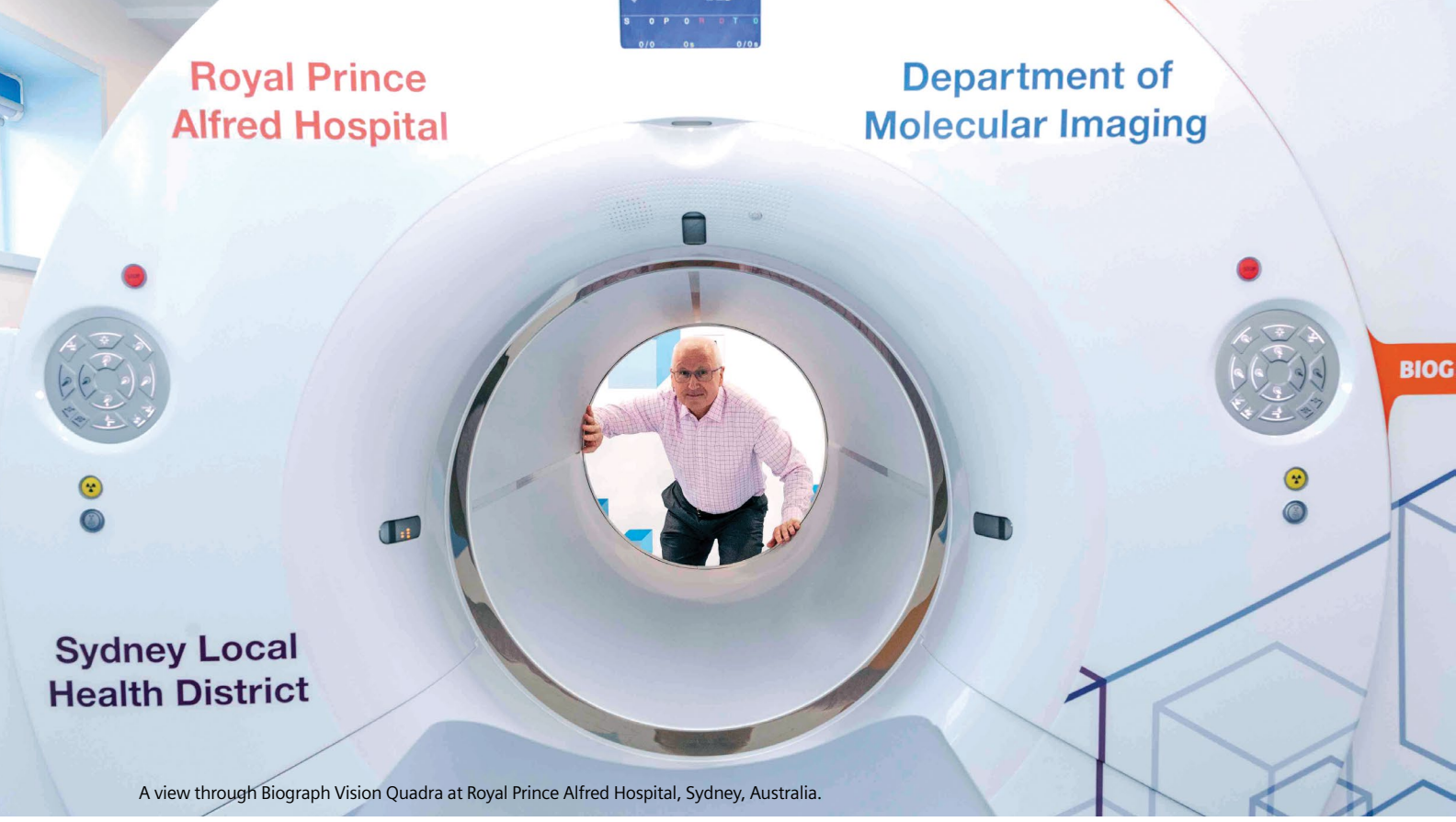

A view through Biograph Vision Quadra at Royal Prince Alfred Hospital, Sydney, Australia.

A champion of PET innovation

An early PET advocate recounts the origins of PET implementation at Royal Prince Alfred Hospital in Australia and today achieves even higher levels of patient care and research using Biograph Vision Quadra™.

By Sameh Fahmy | Data courtesy of Royal Prince Alfred Hospital, Sydney, Australia.

As a pioneer in the use of PET since the late 1980s, Professor Michael Fulham, MBBS, of the Royal Prince Alfred Hospital (RPA) and the University of Sydney in Australia, recalls technical challenges and the difficulty convincing clinicians of the value of positron emission tomography (PET) when he first returned to Australia from the United States.

Those challenges are a distant memory for Fulham and RPA, where he is the director of the Department of Molecular Imaging and the clinical director of Medical Imaging in Sydney Local Health District (SLHD). The hospital recently surpassed the milestone of 120,000 PET and PET/computed tomography (CT) scans and has the distinction of being the first hospital in Australia and the second hospital worldwide to install Siemens Healthineers' Biograph Vision Quadra PET/CT scanner.

With the 106-cm axial PET field of view Biograph Vision Quadra offers, Fulham and his colleagues have achieved an even higher level of patient care and research excellence made possible by whole-body, vertex-to-thighs imaging. "When you can see everything at once—the brain, the heart, the liver, the abdomen, the pelvis—that to me is a game changer," Fulham says. "Why? Because you've got true simultaneity, both for clinical work and for research."

Timeline of changing paradigms in medical imaging

Fulham conducted research on the capabilities of PET in the late 1980s

A crane lowers Biograph Vision Quadra through the roof during the installation at Royal Prince Alfred Hospital, Sydney, Australia, in 2020.

Professor Michael Fulham with Biograph Vision Quadra at Royal Prince Alfred Hospital, Sydney, Australia.

at the National Institutes of Health in Bethesda, MD, USA, before returning to RPA in 1993, shortly after the hospital launched its PET program. RPA, voted as the best hospital in Australia in a 2022 survey, has long been one of Australia's premier tertiary referral hospitals and the principal teaching hospital of the University of Sydney.[1]

Fulham notes that early PET scanners had gantries that could only accommodate the head, but the development of CTI ECAT 951 opened up a new era by enabling the imaging of all body parts. The Siemens ECAT 951 was the scanner installed in RPA in 1992. He recalls that surgical oncologists at RPA, rather than medical oncologists, were the most enthusiastic early adopters of PET imaging. Its utility in guiding and improving treatment for patients with cancer of the skin (melanoma), liver, lung, and stomach formed the foundation that later convinced other clinicians, such as hematologists, respiratory physicians, medical oncologists, radiation oncologists, of its potential. "We aim for the best," Fulham says, "and that's really what's driven our program."

RPA's early adoption of imaging modalities to improve patient care is consistent with its history of medical innovation and leadership, both as a teaching hospital and as a referral hospital that has cared for patients since 1882. Fulham emphasizes that results drive the

"When you can see everything at once—the brain, the heart, the liver, the abdomen, the pelvis—that to me is a game changer. Why? Because you've got true simultaneity, both for clinical work and for research."

Professor Michael Fulham, MBBS, Royal Prince Alfred Hospital, Sydney, Australia

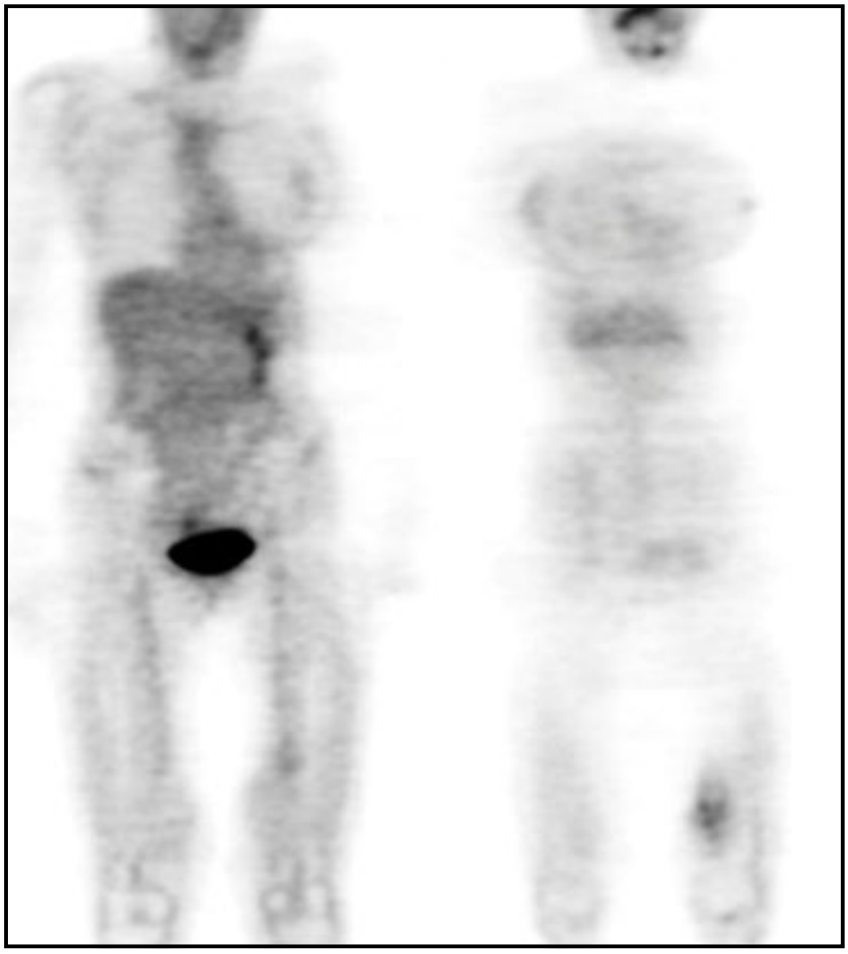

PET (ECAT 951R) "bed positions" scans at RPA in 1992.
Data courtesy of Royal Prince Alfred Hospital, Sydney, Australia.

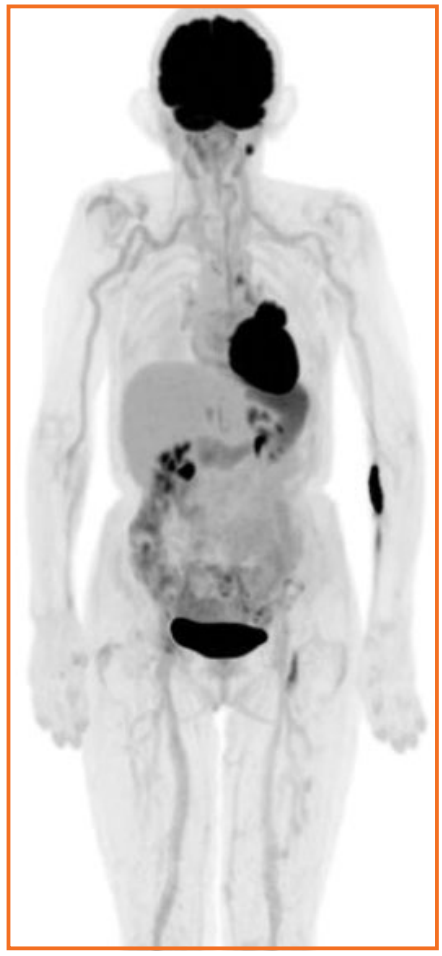

From ECAT to Biograph Vision Quadra in 2021 at RPA (13-minute scan). Data courtesy of Royal Prince Alfred Hospital, Sydney, Australia.

hospital's decision-making and enable him to make the case for new investments in technology.

"My approach is that if you've got meaningful and accurate data, it's very hard to argue against it," he says. "What's important is to demonstrate how imaging with PET changes patient care and how it can be efficient and productive. And we've done all of those things."

Advances in scanner reliability and image quality continued throughout the 1990s, "but when PET/CT was released at RSNA 2000, it was clear that the paradigm would change," Fulham says. At that stage, Fulham said that 8 to 9 scans were the most scans that could be done in one day. Each scan took 64 minutes to acquire data from the base of the skull to the upper thighs. "It's not just about anatomical localization," he added. "It's really about how both work together. The PET in the Biograph™ Duo PET/CT had LSO detectors that were so much faster. So coupled with the anatomical data from the CT, the introduction of PET/CT was a tremendous advance—we could do faster and better scans."

Fulham says the central role that PET/CT now plays in patient care at RPA and how quickly the technology has evolved are perhaps best illustrated by looking back at the number of scans the hospital has performed. When he began working at RPA in the early 1990s, the hospital scanned its first 100 patients over a span of 10 months. Scanning the first 1,000 patients took 25 months. Fast forward to July 2019, and RPA reached a milestone of 100,000 patient scans. By the end of March 2022, it had already reached 120,000 scans.

RPA installed two Biograph Vision™ scanners in 2019. With 3.2-mm LSO crystals that deliver high spatial resolution and fast time of flight, the scanners enabled Fulham and his colleagues to confidently detect small sites of disease that would otherwise be missed.

Metastic lung cancer patient: two positions/12-minute torso and 1-minute legs, using Biograph Vision Quadra. Data courtesy of Royal Prince Alfred Hospital, Sydney, Australia.

"With Biograph Vision, the crystal size was smaller, and the sensitivity increased compared to our Biograph mCTs," he says. "The image quality, which was already very good on the two Biograph mCTs we had, improved yet again, and with it came the confidence in detecting sites of disease in even smaller structures. This, once again, changed patient management."

Today's install increases patient throughput and comfort

By incorporating four detector-block assemblies found in Biograph Vision alongside each other, Biograph Vision Quadra significantly enhances effective sensitivity. Fulham describes the decision to install it at RPA as "a no brainer."

"I had no doubt about its value to patients because it was 16 times more sensitive than most conventional PET/CT scanners and 10 times more sensitive than Biograph Vision, and Biograph Vision

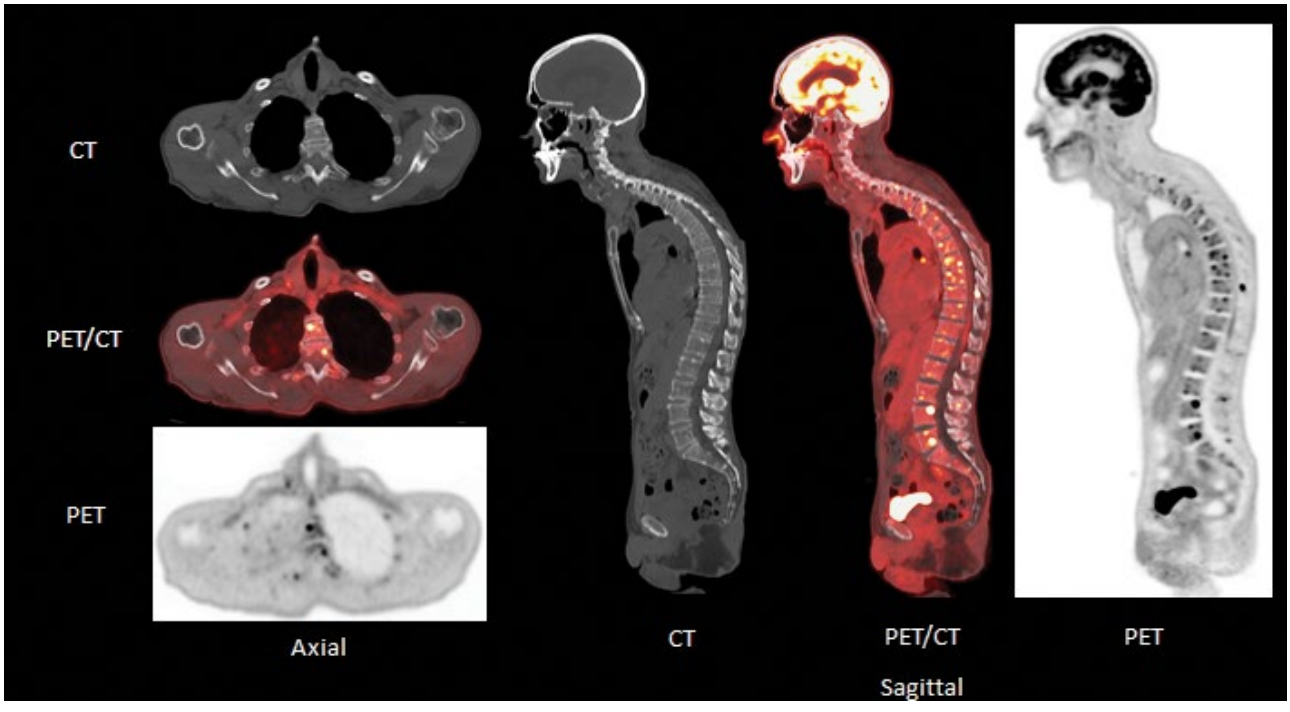

Same patient, cross sectional and side views. Data courtesy of Royal Prince Alfred Hospital, Sydney, Australia.

was the most sensitive scanner that's been made by Siemens Healthineers until Biograph Vision Quadra came along," Fulham says.[a] "So, I knew that we would be able to get more precision in what we did, and everything would be better—the scan duration would be shorter, the dose lower, and we would have superb images."

A workhorse for clinical care and research in PET/CT imaging

Fulham emphasizes the importance of being able to scan multiple organs simultaneously, noting that it enables the assessment of tracer kinetics. He and his colleagues are assessing optimal scan acquisition time and dose and adapting the parameters for different body types. "There's so much potential in Biograph Vision Quadra that it really is untapped," he says. "We're only just starting to scratch the surface of what it can do in our research areas."

In clinical care, Fulham noted that the image quality that Biograph Vision Quadra produces with shorter scan durations and with reduced doses is 'ridiculously good.'

"Nothing can detect disease in small nodes in prostate cancer like a PSMA scan with Biograph Vision Quadra," Fulham says. "We pick up nodes as small as 2 mm that have uptake in them, and the scanner gives you the confidence that it's real, it's there, and it means better patient care." He added that "we have scanned some patients where the image quality at a 1-min acquisition is diagnostic, which is unbelievable."

The rapid scan times that Biograph Vision Quadra enables have increased patient throughput at RPA and, importantly, patient comfort. He recalls a patient with a very high body mass index (BMI =64.2, 419 lb/190 kg) who had been scanned previously on the Biograph Vision scanner. "She was blown away when she was on the bed for 12 minutes," Fulham says. "The patient asked the tech, 'Is it done? The last time I was here I was on the bed for 45 minutes.' This is incredibly meaningful for the patient, and not only that, the image quality was truly unbelievable for a patient with a high BMI."

For Fulham, outcomes such as these reaffirm how the early adoption of new technologies can benefit patients. "The journey has been focused predominantly on making sure that we do the right thing by the patient, having fantastic technology, and a receptive vendor who's prepared to push the envelope," he says. "Our relationship [with Siemens Healthineers] has been based on a solid understanding of what the technology is capable of and what we need."

Fulham emphasizes that RPA plans to continue growing its PET/CT program to better serve its patients and to continue to advance the field through innovative research.

"Was it the right decision to get a Biograph Vision Quadra?" Fulham asks rhetorically. "Yes. And what are we going to do next? Of course, we are going to get another one!"

"We're expanding the department in the near future, and I hope to have a PET/MR as well as a new PET/CT scanner. The workhorse will be Biograph Vision Quadra, and it'll be the workhorse both for research and for clinical care." ●

Sameh Fahmy, MS, is an award-winning freelance medical and technology journalist based in Athens, Georgia, USA.

[a] Based on competitive literature available at the time of publication. Data on file.

[b] The statements by Siemens Healthineers customers described herein are based on results that were achieved in the customer's unique setting. Since there is no "typical" hospital and many variables exist (e.g., hospital size, case mix, level of IT adoption), there can be no guarantee that other customers will achieve the same results.

[c] Biograph Vision Quadra is not commercially available in all countries. Due to regulatory reasons, its future availability cannot be guaranteed. Please contact your local Siemens Healthineers organization for further details.

For More Information

siemens-healthineers.com/molecular-imaging/news/mso-quantum-leap-biograph-vision-quadra

siemens-healthineers.com/molecular-imaging/news/mso-practical-approach-to-cardiac-PET

siemens-healthineers.com/molecular-imaging/pet-ct/biograph-vision-quadra

References

[1] Newsweek. 2022. World's Best Hospitals 2022 - Top 250. [online] Available at: https://www.newsweek.com/worlds-best-hospitals-2022

Your digital nuclear medicine resources

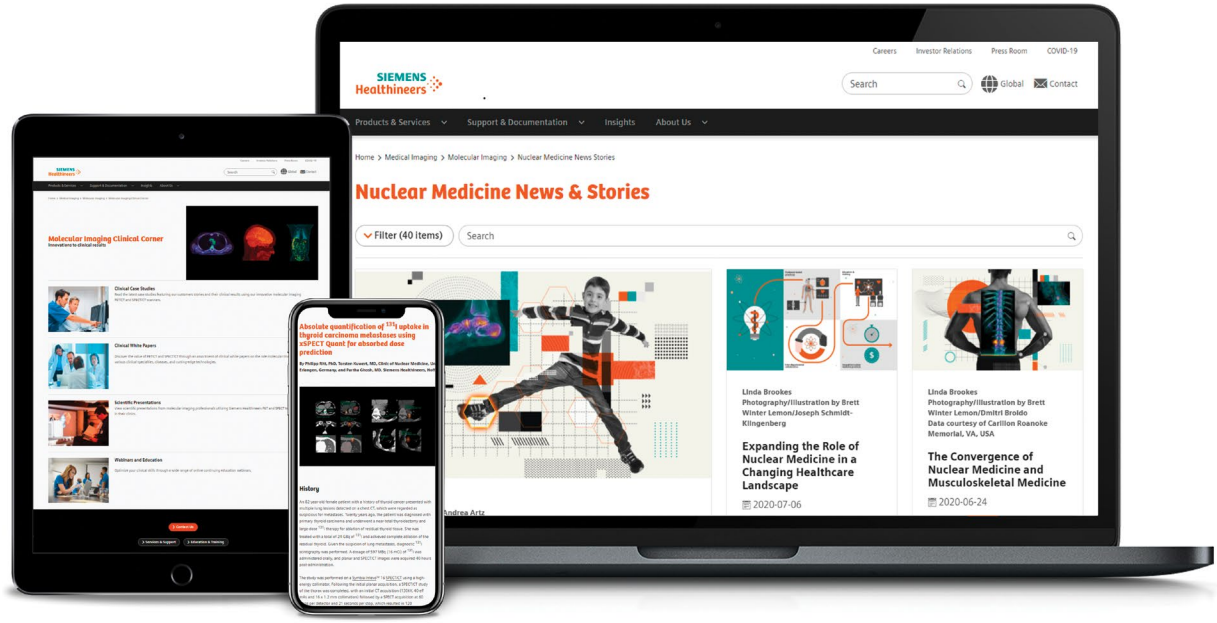

Explore our collection of MI publications, ranging from news to clinical results

Discover the value of PET and SPECT technologies through an assortment of clinical case studies, white papers, and more

Expand your clinical knowledge through a wide range of archived continuing education (CE) webinars

SCAN ME

Read nuclear medicine news & stories anytime, anywhere:
siemens-healthineers.com/nmns

SCAN ME

Access current clinical information whenever, wherever:
siemens-healthineers.com/miclinicalcorner

SIEMENS Healthineers

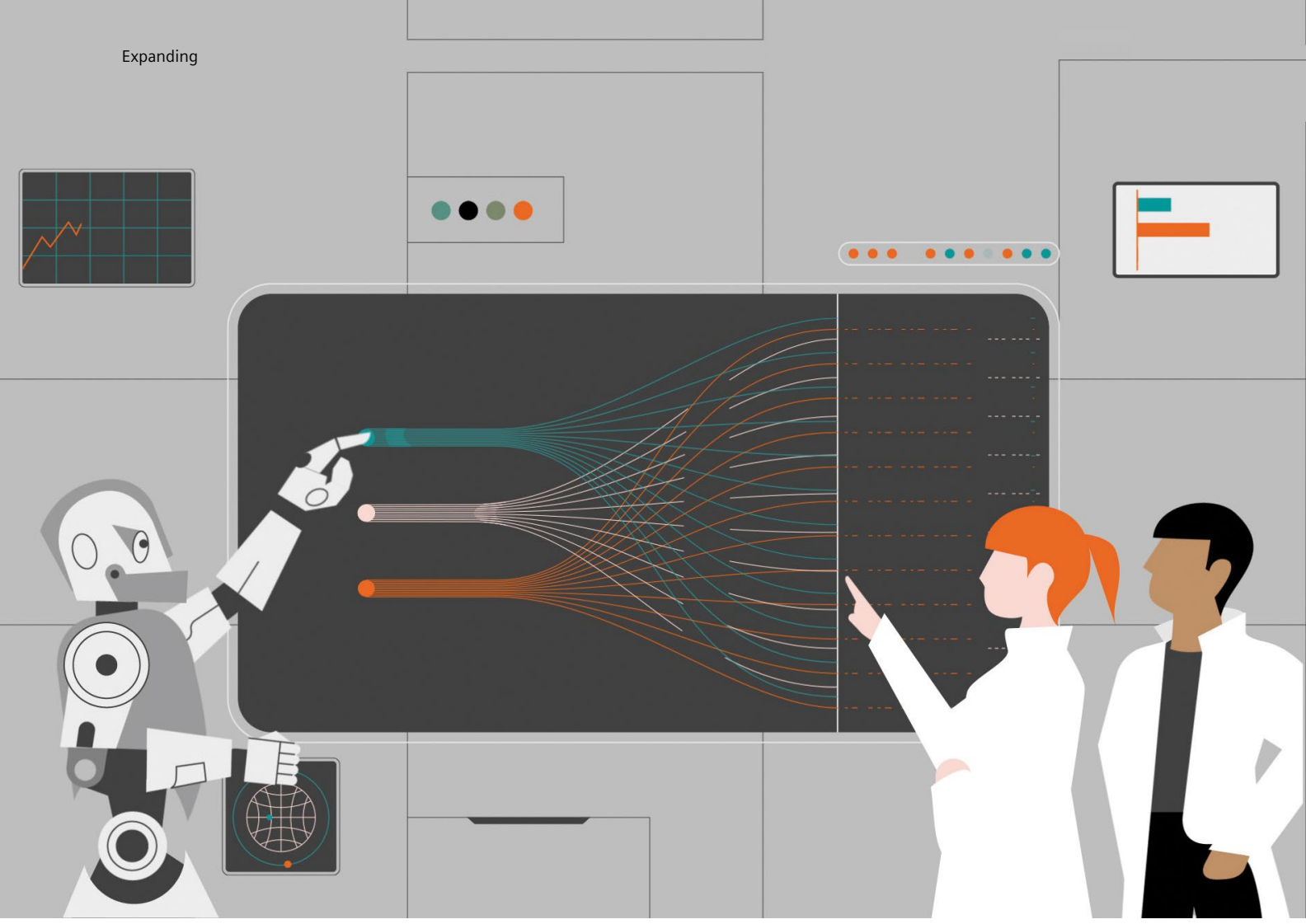

How we developed Auto ID

Selecting a single checkbox alongside the words “Enable Auto ID” brings the power of artificial intelligence into routine clinical use in molecular imaging: an action that saves precious time and streamlines processes that would otherwise be tedious.

By Sameh Fahmy | Photography by Steven Bridges & Lars Berg | Illustration by Joseph Schmidt-Klingenberg

The ease of use physicians might one day take for granted stands in contrast to the years of development, validation, and testing performed by a dedicated team of scientists and physicians who created Lesion Scout with Auto ID.[a] The clinical application—housed within the *syngo* ®.via for Molecular Imaging reading solution—sits at the interface of medicine and artificial intelligence, and opens the door to a future in which care is delivered more efficiently and precisely. The power of Auto ID lies in its potential to dramatically speed workflow for physicians by automatically segmenting and classifying the uptake of ^{18}F-FDG in whole-body PET/CT images as either pathologic or physiologic. Auto ID also enables physicians to calculate whole-body metabolic tumor volume (MTV) and total lesion glycolysis (TLG) within seconds.[b]

"For me, one of the motivations is the potential impact of this type of technology," says Ludovic Sibille, MS, the senior scientist at Siemens Healthineers who developed the algorithm that powers Auto ID. "It has a wide application and a large impact potentially on our customers and on radiology."

A collaborative journey

Collaboration has been an integral part of the journey that has made Auto ID possible. Physicians from the Department of Nuclear Medicine and the European Institute for Molecular Imaging at the University of Münster provided the clinical data that was used to train the artificial intelligence algorithm. In addition, Sibille and his colleagues at Siemens Healthineers have incorporated feedback on early prototypes from meetings and surveys of clinicians and management at institutions ranging from large academic medical centers to smaller regional hospitals.

Carl von Gall, MD, product manager for oncology applications at Siemens Healthineers, recalls showing an early prototype of Auto ID to physicians at the 2019 Annual Congress of the European Association of Nuclear Medicine (EANM) and seeing their marvel.

"There's this 'aha' moment when they would open up their eyes and say, 'You just identified uptake that would need to be included or excluded, with a little help from me, in less

"For me, one of the motivations is the potential impact of this type of technology. It has a wide application and a large impact potentially on our customers and on radiology."

Ludovic Sibille, MS, Siemens Healthineers

Auto ID proposes a selection of foci to be excluded and included from findings creation. Data acquired under IRB-approved protocol. Data on file.

than two minutes,'" he recalls, adding that the current iteration of Auto ID has brought the time down to approximately 10 seconds.[c] "They told us pretty directly that Auto ID will be something that they could use every day."

Grounded in clinical expertise

Auto ID automatically segments and classifies lesions using a type of deep learning algorithm known as a convolutional neural network (CNN). CNNs are often used in image recognition and computer vision, but Sibille explains that the immense amount of data associated with 3D PET/CT images made the development of a CNN that can accurately classify uptake particularly challenging.

Through an iterative process, Sibille worked to refine the parameters that comprise the algorithm. He trained, validated, and tested the algorithm against data grounded in the clinical expertise of Michael Schäfers, MD, and his colleagues at the University of Münster. To create a reference standard to train, validate, and test the algorithm, a board-certified nuclear medicine physician and a board-

certified radiologist from the University of Münster analyzed whole-body PET/CT scans of 629 patients with lung cancer or lymphoma. The experts manually delineated foci with increased ^{18}F-FDG uptake and performed more than 12,000 annotations. Like Sibille, Schäfers says he was motivated by the opportunity to have a meaningful impact on the future of medicine.

"There's hype about artificial intelligence, but most of the approaches suffer from poor data quality or not enough data," Schäfers says. "If you want to use AI as an expert system, to train people, to support people in their decisions, you have to make sure that the data, the ground truth, is not wrong from the beginning."

Sibille, Seifert, Schäfers, and several of their colleagues published their findings in the journal *Radiology*.[1] Lymphoma and lung cancer were chosen for the study because they are relatively common metastatic cancers, but a preliminary internal evaluation that examined melanoma, colorectal cancer, breast cancer, cancers of unknown origin, and inflammatory disease found that Auto ID

"There's hype about artificial intelligence, but most of the approaches suffer from poor data quality or not enough data. If you want to use AI as an expert system, to train people, to support people in their decisions, you have to make sure that the data, the ground truth, is not wrong from the beginning."

Michael Schäfers, MD, University of Münster

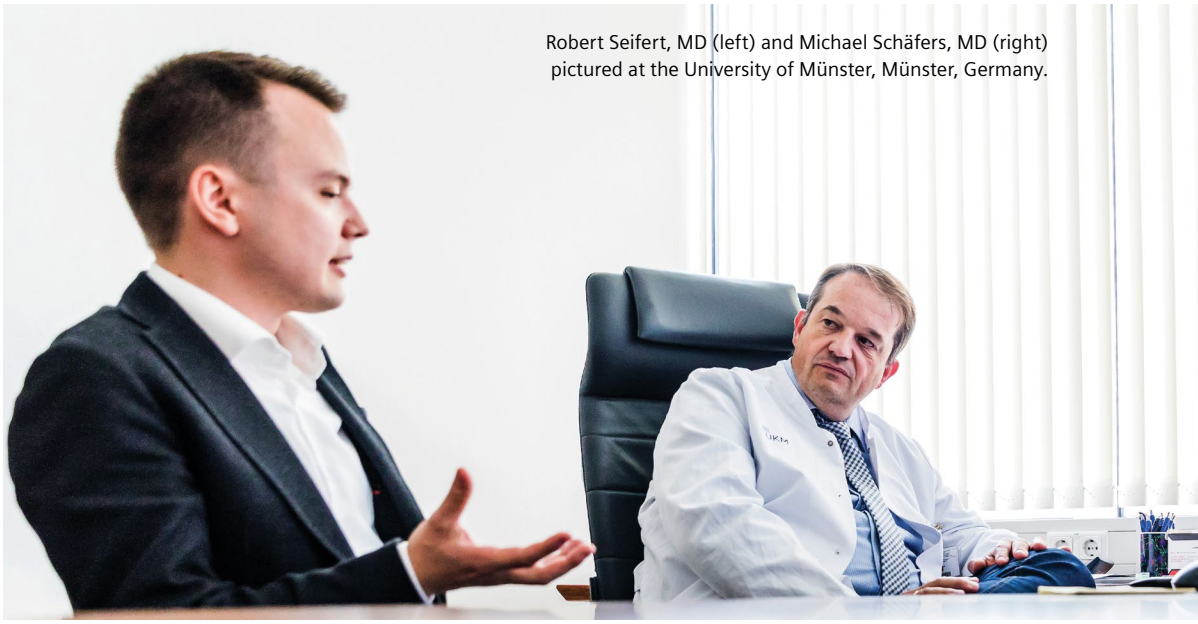

Robert Seifert, MD (left) and Michael Schäfers, MD (right) pictured at the University of Münster, Münster, Germany.

Lobby vestibule of the Department of Nuclear Medicine at the University of Münster

differentiated physiologic vs. pathologic uptake with an overall accuracy of 92%.[d] "The beauty of this is that the physiological uptake pattern is similar in patients and is, to the most degrees, not disease-specific," von Gall says. "Because that pattern is robust, physicians may be comfortable applying that to their daily routine."

Additional retrospective studies have continued to evaluate Auto ID's ability to quantify MTV in lymphoma, breast cancer, and other miscellaneous cancer types. The studies reinforce the workflow of Auto ID when compared to manual segmentation and quantification efforts. The ability of Auto ID to assist in the segmentation and quantification of MTV TLG underscores the prognostic value in the ability to predict overall- and progression-free survival.[2-4]

"The future of our field"

Robert Seifert, MD, of the University of Münster, emphasizes that PET/CT parameters such as MTV and TLG have been shown to provide prognostic value for cancer patients while also potentially providing valuable data for assessing response to treatment. Measuring these parameters has been too tedious and time consuming for routine use, but the speed and accuracy of Auto ID has the potential to enable much broader use.

Seifert and Schäfers point out several additional ways in which artificial intelligence has the potential to enhance clinical care and basic research, including enabling more nuanced staging of cancer, the analysis of dynamic images, and the integration of imaging data with population-level datasets to advance research. "The Auto ID functionality and similar approaches are the future of our field," Seifert says.

"The Auto ID functionality and similar approaches are the future of our field."

Robert Seifert, MD, University of Münster

From its inception in 2013, the development of Auto ID has been guided by the belief that new technologies should support and streamline the work of physicians without adding complexity or burden. Auto ID provides color-coded proposals for uptake that likely should be excluded or included—green for exclude and orange for include, for example—but the reading physician remains in control and ultimately decides the content of the final report.

"AI, if it's truly meaningful, needs to be almost invisible," von Gall says. "Don't change the reader's method—support it, add to it, augment it, but don't change it. So, that's why the only thing that you're going to see from Auto ID in the configuration is one checkbox, which says 'Enable Auto ID.' And that's where the magic happens." ●

Sameh Fahmy, MS, is an award-winning freelance medical and technology journalist based in Athens, Georgia, USA.

"AI, if it's truly meaningful, needs to be almost invisible. Don't change the reader's method—support it, add to it, augment it, but don't change it."

Carl von Gall, MD, Siemens Healthineers

References

1 Sibille L, Seifert R, Avramovic N, et al. ^{18}F-FDG PET/CT Uptake Classification in Lymphoma and Lung Cancer by Using Deep Convolutional Neural Networks. *Radiology*. 2020;294:445-452.

2 Pinochet P, Eude F, Becker S, et al. Evaluation of an Automatic Classification Algorithm Using Convolutional Neural Networks in Oncological Positron Emission Tomography. *Front Med (Lausanne)*. 2021;8:628179. doi:10.3389/fmed.2021.628179.

3 Weber M, Kersting D, Umutlu L, et al. Just Another "Clever Hans"? Neural networks and FDG PET-CT to predict the outcome of patients with breast cancer. *Eur J Nucl Med Mol Imaging*. 2021. doi:10.1007/s00259-021-05270-x.

4 Capobianco N, Meignan M, Cottereau A-S, et al. Deep-Learning ^{18}F-FDG Uptake Classification Enables Total Metabolic Tumor Volume Estimation in Diffuse Large B-Cell Lymphoma. *J Nucl Med*. 2021;61(1):30-36. doi:10.2967/jnumed.120.242412.

[a] Lesion Scout with Auto ID is not available for sale in the United States and is not commercially available in all countries. Future availability cannot be guaranteed. Please contact your local Siemens Healthineers organization for further details.

[b] The lesion classification presented by Auto ID is only a proposal. All findings must be evaluated and accepted by the physician before MTV/TLG is calculated.

[c] Within 10 seconds for cases with 440 matrix size and smaller. Data was obtained using studies with 270 segmentations or less.

[d] Clinical results may vary.

Sequential xSPECT Quant acquisitions for absorbed dose calculation following a therapy dose of ^{177}Lu DOTATATE in a patient with a metastatic neuroendocrine tumor

By Partha Ghosh, MD, Siemens Healthineers, Hoffman Estates, Illinois, USA
Data and images courtesy of Queen Elizabeth Hospital Birmingham, Birmingham, United Kingdom

History

An elderly male with a neuroendocrine tumor (NET) and liver metastases underwent peptide receptor radionuclide therapy (PRRT).

Approximately 7.7 GBq (200 mCi) of ^{177}Lu DOTATATE with concurrent amino acid infusion was administered by intravenous (IV) infusion.

A SPECT/CT acquisition was performed 4 hours after the therapy infusion. Subsequent sequential SPECT/CT acquisitions were also acquired at 24-hours, 96-hours, and 168-hours post therapy.

The study was conducted on Symbia Pro.specta™[a] SPECT/CT, which was calibrated for ^{177}Lu absolute quantification using xSPECT Quant's National Institute of Standards and Technology (NIST)-traceable Selenium 75 (^{75}Se) medium-energy calibration source.

Following the initial low-dose CT, a SPECT acquisition using a medium-energy low-penetration (MELP) collimator was performed at 60 views per detector with a 20-second acquisition per view. The study was acquired for 2 bed positions in order to obtain both the thorax and abdomen, although the focus was primarily on the liver and kidney tracer concentrations.

xSPECT Quant™ reconstructions (128 x 128 matrix, xSPECTEM 24i4s) were subsequently performed using the SPECT and CT data. xSPECT Quant data across multiple timepoints was reviewed on *syngo*®.via to estimate lesion and critical organ tracer concentration in Bq/ml.

Findings

Figures 1 and 2 show maximum intensity projection (MIP) and multiplanar reconstruction (MPR) views of sequential SPECT/CT studies, which demonstrate an initial high uptake of ^{177}Lu DOTATATE within multiple liver metastases with a progressive increase in uptake between 4 hours and 24 hours. The 24-hour study shows the highest lesion uptake with subsequent slow washout revealed on the 96- and 168-hour studies. However, a significant amount of retained tracer is still visualized within the largest liver metastases even at 168 hours post-therapy administration. On the contrary, the bilateral renal cortex shows normal thickness and high initial tracer uptake but with progressive washout. There is slow clearance of tracer between 4 hours and 24 hours in the renal cortex but with faster clearance and low renal tracer uptake at 168 hours. This visual impression suggests prolonged retention of the radionuclide within the liver metastases and fast tracer transit with fast washout in the renal cortex. This implies the possibility of high absorbed dose to the liver metastases due to the longer tracer retention following radionuclide therapy but low renal cortical absorbed dose due to fast clearance.

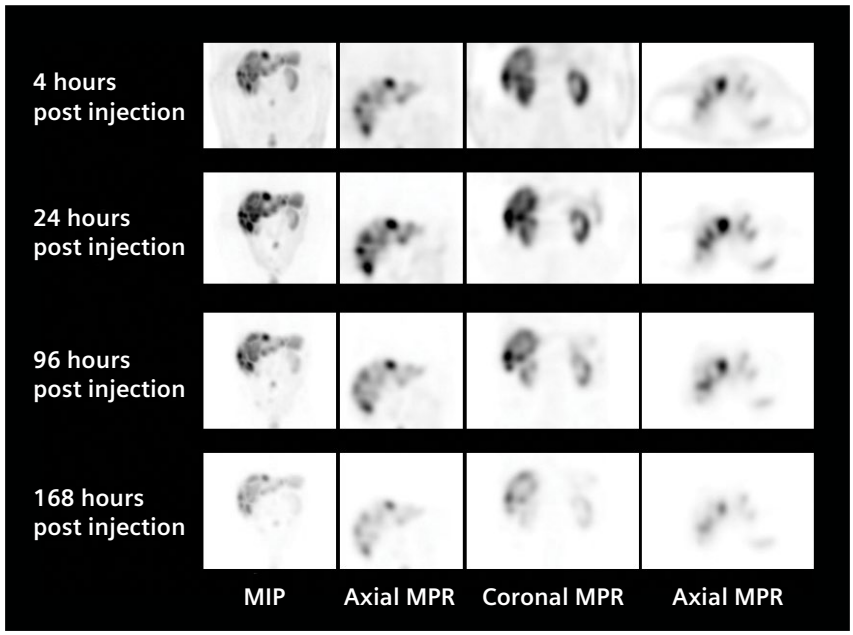

1 **Sequential SPECT/CT with xSPECT Quant performed at 4 hours, 24 hours, 96 hours, and 168 hours following a therapy dose of 7.7 GBq (200 mCi) of ^{177}Lu DOTATATE in a patient with a metastatic NET and multiple liver metastases shows a gradual increase in tracer concentration in the liver lesions with the peak at 24 hours and slow washout shown on the 168-hour study. Renal cortical tracer concentration shows initial high uptake with progressive washout.**

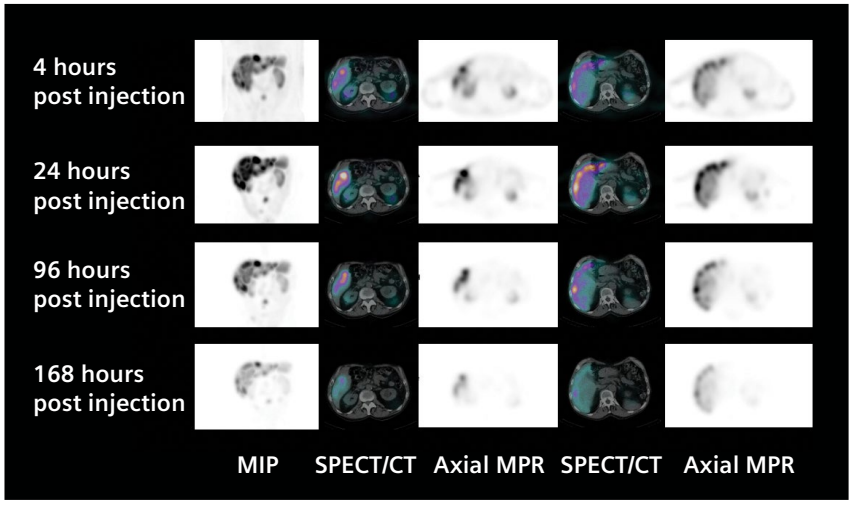

2 **Additional SPECT and SPECT/CT slices through liver metastases acquired across multiple timepoints show a gradual increase in tracer concentration within liver lesions between 4 hours and 24 hours after tracer administration with slow washout. SPECT/CT images also demonstrate normal renal cortical thickness and initial high renal cortical uptake at 4 hours with progressive washout and minimal renal cortical retention at 168 hours.**

As shown by the quantitative evaluation of tracer concentration in liver metastases by sequential xSPECT Quant studies (Figure 3), there is an increase in tracer concentration between 4 hours and 24 hours with the maximum reached at 24 hours with slow washout. Tracer retention within liver lesions at 168 hours is approximately 35% of the maximum concentration achieved at 24 hours. However, the renal clearance is rapid with maximum concentration in the renal cortex achieved by 4 hours with progressive clearance with less than 20% of the maximum concentration remaining at 168 hours.

xSPECT Quant and CT DICOM data were transferred to third-party dosimetry software[b] for calculation of absorbed dose. Tracer concentration values from 4 time points were used to generate time-activity curves (TACs) for every voxel followed by dose calculation using a linear Boltzmann transport equation (LBTE) solver. LBTE simulates an infinite number of radiation particles interacting with the heterogeneous media. CT and SPECT images across multiple timepoints were aligned and the automatic segmentation of the critical organs—lungs, kidneys, and liver—was performed to generate volumes of interest (VOIs). Liver metastases were identified using SPECT images with automated gradient-based VOI generation in *syngo*.via's RT image suite.

The dose volume histogram shows a relatively small portion of the lesion receiving 16.8 Gy, which is evident from the isodose lines and dose volume histogram. The kidneys show low levels of renal cortical absorbed dose as predicted from the quantitative SPECT data, which showed fast washout after initial peak. The mean renal dose was 1.74 Gy for the left kidney and 2.14 Gy for the right kidney. The mean lung dose was also low at approximately 0.1 Gy for both lungs.

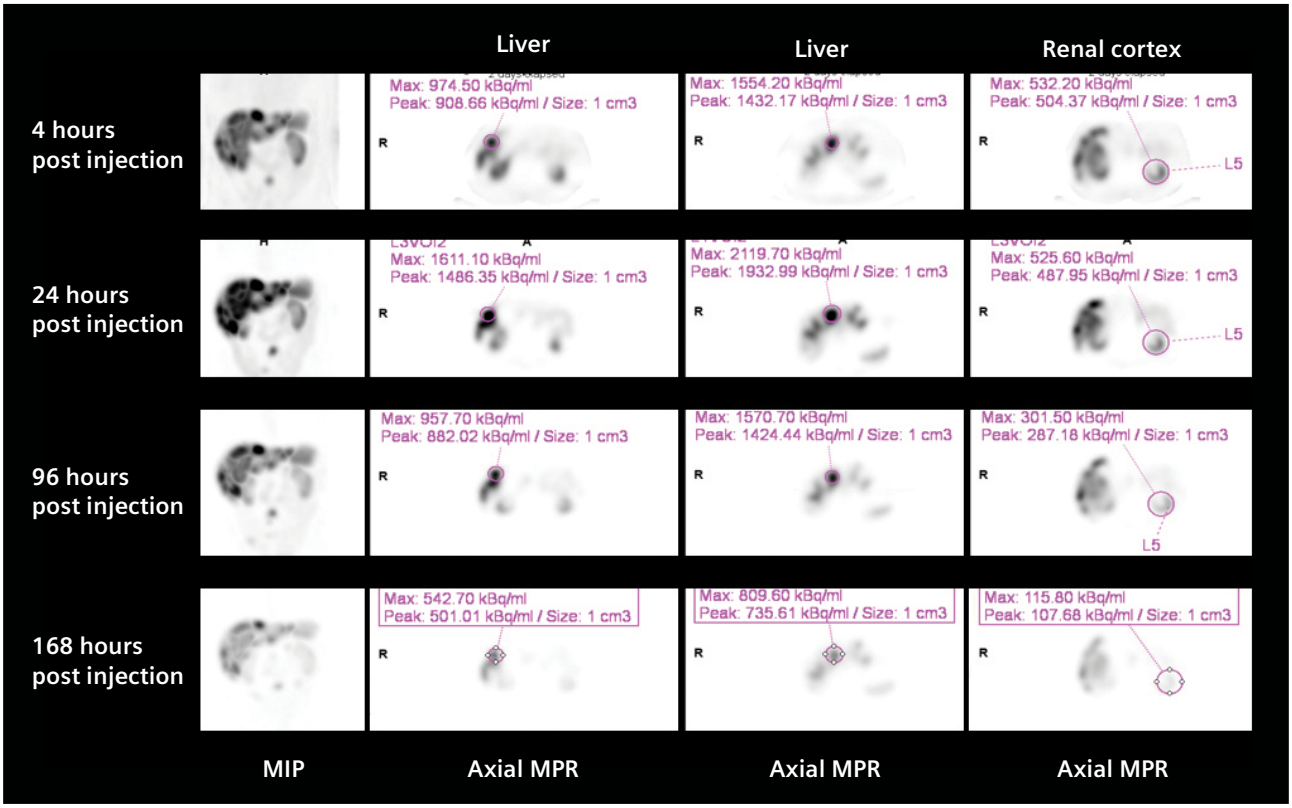

3 **Sequential SPECT images demonstrate absolute tracer concentration obtained from xSPECT Quant reconstructions (128 x 128 matrix, xSPECTEM 24i4s) performed from sequential SPECT/CT data. Maximum and average tracer concentration in kBq/ml within 2 liver metastases and the renal cortex are displayed. Tracer concentration of liver metastases reaches a maximum at 24 hours with subsequent slow washout. Renal cortical tracer concentration is highest at 4 hours and then shows progressive reduction.**

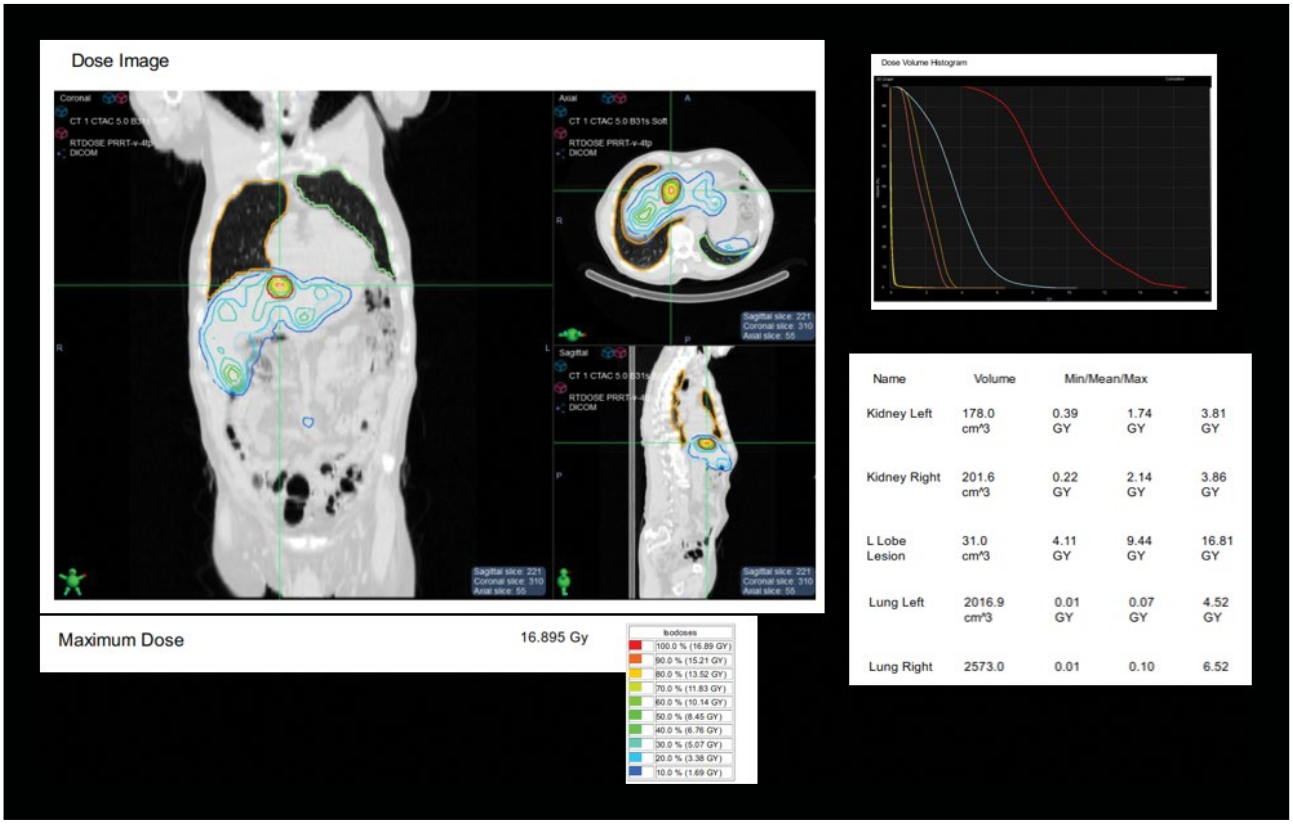

4 **Isodose lines show high dose associated with the largest liver metastases along with a dose volume histogram displaying absorbed dose values in lesions and critical organs. Dosimetry results for the largest liver lesion show the liver metastases with the maximum absorbed dose of 16.8 Gy with the mean dose being 9.4 Gy. The kidneys show low levels of renal cortical absorbed dose with a mean renal dose of 1.74 Gy for the left kidney and 2.14 Gy for the right kidney.**

Discussion

In this clinical case example, xSPECT Quant reconstructions from the sequential SPECT/CT data enabled the evaluation of absolute tracer concentration. This enabled a standalone dosimetry software to load the quantitative data and seamlessly co-register the SPECT and CT as well as the SPECT/CT images across multiple timepoints to calculate TACs for every voxel for 3D voxel-based dosimetry.

The resultant images with isodose lines visualized on CT images, as well as dose volume histograms, show high maximum and mean absorbed dose to the liver lesion. The renal and lung dose is low, which ensures the possibility of multiple therapy cycles in this patient. Assuming a cumulative renal absorbed dose threshold of 23 Gy, there is a possibility of more than 6 cycles of therapy in this patient with the assumption that renal dose will remain in the same range for subsequent therapies. This assumption may not apply since tumor shrinkage and decrease in uptake following response to radionuclide therapy may lead to higher levels of tracer clearance and retention in the renal cortex, ultimately leading to a higher absorbed dose in subsequent studies. Thus, sequential SPECT/CT for subsequent therapy cycles is also important for proper management of this patient.

xSPECT Quant enables accurate, reproducible quantification of ^{177}Lu-DOTATATE concentration within lesions and critical organs due to NIST-traceable, source-based system calibration, CT attenuation correction (CTAC), scatter correction, as well as corrections for detector deflection and other variables. Absolute tracer concentration in SPECT datasets using xSPECT Quant can be intrinsically read by third-party dosimetry software without the need for any additional calibration factor for dosimetry calculation. In this patient, the mean absorbed dose to the largest liver lesion (9.4 Gy) is comparable to values obtained from other similar studies. Kairemo et al performed 3D voxel-based dosimetry using sequential SPECT/CT following 7.4 GBq (200 mCi) dose of ^{177}Lu DOTATATE and obtained tumor doses, which varied from 2-10 Gy, while renal dose varied from 3-12 Gy.[1]

Conclusion

This case demonstrates the value of using xSPECT Quant for the reproducible quantification of tracer concentration in SPECT/CT, which is instrumental for accurate dosimetry. Additionally, the high-quality, thin-slice, low-dose CT from Symbia Pro.specta enabled accurate organ volume segmentation in order to generate organ-dose estimates, which is key in guiding the feasibility of additional radiopharmaceutical or external beam treatments. ●

The outcomes achieved by the Siemens Healthineers customers described herein were achieved in the customer's unique setting. Since there is no "typical" hospital and many variables exist (eg, hospital size, case mix, level of IT adoption) there can be no guarantee that others will achieve the same results.

Symbia Pro.specta is not commercially available in all countries. Future availability cannot be guaranteed. Please contact your local Siemens Healthineers organization for further details.

Velocity™ research dosimetry software for ^{177}Lu is not recognized by the US FDA as being safe and effective and Siemens Healthineers does not make any claims regarding its use. Due to regulatory reasons, its future availability cannot be guaranteed. Please contact your local Siemens Healthineers organization for further details.

Examination protocol

Scanner: Symbia Pro.specta

SPECT	
Injected dose	7.7 GBq (200 mCi) ^{177}Lu DOTATATE
Acquisition	2 bed positions/60 stops per detector, 20 seconds per stop
Image reconstruction	128 x 128 matrix, xSPECTEM 24i4s

CT	
Tube voltage	130 kV
Tube current	40 ref mAs
Slice collimation	32 x 0.7 mm
Slick thickness	4 mm

References

[1] Kairemo K, Kangasmäki A. 4D SPECT/CT acquisition for 3D dose calculation and dose planning in (177)Lu-peptide receptor radionuclide therapy: applications for clinical routine. *Recent Results Cancer Res.* 2013;194:537-50. doi:10.1007/978-3-642-27994-2_31.

^{99m}Tc MDP SPECT/CT imaging in the evaluation of mandibular osteomyelitis severity

By Partha Ghosh, MD, Siemens Healthineers, Hoffman Estates, IL, USA
Data and images courtesy of Chiba Aoba Municipal Hospital, Chiba, Japan

History

A 67-year-old female reported chronic pain and limited movement in her right temporo-mandibular joint along with difficulty opening her jaw.

Clinical examination showed ankylosis of the right-mandibular joint with extremely restricted movement, suggesting that surgical replacement of the affected mandible with a prosthesis may be difficult.

A ^{99m}Tc MDP bone scintigraphy with whole-body planar and SPECT/CT of the head-and-neck region was performed to delineate the extent of mandibular pathology.

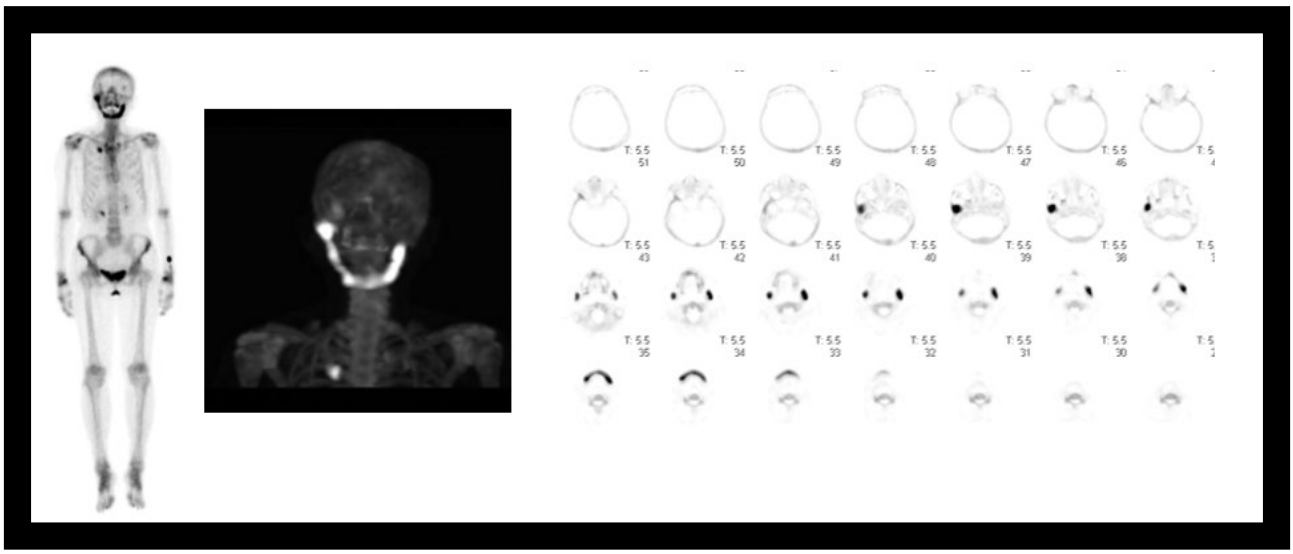

1 **Whole-body planar, SPECT MIP, and axial sections of the ^{99m}Tc MDP bone study show intense hypermetabolism in the mandible, especially in the right mandibular condylar process. The right mandibular ramus and body also show a moderate increase in uptake, while the body and part of the ramus on the left side of the mandible reflect intense uptake. The left condylar process is free of any hypermetabolism. MIP and axial slices of the SPECT study indicate relative similarity in uptake intensity in the right mandibular condylar process and the left ramus.**

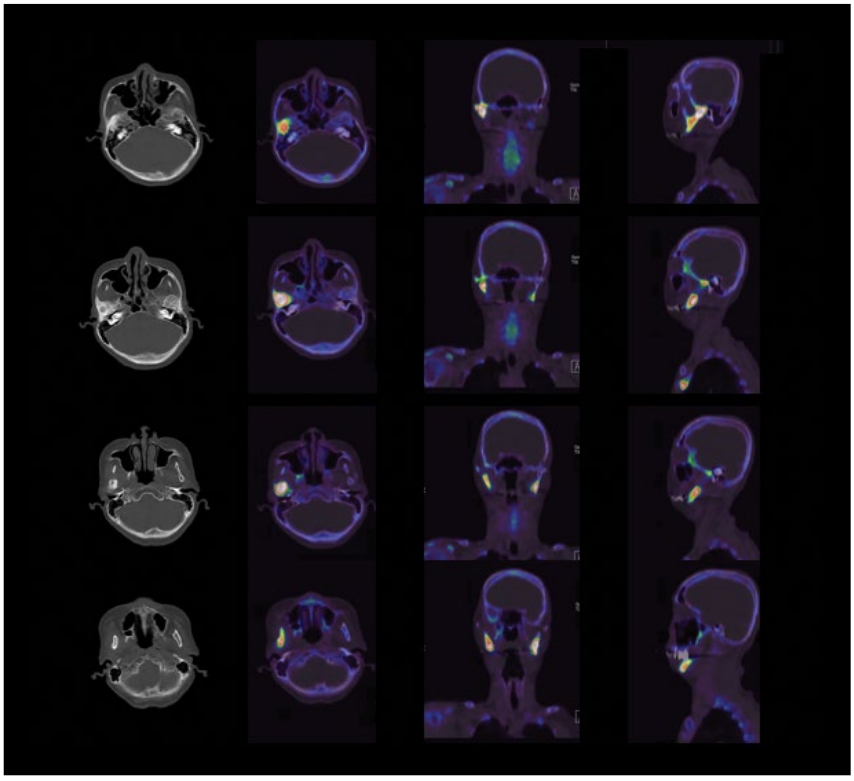

2 **Axial CT and fused SPECT/CT images in different orientations show intense sclerosis involving the right mandibular condylar process with corresponding intense hypermetabolism in the condyle as well as the adjacent ramus correlating with ankylosis of the right temporo-mandibular joint. The fused images also show intense hypermetabolism in the right as well as the left mandibular ramus.**

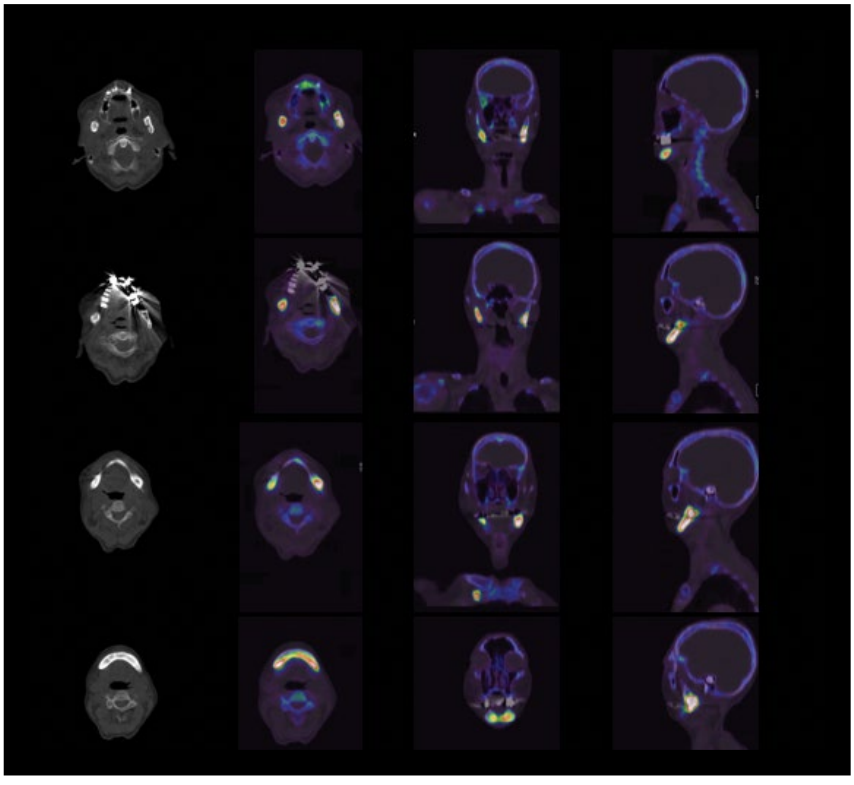

3 **Axial CT slices and fused SPECT/CT slices in various orientations show sclerosis within the ramus and the body of the right and left sides of the mandible with corresponding hypermetabolism, suggesting involvement of the entire mandible except for the left condylar process.**

As indicated in Figures 1-3, the initial SPECT/CT study showed severe sclerosis and hypermetabolism in the right mandibular condylar process with ankylosis of the right mandibular joint along with involvement of the entire ramus and body of the right and the left mandible. Both the sclerosis and hypermetabolism were particularly high and of similar intensity in the right condylar process and left ramus, suggesting two foci of particular intensity in these areas with a lower level of involvement in the rest of the mandibular body. The sparing of the left mandibular condylar process and the left temporo-mandibular joint of any pathology is clearly defined in the MIP and the fused images.

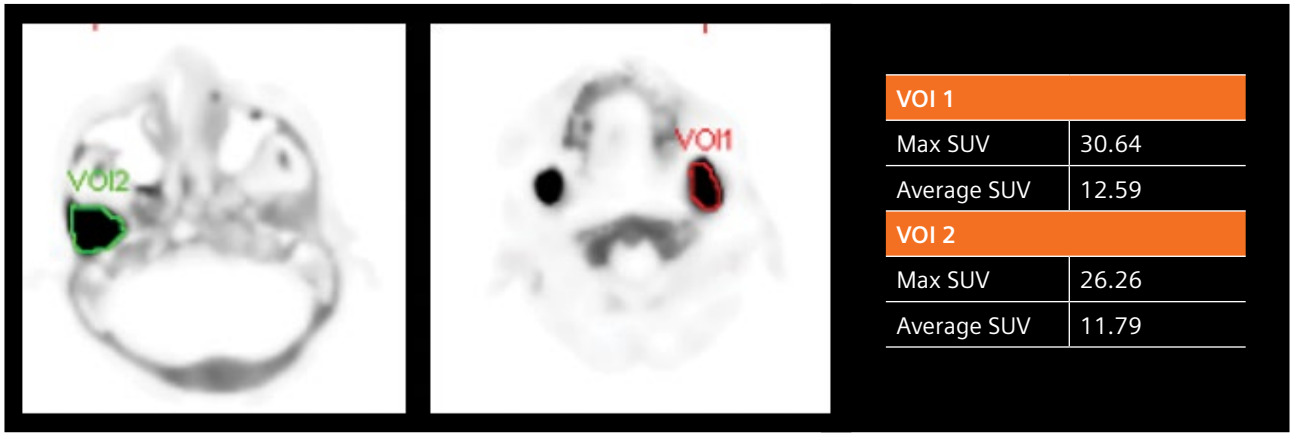

VOI 1	
Max SUV	30.64
Average SUV	12.59
VOI 2	
Max SUV	26.26
Average SUV	11.79

4 SUV estimation from xSPECT Quant denotes an SUV_{max} of 30.6 in the right mandibular condyle (Vol 2-Green) and an SUV_{max} of 26.2 in the left ramus (Vol 1-Red). The quantitative SPECT/CT enables the evaluation of SUV_{max} and SUV_{peak} to establish a quantitative benchmark for subsequent follow-up.

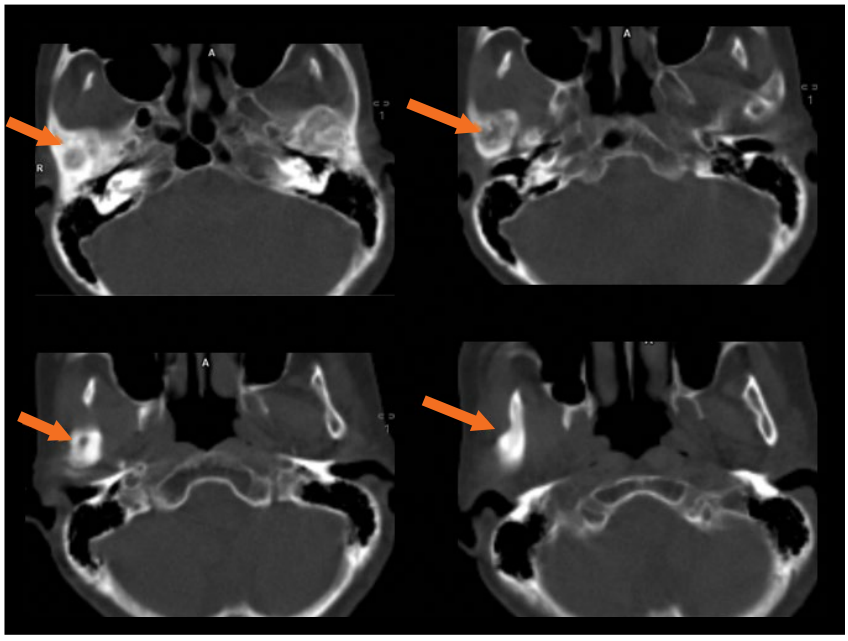

5 The zoomed image of the CT axial slices through the mandibular condylar process and the upper part of the mandibular ramus shows osteosclerosis, periosteal, and cortical bone thickening as well as perforations or breakage of the cortical bone at some points in the right and the left mandibular ramus. These features suggest the possibility of osteonecrosis or osteomyelitis of the mandible.

Findings

The SPECT/CT findings show typical CT changes of osteosclerosis, periosteal, and cortical bone thickening, as well as an intense and variegated hypermetabolism in the mandible with particularly intense foci in the right mandibular condylar process; in addition, the ankylosis of the right mandibular joint along with an intense hypermetabolism and sclerosis in the left mandibular ramus, suggest the possibility of severe and diffuse mandibular osteomyelitis. This may be due to a gingival infective foci or osteomyelitis secondary to a mandibular osteonecrosis, which could be related to diphosphonate use. In review of the age and gender of the patient (67-year-old female), the possibility of mandibular osteonecrosis secondary to diphosphonate use is deemed a distinct possibility and needs to be ruled out by conducting a thorough assessment of her medication history. The patient was treated conservatively with antibiotics but continued to display symptoms of pain and extremely restricted jaw movement. A $^{Ga}67$ scintigraphy conducted two years prior showed limited active osteomyelitis (right mandibular joint; left mandibular superior branch), ruling out multiple myeloma.

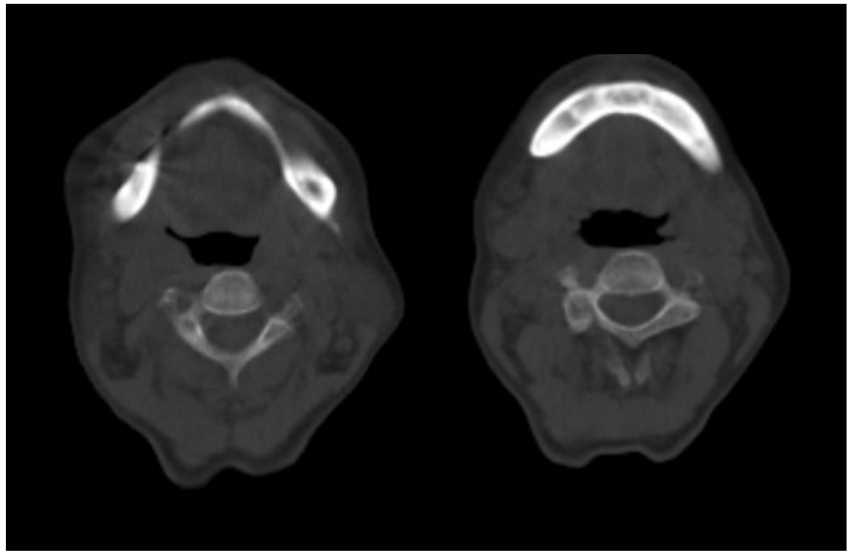

6 **The lower part of the ramus and the body of the mandible visualize osteosclerosis and cortical bone thickening, reflecting osteonecrosis or osteomyelitis.**

Two years following the initial $^{Ga}67$ scintigraphy, the patient underwent a ^{99m}Tc MDP SPECT/CT study on a Symbia Intevo™ scanner equipped with xSPECT Bone™ and xSPECT Quant™ to assess the morphological and metabolic change to the mandibular osteomyelitic process. The study was performed 3 hours following an intravenous IV injection of 23.7 mCi (878.7 MBq). A whole-body planar study was performed followed by a SPECT/CT. Additionally, xSPECT Bone and xSPECT Quant reconstructions were performed and fused with CT for evaluation.

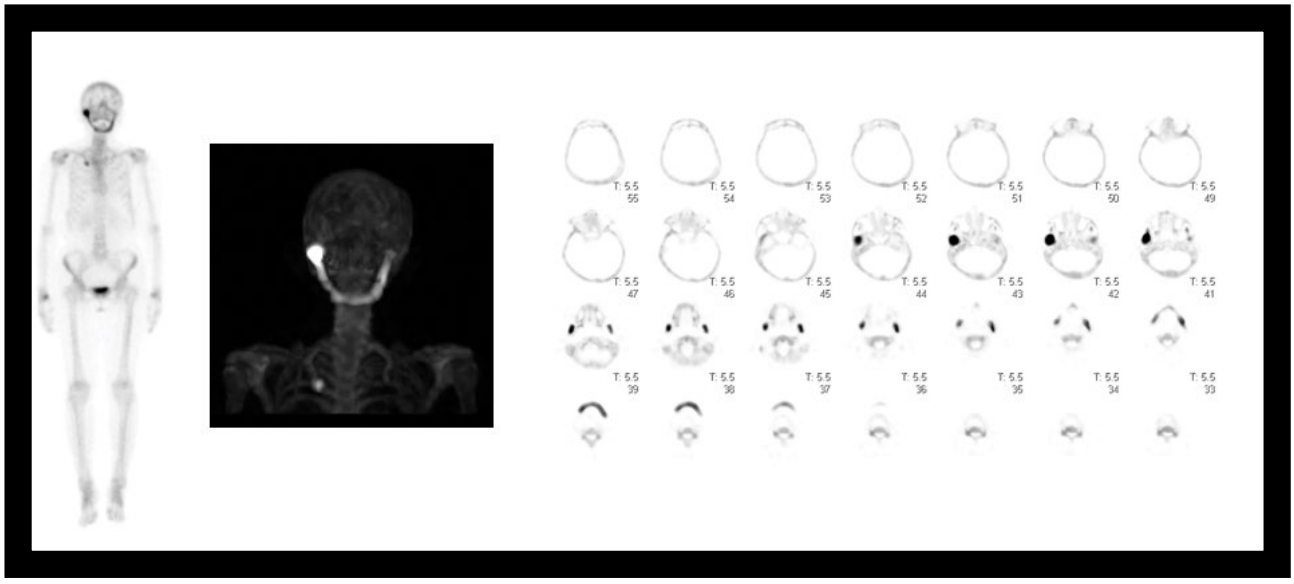

7 **Whole-body planar, MIP, and axial slices of the SPECT study reveal intense uptake in the right mandibular condylar process with lower intensity of uptake in the right and left ramus in addition to the body. The left mandibular condyle is free of any hypermetabolism.**

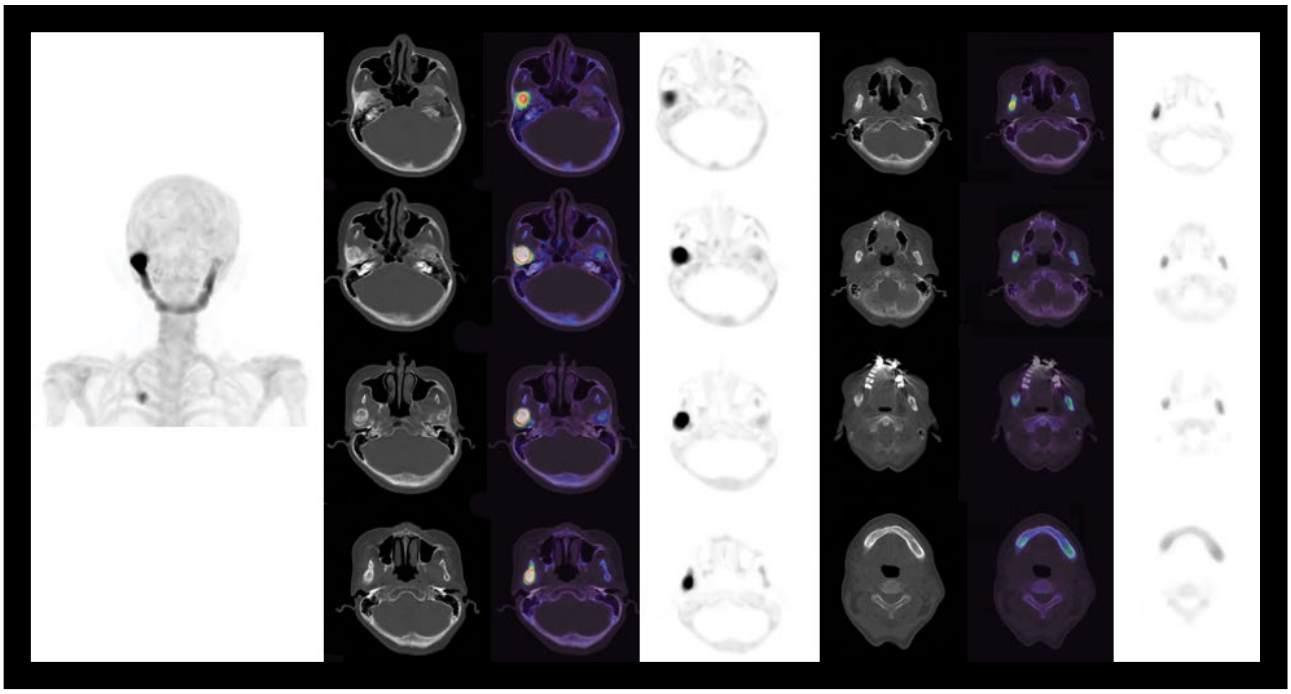

8 MIP, xSPECT Bone, CT, and fused SPECT/CT axial slices show intense uptake in the right mandibular condylar process comparable to the initial study but with slightly lower uptake intensity in the rest of the mandible, especially in the left ramus. The level of osteosclerosis remains similar to that of the initial study.

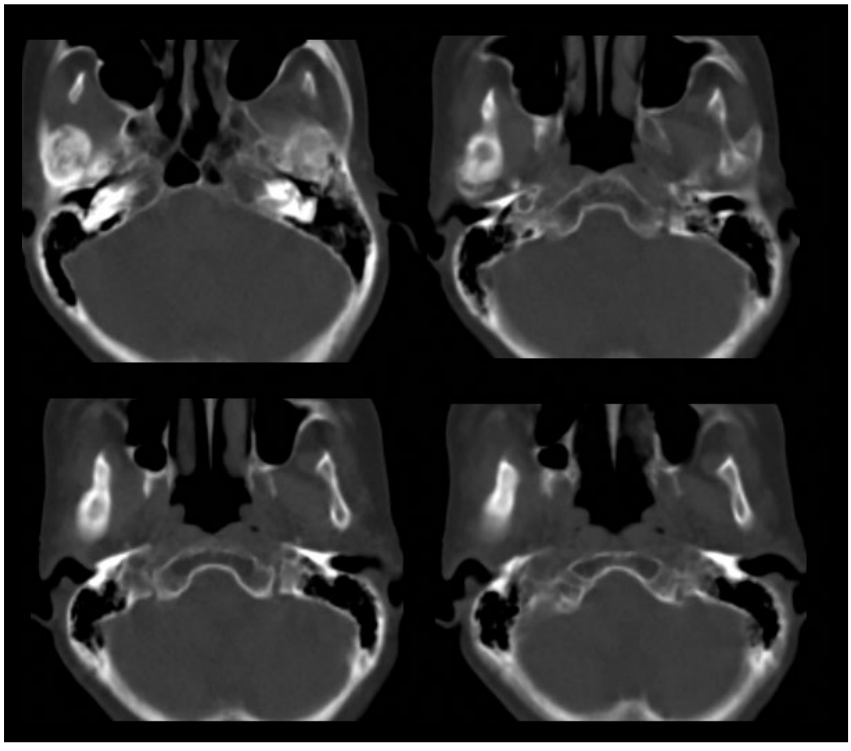

9 The zoomed CT images from the follow-up study also show osteosclerosis with small focal areas of osteolysis along with cortical and periosteal thickening and cortical perforation in the right mandibular condylar process, as well as the adjacent right and left mandibular ramus. The sclerosis intensity is similar to that of the initial study.

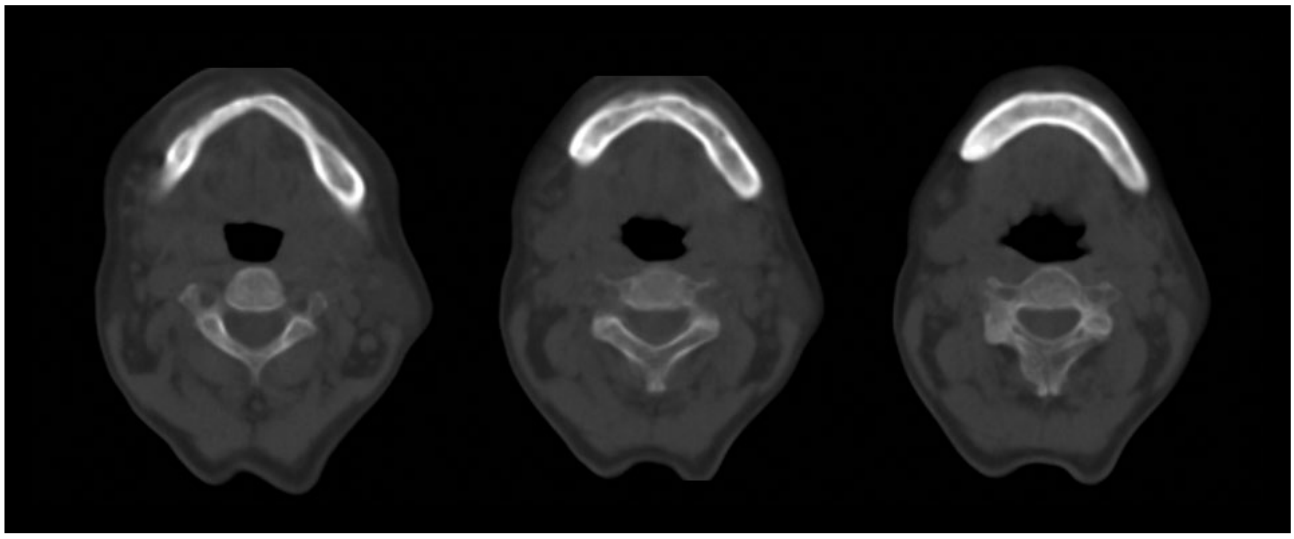

10 Axial slices through the body of the mandible show focal sclerosis, cortical bone thickening, periosteal thickening, and cortical perforations typical of mandibular osteomyelitis.

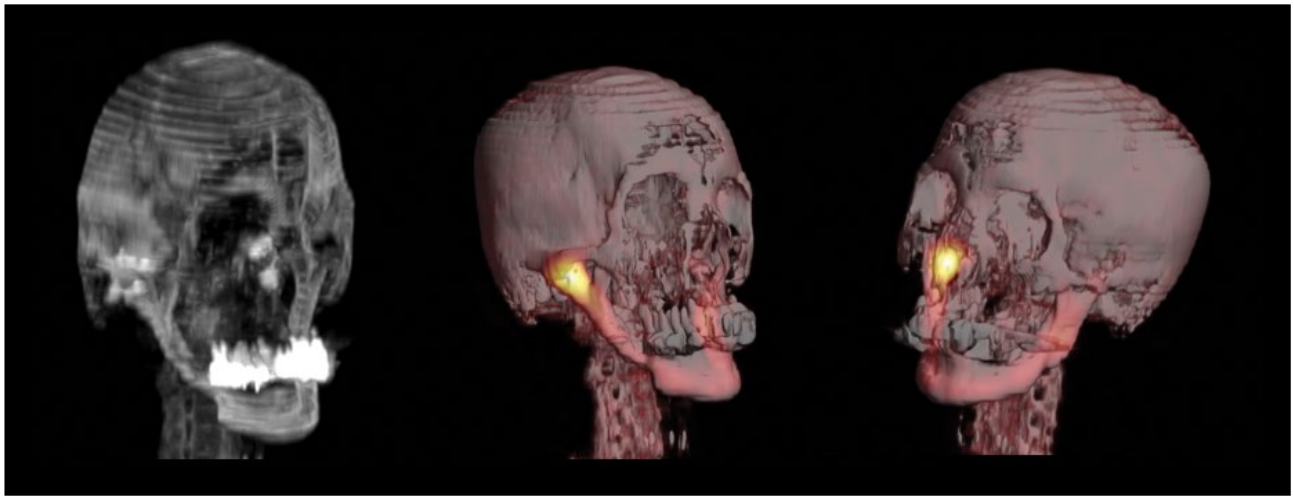

11 CT MIP as well as volume rendering of fused SPECT/CT reveal sclerosis with corresponding intense hypermetabolism in the right mandibular condylar process and the right temporo-mandibular joint. The ramus and body of the mandible highlight cortical sclerosis but with lesser extent of hypermetabolism. The dental implants in the upper jaw cause beam-hardening artifacts in the CT, impacting the visualization of parts of the mandibular ramus.

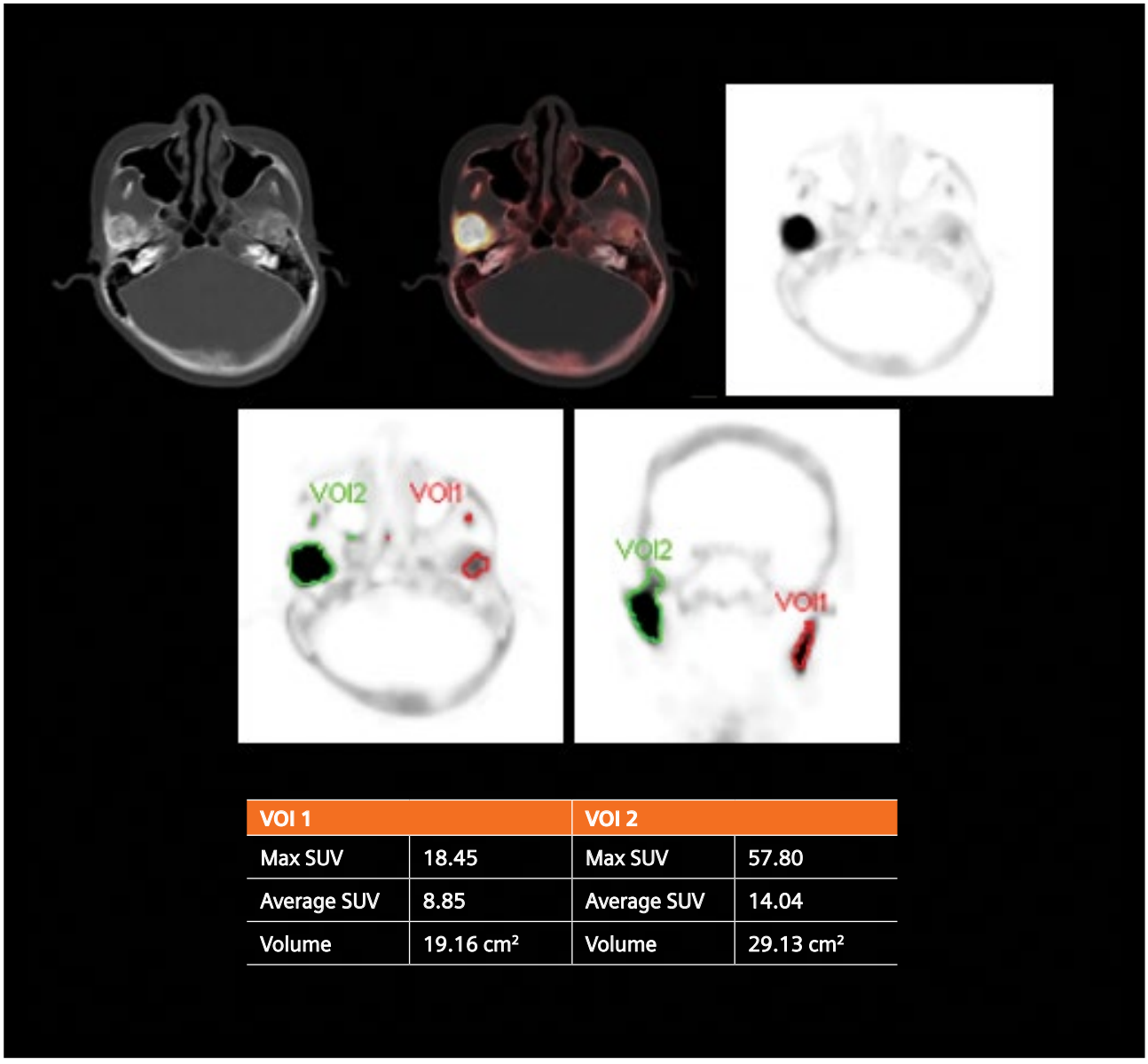

VOI 1		VOI 2	
Max SUV	18.45	Max SUV	57.80
Average SUV	8.85	Average SUV	14.04
Volume	19.16 cm²	Volume	29.13 cm²

12 **xSPECT Quant-based SPECT/CT quantification shows SUV_{max} in the right mandibular condylar process (Vol 2-Green) to be 57.8 and the left mandibular ramus (Vol 1-Red) to be 18.4.**

Although the visual impression of the sequential SPECT suggests a resolution of the intensity of uptake in the left ramus—including the continuation of similar hypermetabolism levels in the right mandibular condylar process—the xSPECT Quant quantitative evaluation confirms the significant increase in hypermetabolism in the right mandibular condyle in addition to and the decrease in left ramus uptake. Likewise, the follow-up SPECT suggests a resolution of the intensity of uptake in the left ramus—including the continuation of similar hypermetabolism levels in the right mandibular condylar process. However, the xSPECT Quant quantitative evaluation confirms the significant increase in hypermetabolism in the right mandibular condyle. The decrease in the left ramus reflects a variegated response to antibiotic therapy with complicating processes of ankylosis in the right mandibular joint, which may further increase the osteosclerotic and osteolytic processes, leading to higher metabolism.

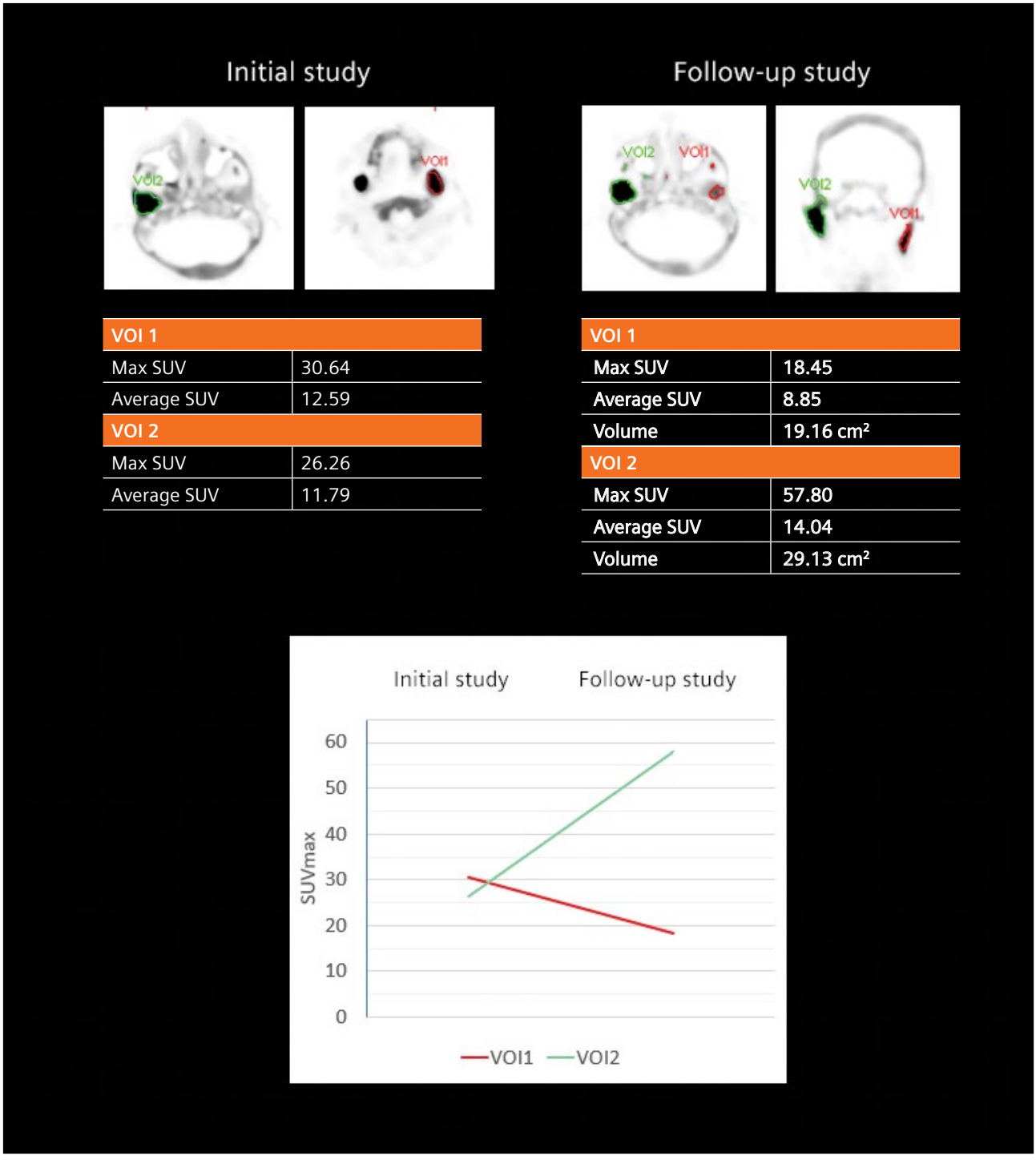

VOI 1	
Max SUV	30.64
Average SUV	12.59
VOI 2	
Max SUV	26.26
Average SUV	11.79

VOI 1	
Max SUV	18.45
Average SUV	8.85
Volume	19.16 cm²
VOI 2	
Max SUV	57.80
Average SUV	14.04
Volume	29.13 cm²

13 **The comparison of SUV_{max} between the initial and follow-up xSPECT Quant studies shows a significant increase in SUV_{max} in the right mandibular condylar process pathology. This significant increase from 26.2 to 57.8 suggests advanced severity of the mandibular osteomyelitis with a higher hypermetabolism reflecting advanced ankylosis and sclerosis. However, the hypermetabolic area of the osteomyelitis in the left mandibular ramus shows a decrease in SUV_{max} from 30.5 to 18.4—which is also reflected in the visual intensity of uptake in the left mandibular ramus—suggesting a partial resolution of the osteomyelitic process in that segment of the mandible. The SUV_{max} trend chart also reflects the differential response of SUV_{max} in two different mandibular zones.**

Discussion

Mandibular osteomyelitis may be caused by bacterial infections of the teeth and gums and may occur secondary to medication-related osteonecrosis of the mandible and maxillofacial region.[1] Medication-related osteonecrosis of the jaw is often related to bisphosphonate therapy for osteoporosis in the elderly.

In this patient, the severity of osteomyelitis was advanced in the right mandibular condylar process with gross sclerosis and fibrosis with ankylosis of the right temporo-mandibular joint. However, the osteomyelitis process also spread to the right mandibular ramus and body and also to the left body and ramus, thereby involving nearly the entire mandible and sparing only the left mandibular condyle and left temporo-mandibular joint.

The CT changes of sclerosis, focal osteolysis, cortical and periosteal thickening, and cortical perforations are typical of mandibular osteomyelitis, although it is not possible to differentiate between bacterial infection-related mandibular osteomyelitis and osteomyelitis secondary to medication-related osteonecrosis of the jaw.[2] Furthermore, the CT changes are not reflective of a response of the osteomyelitic process following antibiotic therapy, since the established sclerosis is not altered with therapy.

In this context, quantitative SPECT/CT may be helpful in assessing response and progression of disease process, as evident from the SUV evaluation using sequential xSPECT Quant, which clearly shows resolution in the left ramus with progression in the right mandibular condylar process. Ogura et al performed a quantitative SPECT/CT in 9 patients with medication-related jaw osteonecrosis and 4 patients with chronic mandibular osteomyelitis. The SUV_{max} was consistently higher in chronic osteomyelitis (mean SUV_{max} 10.16) compared to that in medication-related osteonecrosis (mean SUV_{max} 5.50).[3] The estimation of total bone uptake—attained by multiplying the SUV_{mean} with the metabolic bone volume measured by the volume of interest (VOI) around the lesion—was also significantly higher in chronic osteomyelitis.

Although the current study is focused on SUV_{max} within lesions, the estimations of metabolic bone volume from the VOI may be easily obtained for calculation of total bone uptake from the xSPECT Quant data using *syngo*®.via software. This could further improve evaluation of extensive disease processes, which in this case, involves nearly the entire mandible. The severity of SUV_{max} increase in the right mandibular joint may have multi-factorial causes, including progression of the chronic osteomyelitic process and progressive ankylosis, limitation of movement, and further alteration of bone metabolism. The left ramus lesion appears to have responded to therapy, as reflected in the decrease in SUV_{max}.

Conclusion

xSPECT Quant helps provide a reproducible and automated quantitative solution for the sequential evaluation of complicated disease processes. In combination with CT changes evaluated using diagnostic CT as part of the SPECT/CT process, this offers a comprehensive assessment of mandibular osteomyelitis. ●

Examination protocol

Scanner: Symbia Intevo 6

SPECT		CT	
Injected dose	23.7 mCi (878.7 MBq) ^{99m}Tc MDP	Tube voltage	130 kV
Post-injection delay	3 hours	Tube current	13 eff mAs
Acquisition	30 stops/detector, 20 seconds/stop	Slice collimation	6 x 2 mm
		Slice thickness	5 mm
		Reconstruction kernel	B70s

The outcomes achieved by the Siemens Healthineers customers described herein were achieved in the customer's unique setting. Since there is no "typical" hospital and many variables exist (e.g. hospital size, case mix, level of IT adoption) there can be no guarantee that others will achieve the same results.

References

[1] Kato H, Uchibori M, Nakanishi Y, Kaneko A. A Case of Osteomyelitis of the Mandibular Condyle Secondary to Bisphosphonate-related Osteonecrosis of the Jaw. *Tokai J Exp Clin Med*. 2020;45(3):126-130. PMID:32901900.

[2] Malina-Altzinger J, Klaeser B, Suter VGA, Schriber M, Vollnberg B, Schaller B. Comparative evaluation of SPECT/CT and CBCT in patients with mandibular osteomyelitis and osteonecrosis. *Clin Oral Investig*. 2019;23(12):4213-422. doi:10.1007/s00784-019-02862-8.

[3] Ogura I, Kobayashi E, Nakahara K, Igarashi K, Haga-Tsujimura M, Toshima H. Quantitative SPECT/CT imaging for medication-related osteonecrosis of the jaw: a preliminary study using volume-based parameters, comparison with chronic osteomyelitis. *Ann Nucl Med*. 2019;33(10):776-782. doi:10.1007/s12149-019-01390-5.

Delineation of multivessel coronary artery disease and post-therapy stent occlusion with ^{82}Rb myocardial perfusion PET/CT and blood flow estimation

By Parthiban Arumugam, MD and Yahya Al-Najjar, MD, Manchester Royal Infirmary, Manchester, United Kingdom
Data and images courtesy of Manchester Royal Infirmary, Manchester, United Kingdom

History

A 62-year-old female presented with atypical chest pain and a history of major risk factors for coronary artery disease (CAD), including obesity (high body mass index, height of 168 cm [5'5"], and a weight of 103 kg [227 lb]), hypertension, diabetes, hyperlipidemia, and a family history of CAD.

The patient underwent a Rubidium 82 (^{82}Rb) PET/CT myocardial perfusion study on a Biograph Vision™ PET/CT system. The initial dynamic acquisition at rest was performed following ^{82}Rb infusion. Following adenosine stress infusion, the patient received a 20 mCi (740 MBq) intravenous (IV) injection of ^{82}Rb followed immediately with a 5-minute dynamic list-mode acquisition.

A low-dose CT was acquired prior to the rest image acquisition for attenuation correction (AC).

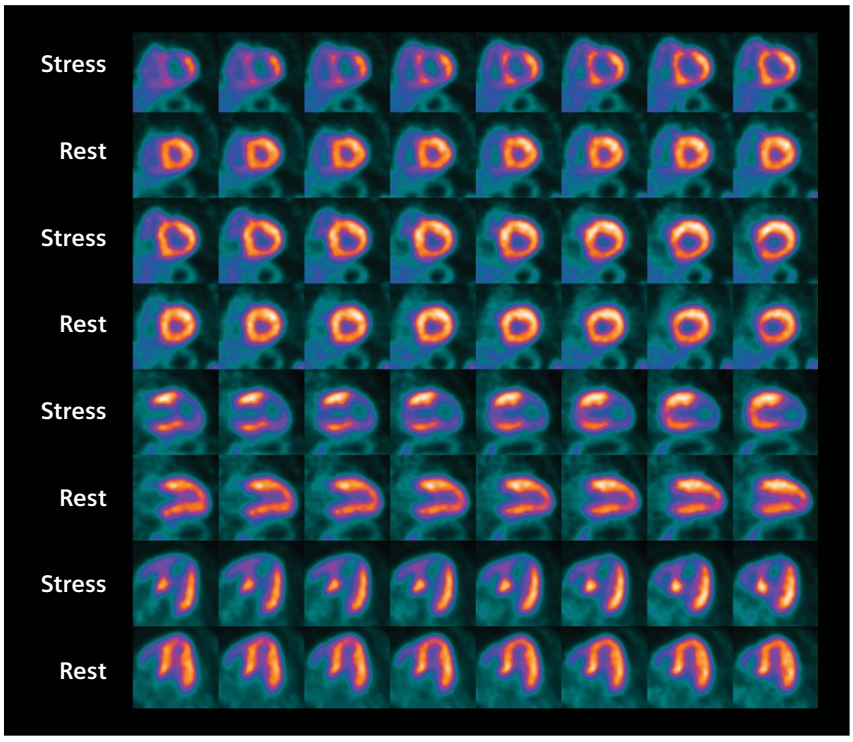

1 **Stress-rest relative perfusion PET images show severely decreased but reversible perfusion abnormality in the anterior wall, septum, and apex. The inferior wall also shows moderate reversible perfusion abnormality.**

Findings

As seen in Figure 1, the perfusion study reflects severe multivessel CAD with significant stress-induced left ventricular (LV) cavity dilation. There is severe reduction in tracer uptake at the apex and all peri-apical segments along with a mild reduction to the mid/basal inferior myocardium at peak stress. The tracer uptake at rest is within normal limits reflecting a large area of stress-inducible ischemia in the left anterior descending (LAD) territory as well as moderate ischemia in the right coronary artery (RCA) territory.

The gated PET study seen in Figure 2 demonstrates a dyskinetic septum along with a hypokinetic apex and adjoining periapical segments at peak stress. The left ventricle appears dilated with an ejection fraction of 60%. There is no regional wall motion abnormality at rest with an ejection fraction of 74%. Such severe post-stress dilatation and decrease in the left ventricular ejection fraction at peak stress reflects advanced multivessel CAD.

The myocardial blood flow (MBF) assessment using dynamic list-mode data performed on *syngo*®.via (Figure 3) shows decreased stress MBF in LAD and RCA territories with low myocardial blood flow reserve (MBFR) of 1.9 and 1.6, reflecting severe ischemia with normal resting blood flow. The left circumflex (LCX) territory shows normal stress blood flow value and normal MBFR. In view of the presence of hypertension and high resting heart rate, the MBF values were normalized to the resting heart rate of 97 beats per minute (BPM) and resting systolic blood pressure of 149 mm Hg. Polar plots of the MBF and MBFR reveal severe ischemia in the apex and peri-apical anterior wall and septum. Evaluation of the extent of stress perfusion

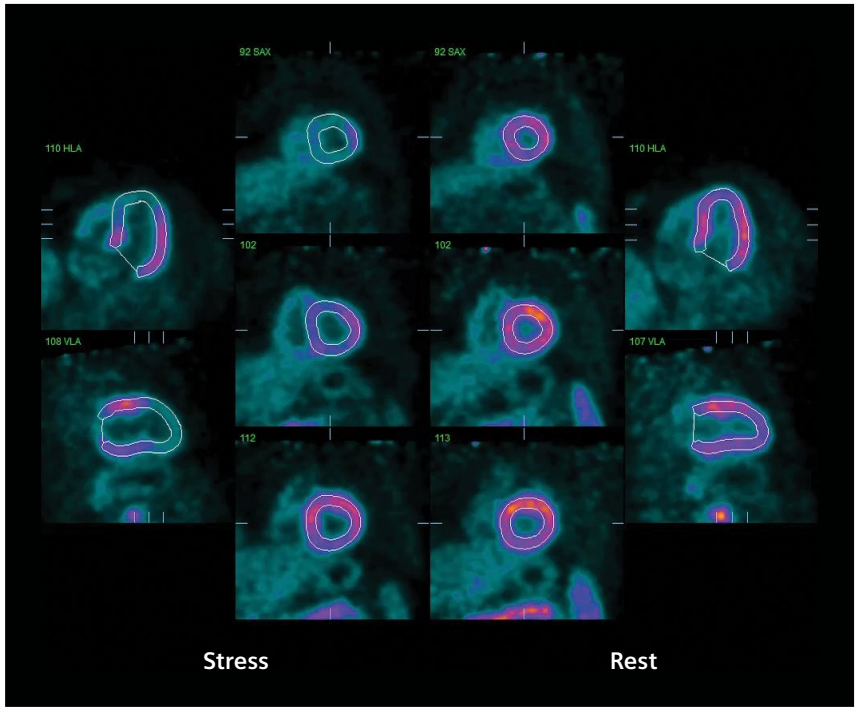

2 **The end diastolic cross section of the left ventricle at stress and rest obtained from the gated PET studies shows LV dilation at peak stress along with severe hypoperfusion in the apex, periapical region, anterior wall, septum, and the inferolateral wall. The resting images show significantly reduced LV cavity size with normalization of perfusion in the LAD and RCA territory at rest.**

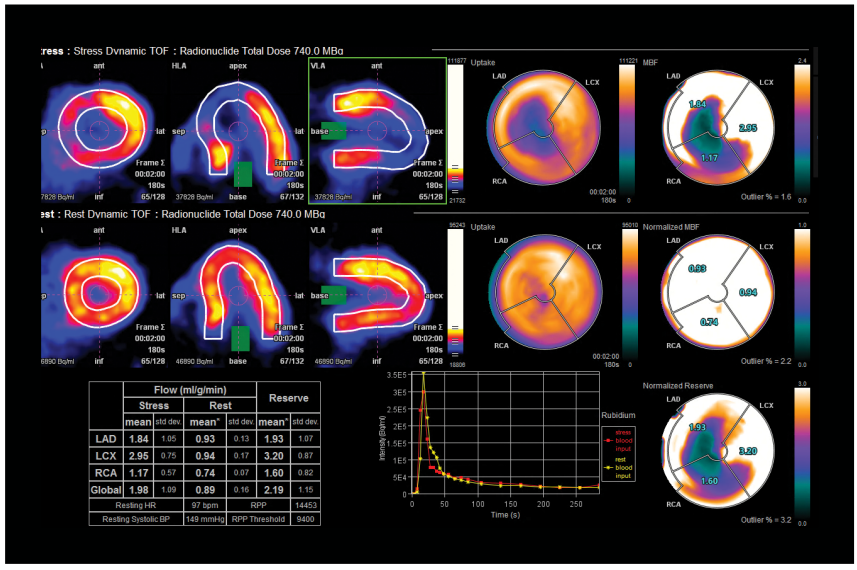

3 **MBF estimation using *syngo*.via shows severely reduced blood flow at stress in the LAD and RCA territories with normalization of blood flow at rest with decreased MBFR in both territories.**

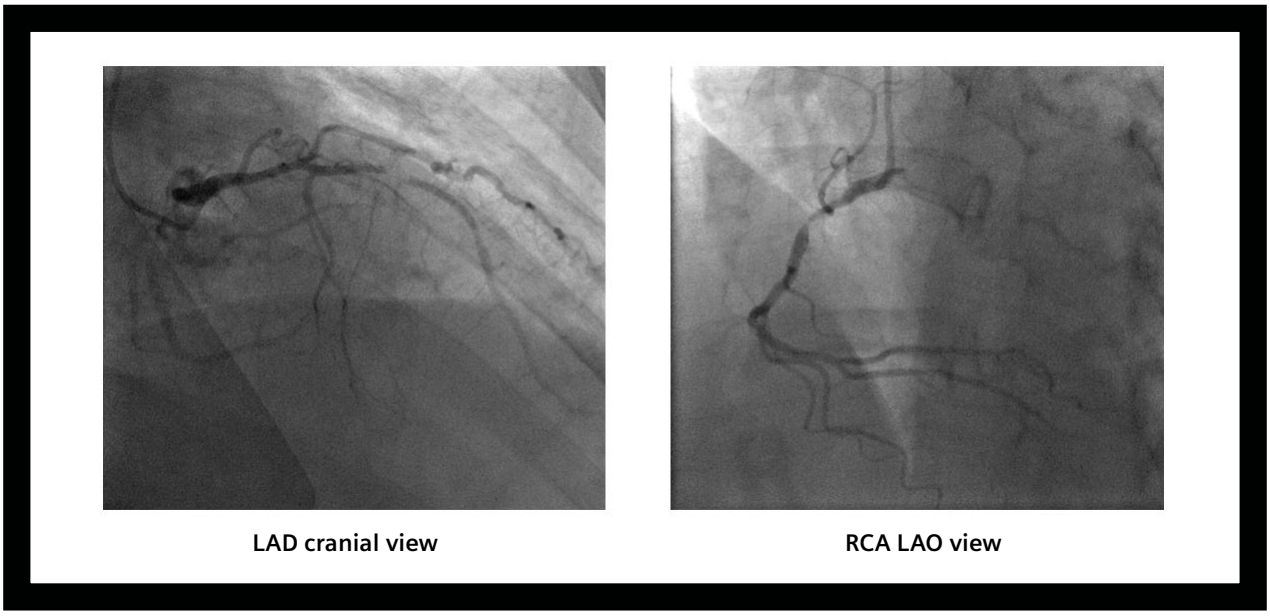

4 **Coronary angiography shows severe stenosis in the mid-LAD as well as proximal-RCA.**

defect and blood flow abnormalities was consistent with multivessel pattern of ischemia and evidence of post-ischemic stunning. Significant stress-inducible ischemia involved at least 10/20 myocardial segments with a predominant LAD distribution. Normal resting LV systolic function and uniform normal resting perfusion reflects the complete reversibility of the stress-induced perfusion defects.

The patient subsequently underwent coronary angiography.

Coronary angiography revealed severe stenosis in mid-LAD and proximal-RCA. Both lesions were subsequently treated with balloon angioplasty and stent insertion. Post-percutaneous coronary intervention (PCI) images (Figure 5) show restoration of normal vascular flow in the LAD and RCA.

As evident in Figure 6, coronary angiography demonstrated luminal irregularities in the mid-LCX artery which was identified as residual disease but not deemed severe enough for intervention with adequate contrast flow to the distal-LCX, obtuse margin 1 (OM1), and obtuse margin 2 (OM2).

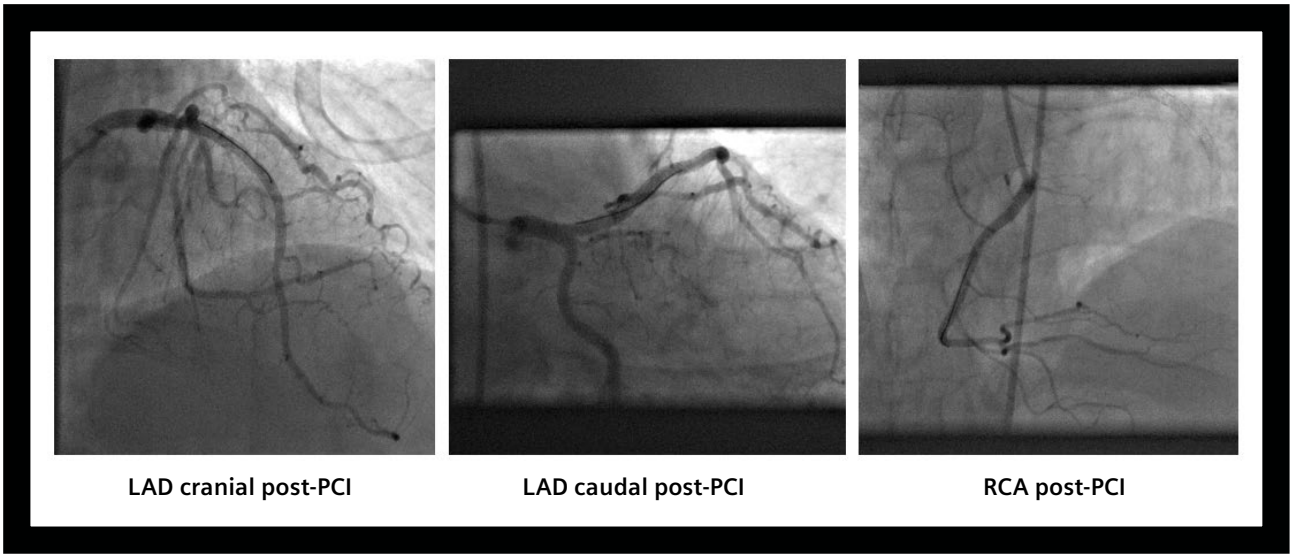

5 **The post-PCI images show guidewires across the LAD and RCA stenotic segments with normal vascular flow in both coronary vessels reflecting successful angioplasty. However, coronary angiography revealed minor residual disease in the LCX (Figure 6) which was not treated.**

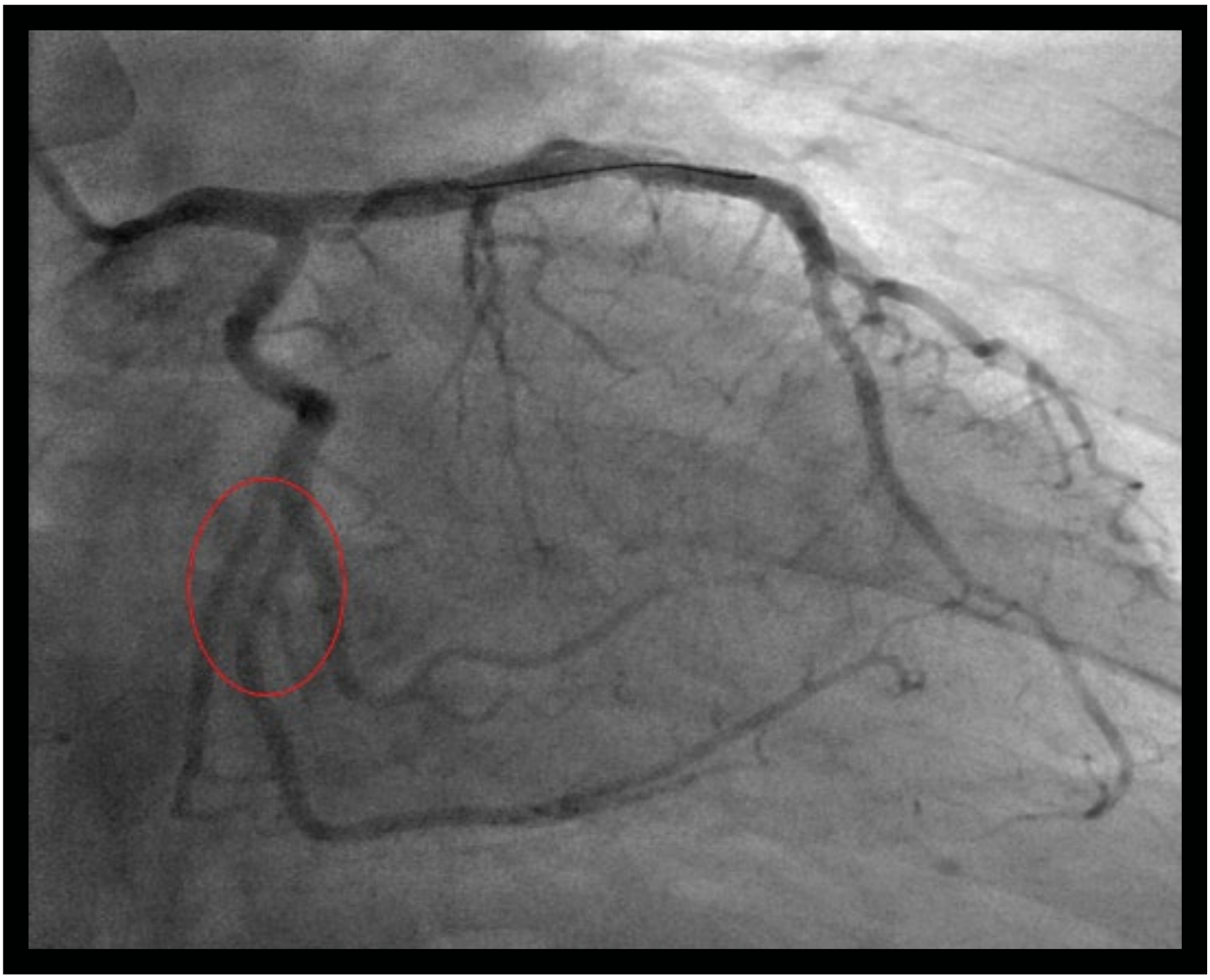

6 **Post-PCI angiography shows minor residual CAD in mid-LCX artery as evident in the luminal irregularities defined within the circle.**

Immediately following the PCI, the patient was re-admitted with hypoxemic (Type 1) respiratory failure. Lung perfusion SPECT/CT was negative for pulmonary embolism, and the serum troponin was also negative. The patient recovered following ventilatory support. However, there was another subsequent admission 6 months post-PCI with chest pain and respiratory distress. In the second instance, the serum troponin was also negative.

Due to repeated chest pain, a repeat PET/CT myocardial perfusion study was requested. The ^{82}Rb myocardial perfusion PET/CT study was performed on the Biograph Vision system with acquisition parameters similar to the initial study.

There is mild stress-induced LV cavity dilatation which reflects severe ischemia. However, the resting LV cavity size is normal.

As evident in the post-PCI PET/CT myocardial perfusion study (Figures 7-9), there is functionally significant ischemia in the inferior wall and infero-septal segment while the LAD and LCX territory shows normal stress perfusion. When compared to the previous study, there is complete resolution of LAD ischemia. However, the presence of a large perfusion defect in the inferior and inferoseptal segments suggests a new significant ischemia in the posterior descending artery (PDA) distribution (6/20 segments). LV systolic function is normal reflecting the moderate degree of ischemia at peak stress.

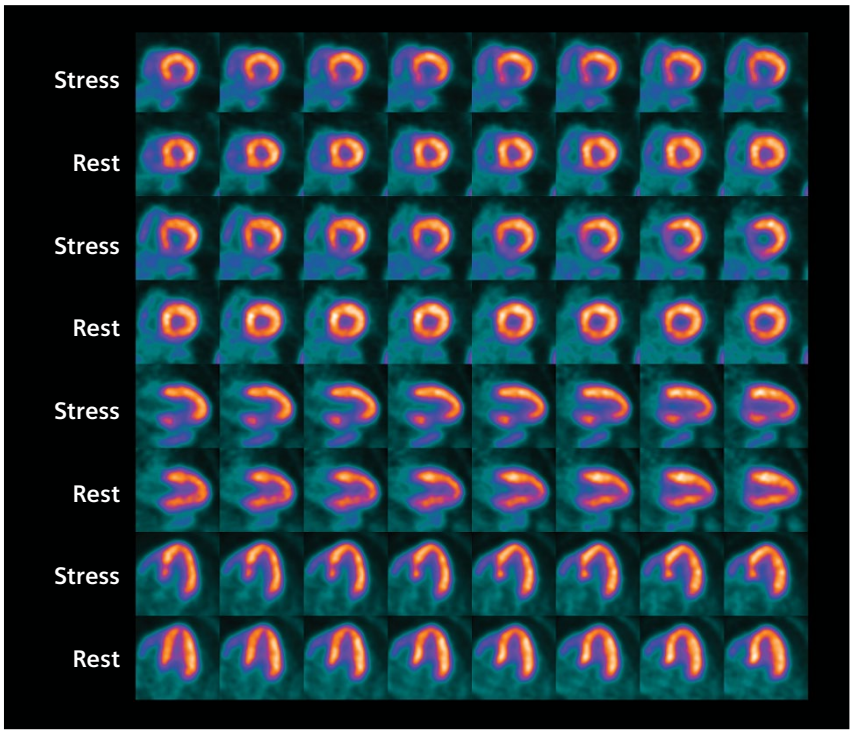

7 **Stress-rest ^{82}Rb myocardial perfusion PET images show moderate to severe reduction in tracer uptake to the mid/basal septum and inferior wall myocardium at peak stress which nearly normalizes at rest.**

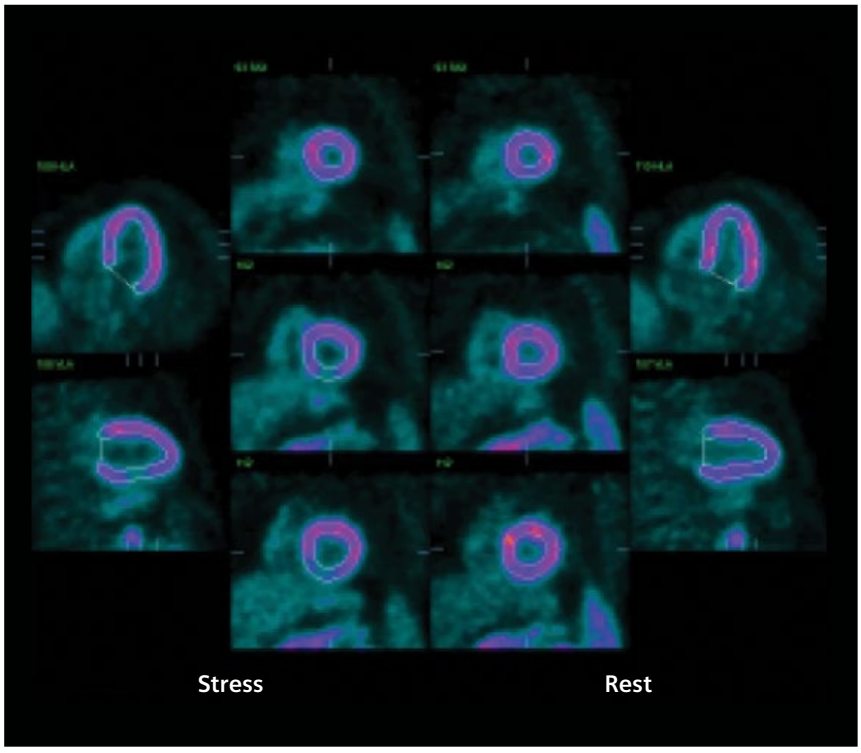

8 **The end diastolic slices from gated stress (left) and gated rest (right) acquisitions show absence of significant regional wall motion abnormality both during stress and rest. The calculated ejection fraction is within normal limits both in stress and rest.**

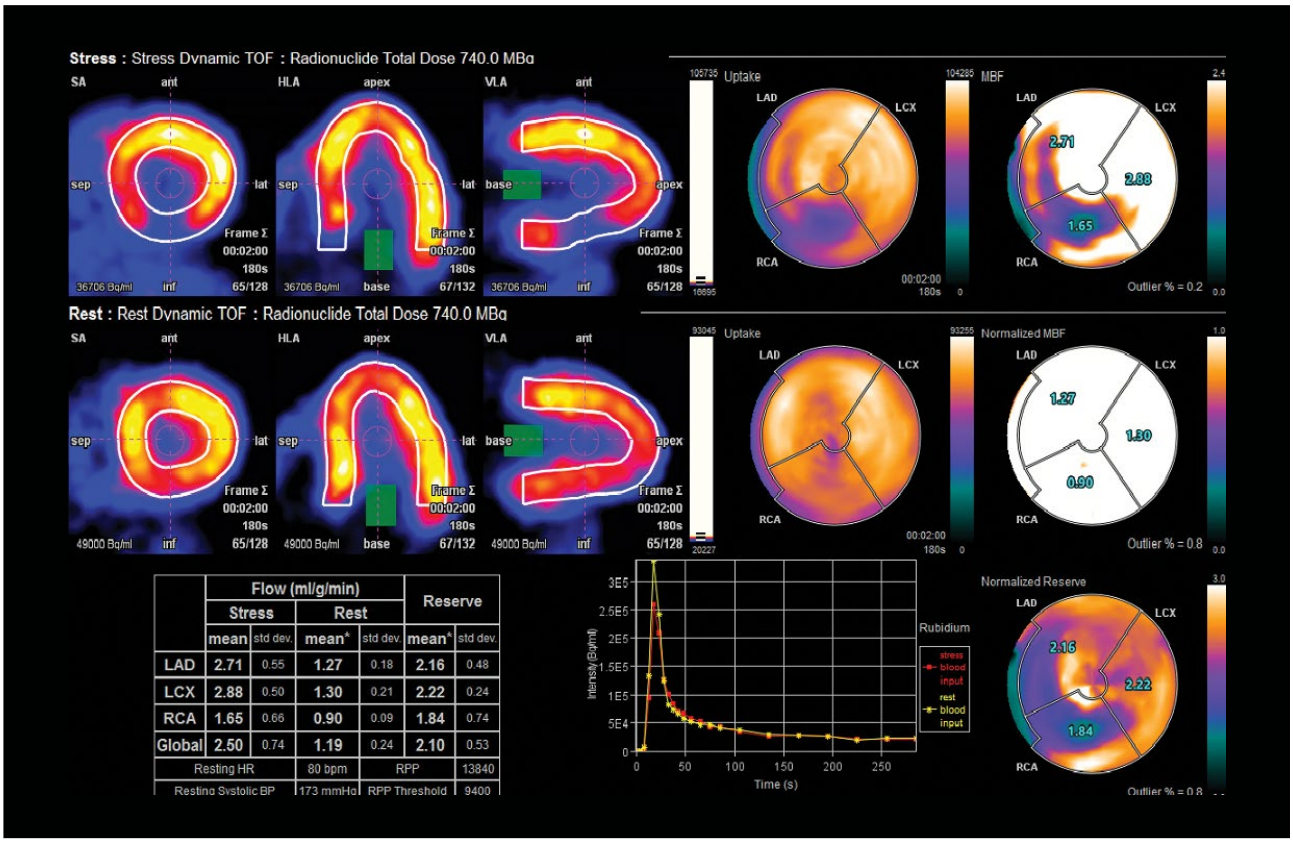

	Flow (ml/g/min)				Reserve	
	Stress		Rest			
	mean	std dev.	mean*	std dev.	mean*	std dev.
LAD	2.71	0.55	1.27	0.18	2.16	0.48
LCX	2.88	0.50	1.30	0.21	2.22	0.24
RCA	1.65	0.66	0.90	0.09	1.84	0.74
Global	2.50	0.74	1.19	0.24	2.10	0.53
Resting HR			80 bpm		RPP	13840
Resting Systolic BP			173 mmHg		RPP Threshold	9400

9 **Stress-rest MBF estimation performed on *syngo*.via shows decreased stress perfusion in the inferior wall and inferoseptal region. MBFR is also reduced in the same area. Remaining LV myocardium including the LAD and LCX territories show normal values at stress and rest with normal MBFR. Resting perfusion in the inferior wall shows normal absolute values (0.90 ml/g/min), which are significantly lower than the resting flow values in the LAD and LCX territories (1.3 ml/gm/min).**

The patient then underwent a follow-up coronary angiography.

Coronary angiography revealed complete occlusion of the RCA stent along with significant flow impairment related to the luminal irregularity in the distal-LCX, which together contribute to the reversible ischemia in the inferior wall and inferoseptal region. The lateral and postero-basal walls are normally perfused since the proximal and mid-LCX show normal luminal flow. The distal LCX irregular luminal lesion with reduced FFR of 0.6 contributes to the inferior wall ischemia while the completely occluded RCA contributes to the inferoseptal as well as the inferior wall ischemia.

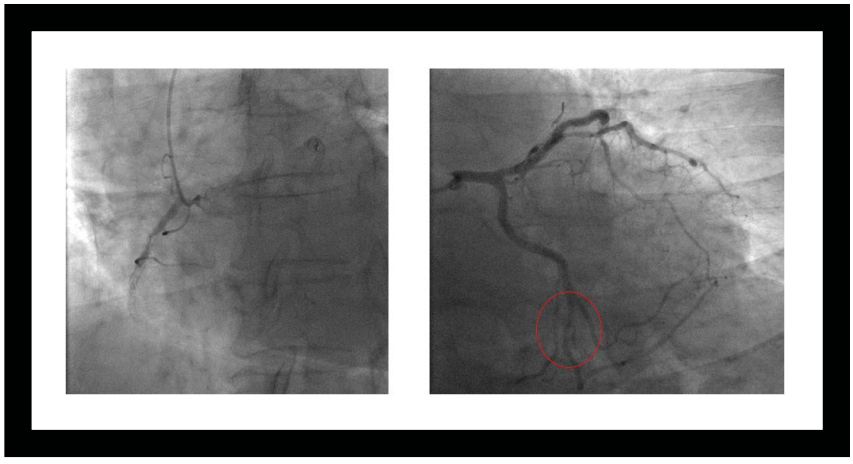

10 **Coronary angiography reflects occlusion of the RCA stent (left) along with luminal irregularities in the distal-LCX (right) with a reduced fractional flow reserve (FFR) of 0.6, which suggests significant flow impairment. In comparison to the previous coronary angiography, the luminal narrowing in the distal-LCX appears to have slightly increased.**

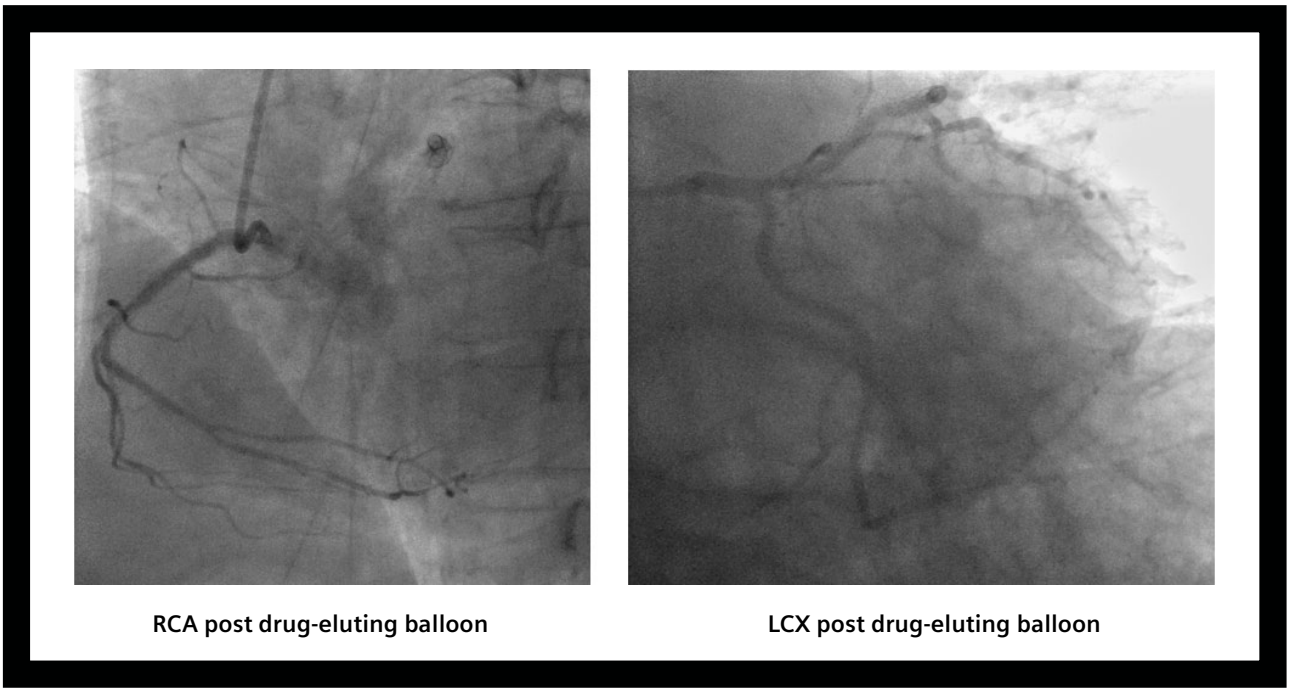

11 **The coronary angiography following the drug-eluting balloon angioplasty of the RCA and distal LCX shows normal distal flow in the RCA, PDA as well as in the distal LCX and OM1 and OM2, reflecting successful restoration of luminal flow in both coronary arteries.**

In view of the coronary angiography results, the patient underwent drug-eluting balloon angioplasty of both the RCA and distal LCX. Normal distal flow was restored in both vascular territories following the angioplasty.

Discussion

This clinical case example illustrates the value of ^{82}Rb PET/CT myocardial perfusion imaging with MBF estimation in detecting multivessel CAD and guiding therapeutic intervention as well as detecting restenosis on follow-up. The severity of the stress-induced perfusion defect in the initial study along with the reduction in absolute value of stress MBF in the affected LAD and RCA territories compared to the normal LCX territory reflects the image quality and quantification advantage of myocardial perfusion PET/CT, especially with current-generation silicon photomultiplier (SiPM) systems like Biograph Vision with excellent time-of-flight (ToF) performance, high count-rate capability, and low detector saturation.

The average LAD territory MBF was 1.84 ml/gm/min at peak stress while that of the normally perfused LCX territory was 2.95 ml/gm/min, although the resting blood flow in both territories was similar. This difference in stress MBF of nearly 40% between ischemic and normally perfused myocardium reflects the quantitative accuracy of PET blood flow estimation. Stress-induced LV dilatation and wall-motion abnormalities evident on static and gated stress PET images reflect multivessel disease while normal resting myocardial perfusion and left ventricular ejection fraction (LVEF) confirm the complete reversibility of the ischemic segments. The stress MBF in the inferior wall (RCA territory) shows further reduction compared to the LAD territory with a stress MBF value of 1.17 ml/gm/min, which reflects the severity of the hemodynamic impairment due to the RCA stenosis as compared to that of the LAD. Even resting perfusion in the RCA territory is significantly lower compared to that of the LAD, although it is within the normal range. Although MBF is impacted by multiple factors over and above stenosis severity, including the state of collateral circulation and microvascular disease, studies have shown a correlation between absolute MBF and coronary flow reserve (CFR) with stenosis severity.

In a study performing ^{82}Rb dynamic PET for MBF estimation compared with stenosis estimation by quantitative coronary angiography, 15 patients with angiographically documented CAD and 7 age-matched asymptomatic controls without CAD

risk factors were studied. Rest and stress MBF in regions subtended by vessels with < 50% stenosis was similar to that of the individuals without risk factors for CAD. MBFR was similar in the two groups (average 1.9 compared to 2.2). MBFR values were able to differentiate coronary lesions with 70% to 89% stenosis from those with 50% to 69% stenosis (average MBFR of 1 compared to 1.7 for the group with lower stenosis levels). MBF at peak stress and MBFR were inversely correlated to the percent diameter stenosis on angiography. The absolute MBF and MBFR values in the ischemic segments in the present study are comparable to that of published studies.[1]

In-stent restenosis is an established complication following coronary stenting, although the incidence is less than 10% for drug-eluting stents.[2] As in this case example, restenosis can precipitate acute ischemic episodes, including hypoxemic respiratory failure. The follow-up ^{82}Rb PET/CT myocardial perfusion study clearly demonstrates the reversible perfusion defect in inferior and inferoseptal wall, which reflected involvement of the RCA territory, more specifically the PDA distribution. The RCA territory average MBF was 1.65 ml/gm/min at peak stress, which was significantly higher than the value in the initial study. The resting RCA MBF was also higher at 0.90 ml/gm/min. The coronary angiography confirmed in-stent restenosis of the RCA along with identification of the distal LCX luminal irregularities as hemodynamically significant due to the reduced FFR of 0.6. Both of the lesions contributing to the inferior wall and inferoseptal ischemia were treated with drug-eluting balloon angioplasty, which has been shown to have a lower incidence of restenosis. The normal stress and resting LVEF, absence of stress-induced wall-motion abnormalities, and normal resting perfusion reflect the moderate nature of the ischemia and the complete reversibility of the ischemic myocardium.

Conclusion

A ^{82}Rb stress-rest PET/CT myocardial perfusion study with absolute quantification of MBF is an accurate technique for detection and characterization of myocardial ischemia in order to guide therapy as well as a follow-up procedure to detect post-PCI complications such as in-stent restenosis, stenosis progression, or development of fresh coronary stenosis. Absolute values of stress MBF, MBFR, and post-stress LV cavity dimensions also contribute to the assessment of disease severity and reversibility of ischemic segments. ●

Biograph Vision is not commercially available in all countries and its future availability cannot be guaranteed. Please contact your local Siemens Healthineers organization for further details.

Examination protocol

Scanner: Biograph Vision

PET	
Injected dose	20 mCi (740 MBq) ^{82}Rb
Post-injection delay	Immediate post-injection dynamic list-mode acquisition
Acquisition	5-minute dynamic list-mode acquisition
Scan time	5-minute dynamic rest and stress acquisition

The outcomes achieved by the Siemens Healthineers customer described herein were achieved in the customer's unique setting. Since there is no "typical" hospital and many variables exist (eg, hospital size, case mix, level of IT adoption) there can be no guarantee that others will achieve the same results.

References

[1] Anagnostopoulos C, Almonacid A, El Fakhri G, et al. Quantitative Relationship Between Coronary Vasodilator Reserve Assessed by Rubidium-82 PET Imaging and Coronary Artery Stenosis Severity. *Eur J Nucl Med Mol Imaging.* 2008;35(9):1593–1601. doi:10.1007/s00259-008-0793-2.

[2] Buccheri D, Piraino D, Andolina G, Cortese B. Understanding and managing in-stent restenosis: a review of clinical data, from pathogenesis to treatment. *J Thorac Dis.* 2016;8(10):E1150–E1162. doi:10.21037/jtd.2016.10.93.

Single-bed, whole-body ^{68}Ga DOTATATE PET/CT delineation of neuroendocrine tumor metastases

By Partha Ghosh, MD, Siemens Healthineers, Hoffman Estates, IL, USA
Data courtesy of Inselspital, Bern, Switzerland

History

A 74-year-old male with a primary duodenal neuroendocrine tumor was referred for ^{68}Ga DOTATATE PET/CT staging to evaluate suspected metastases.

One hour and 17 minutes following a 4.3 mCi (158 MBq) intravenous (IV) injection of ^{68}Ga DOTATATE, the patient underwent a 10-minute, single-bed, whole-body PET/CT acquisition on a Biograph Vision Quadra™ scanner.

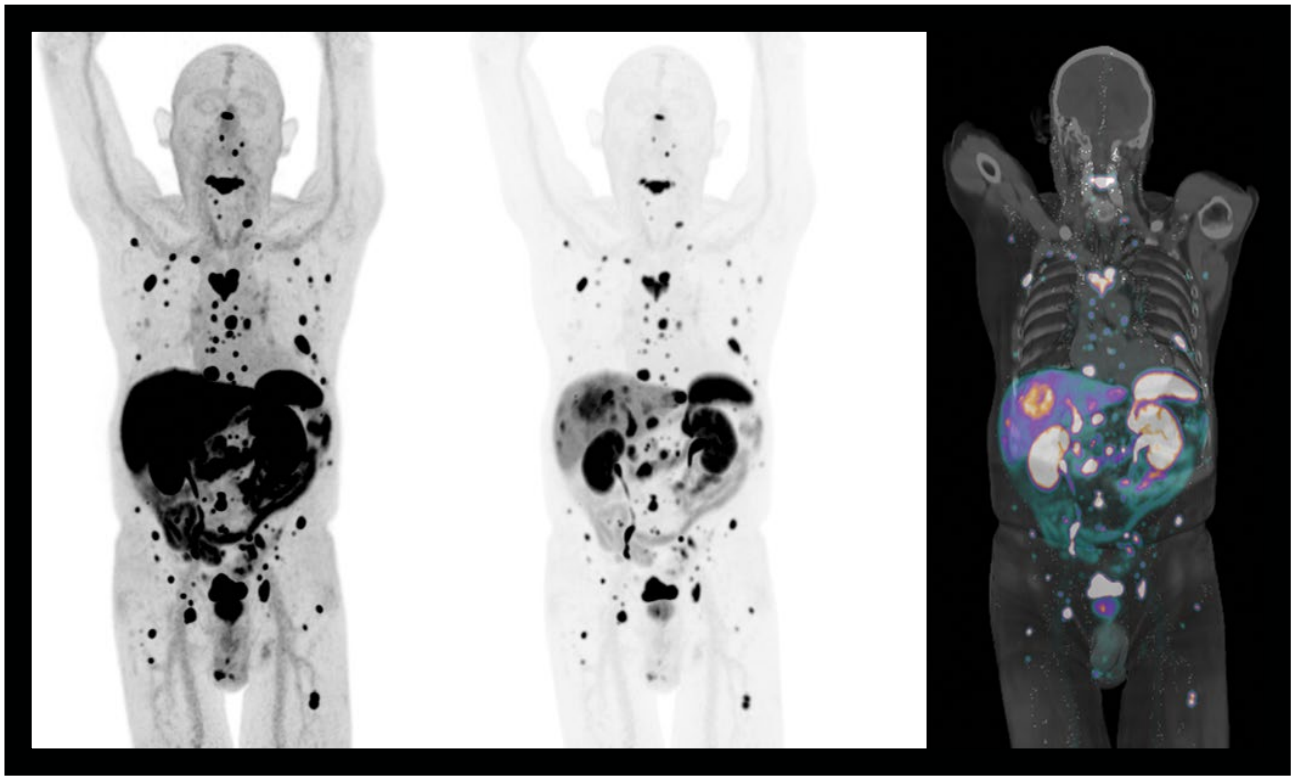

1 **Whole-body PET MIP images show extensive metastases throughout the body ranging from the vertex to the thighs, including multiple metastases in the thorax, liver, intestines, spine, pelvis, and bilateral femur. The PET MIP with a wider window setting (middle) helps differentiate between normal liver and ^{68}Ga DOTATATE-avid liver metastases. The volume-rendered PET/CT image (right) also shows extensive metastases in the bones, liver, and intestines.**

Findings

As seen in Figure 1, there are extensive metastases observed throughout the body with lesions in the bone, liver, and intestines. The physiological uptake of radionuclides in the normal liver parenchyma, spleen, kidney, ureter, bladder, bilateral adrenal glands, and pituitary gland appears within normal limits.

As observed in Figures 2 and 3, the upper- and lower-most metastatic lesions—ranging from the skull base to the thighs—are sharply defined with equally high contrast-to-background levels due to the Biograph Vision Quadra's 106 cm axial PET field of view (FoV), which enabled the single-bed, whole-body acquisition for this particular patient measuring 172 cm (5'7") in height.

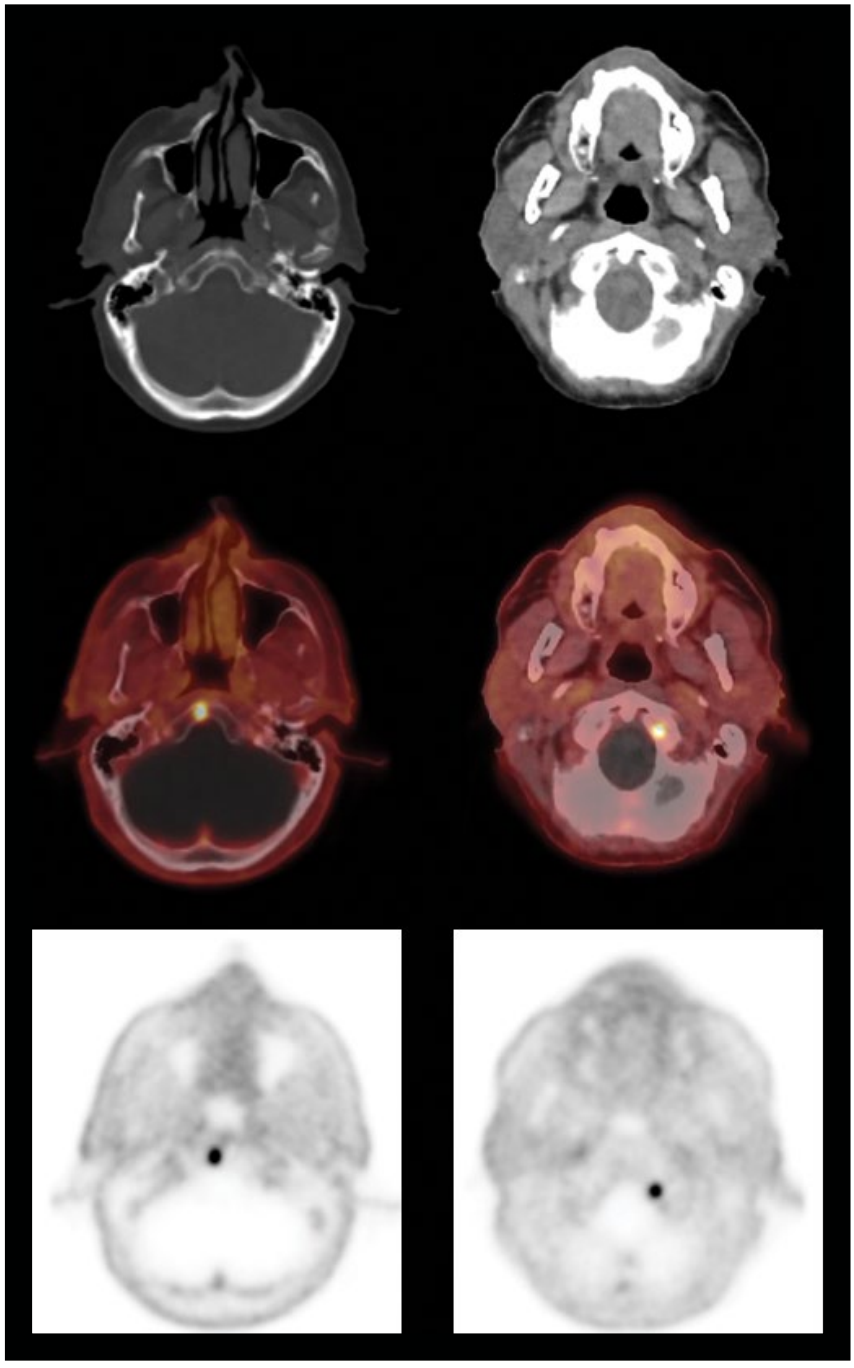

2 **Axial CT, PET/CT, and PET images show the uppermost (near vertex) small bony metastases in the skull base and the upper cervical vertebrae. These lesions are defined with a high contrast to the background similar to the rest of the body.**

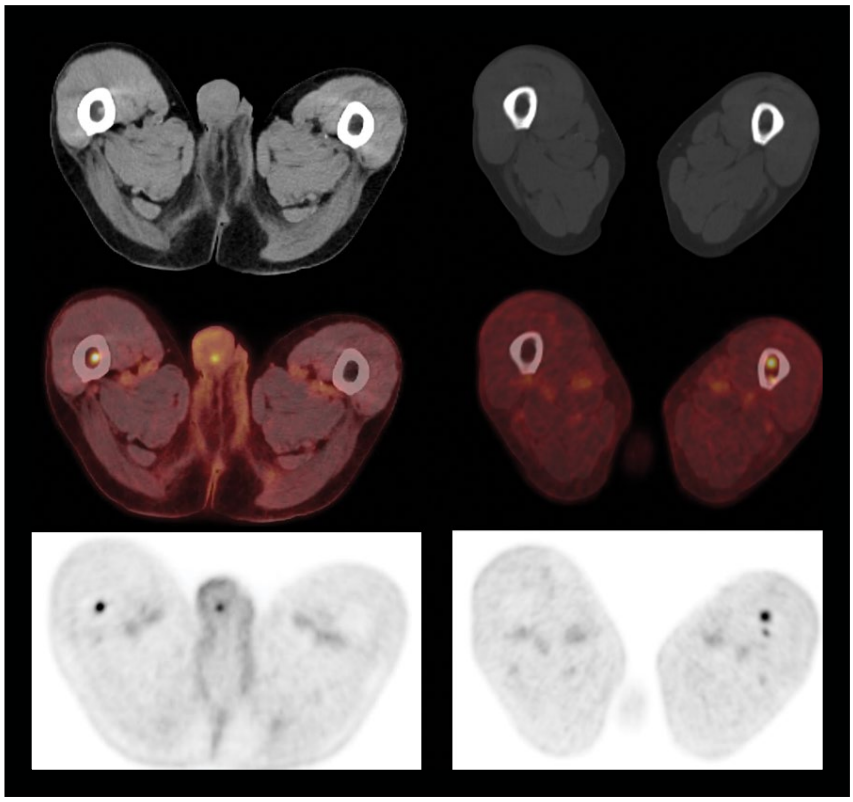

3 **Axial CT, PET/CT, and PET images show the lowermost (near mid-thigh) metastatic lesions within the bone marrow shaft of both femurs. A small metastatic lesion in the cortex of the left femoral shaft and an additional small lesion in the scrotal wall are also visualized.**

There are multiple metastases visualized from the primary neuroendocrine tumor, indicating high somatostatin-receptor density and intense avidity for ^{68}Ga DOTATATE. These findings help inform the recommendation for the patient to proceed with ^{177}Lu DOTATATE radionuclide therapy. By using DOTATATE-labeled ligands, this will help ensure that a similar level of therapeutic tracer intensity within lesions can be achieved for a high and sustained radiation dose to the metastatic lesions without undue normal tissue irradiation.

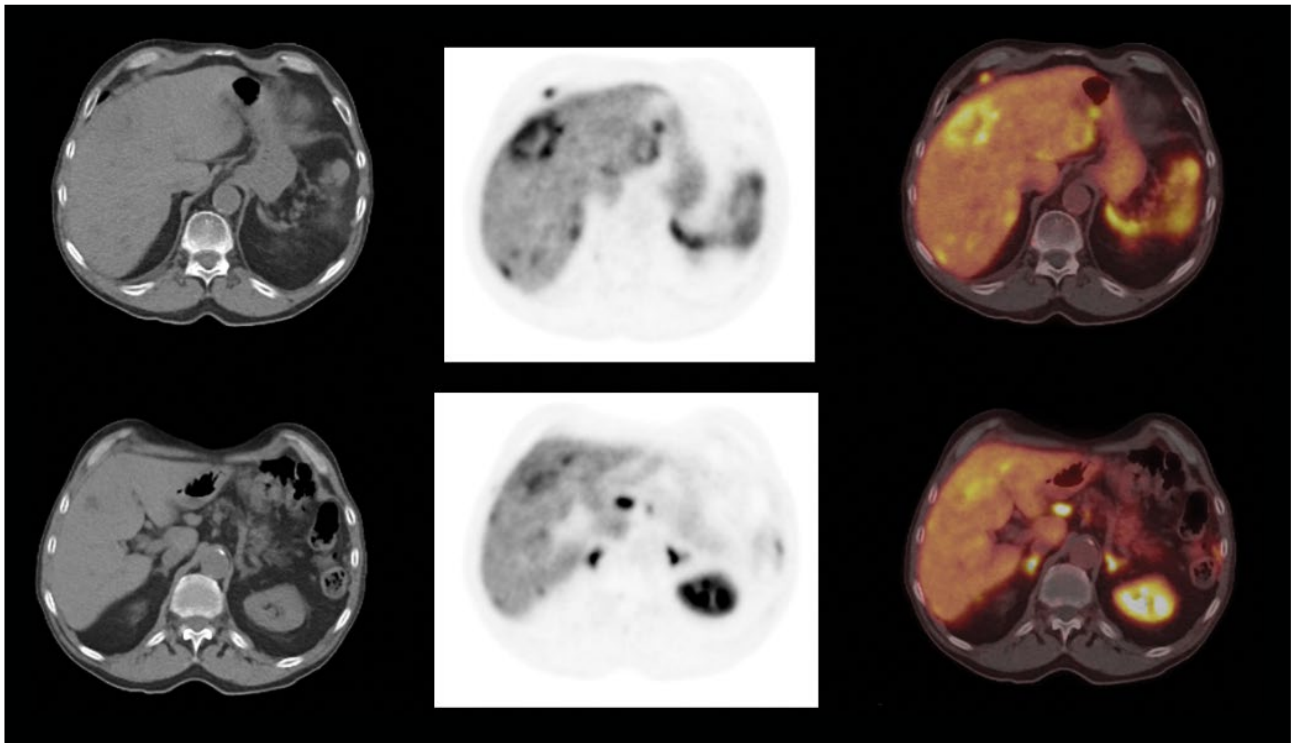

4 **Axial CT, PET, and PET/CT images at two different levels through the liver show large liver metastases in segment 8 with central necrosis. Additional lymph node metastases at the porta-hepatis level as well as intense uptake in the bilateral adrenals are also visualized.**

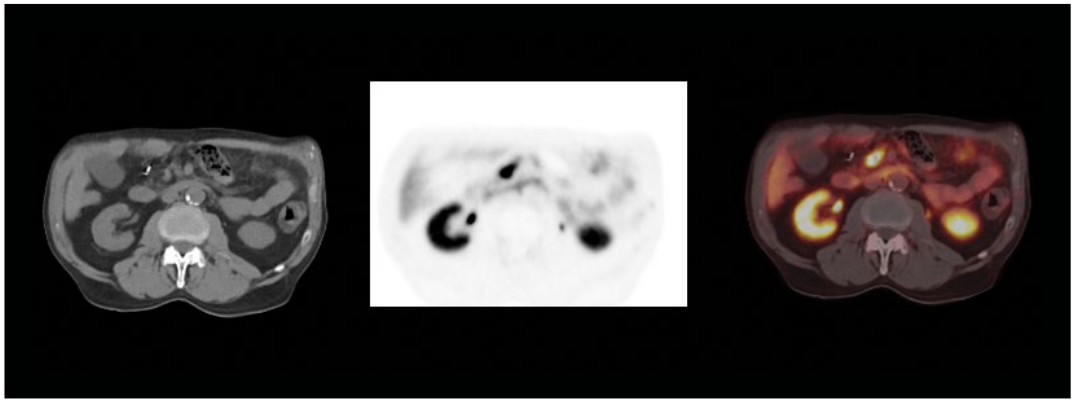

5 **Axial CT, PET, and PET/CT images show intense ^{68}Ga DOTATATE uptake in the intestinal lesions with a high level of renal cortical tracer retention.**

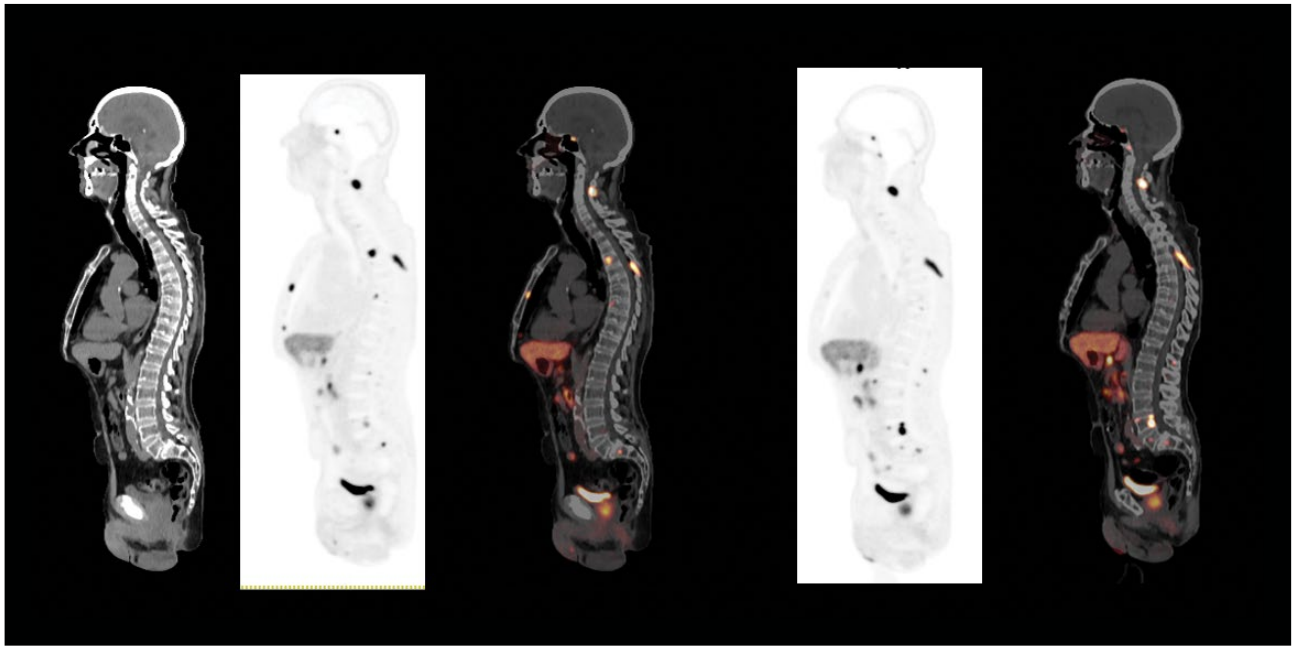

6 **Sagittal CT, PET, and PET/CT images show multiple skeletal metastases with high ^{68}Ga DOTATATE uptake in the L4 lumbar vertebral body and upper sacrum in addition to the spinous process of the thoracic spine and the sternum. The sagittal CT shows focal lytic changes in the lumbar vertebral lesion.**

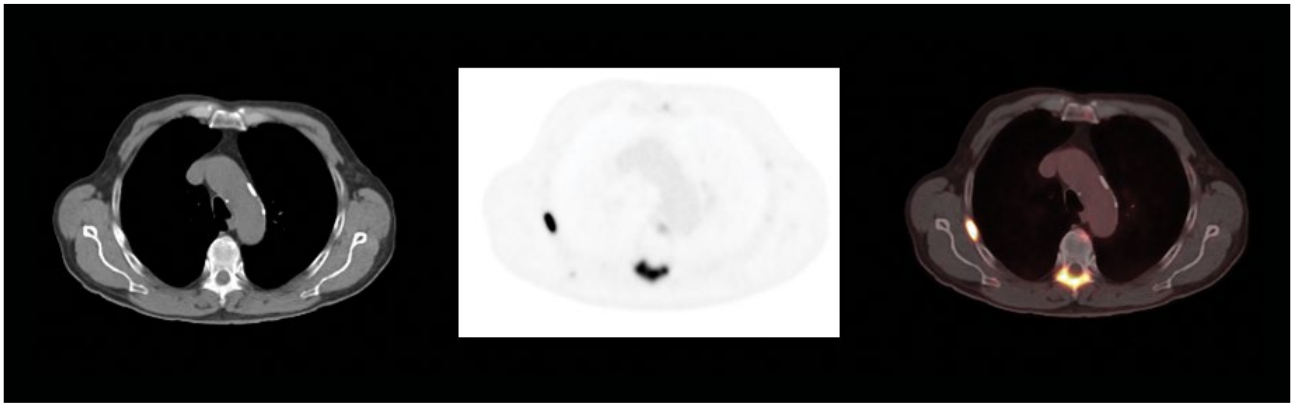

7 **Axial CT, PET, and PET/CT images of the thoracic vertebral level show intense ^{68}Ga DOTATATE uptake in the spinous process and bilateral lamina of the T5 vertebrae, demonstrating the high somatostatin-receptor density of the skeletal metastases. A rib lesion with similar uptake intensity is also visualized.**

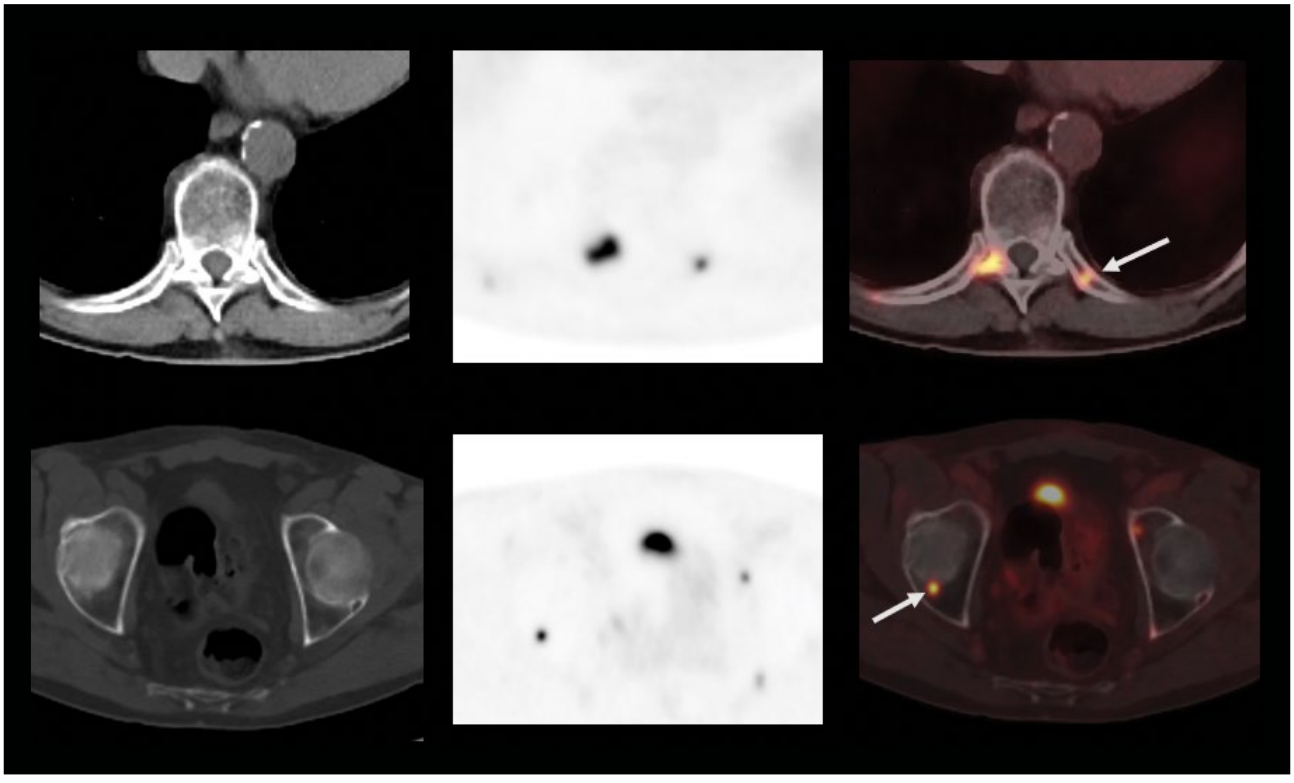

8 **Axial CT, PET, and PET/CT images show small (6 mm in diameter) skeletal metastases in the rib and acetabular margin with high lesion contrast.**

Discussion

Although skeletal lesions are possible in the extremities of a patient with a neuroendocrine tumor, metastatic lesions are primarily expected in the vertex-to-mid-thigh region. In this particular case, the 106 cm axial PET FoV enabled vertex-to-mid-thigh imaging, thus providing the accurate visualization of the smallest lesion in the skull base at one end of the FoV as well as the focal marrow metastases in the shaft of the femur at the other end of the FoV—all within a single bed acquisition. Even the smallest lesions with dimensions of 5-6 mm are visualized with precise delineation.

There are clinical benefits to be acknowledged in having the ability to conduct single-bed, whole-body imaging, which include reduced scan times and effective doses. In general, the use of the 106 cm axial PET FoV in the PET/CT oncology setting should be adequate in meeting most clinical requirements for oncological conditions requiring vertex-to-mid-thigh imaging.

Conclusion

This case demonstrates the role of ^{68}Ga DOTATATE PET/CT imaging in the evaluation of somatostatin-receptor density within neuroendocrine tumor metastases. The 10-minute, single-bed, whole-body images acquired with Biograph Vision Quadra's 106 cm axial PET FoV helped define metastatic burden and inform radionuclide therapy plans that involved the use of DOTATATE-labeled ligands. ●

Examination protocol

Scanner: Biograph Vision Quadra

PET		CT	
Injected dose	4.3 mCi (158 MBq) ^{68}Ga DOTATATE	Tube voltage	120 kV
Post-injection delay	1 hour and 17 minutes	Tube current	80 ref mAs
Acquisition	Single-bed, whole-body; 440 x 440 matrix, PSF+TOF 4i5s, Gaussian filter 2	Slice collimation	32 x 1.2 mm
Scan time	10 minutes		

From innovations to clinical results

Visit Molecular Imaging Clinical Corner to explore the latest in molecular imaging

Read case studies from international healthcare institutions

Discover the value of PET and SPECT technologies through an assortment of clinical white papers

Expand your clinical knowledge through a wide range of archived continuing education (CE) webinars

Access current clinical information anytime, anywhere:
siemens-healthineers.com/miclinicalcorner

Images courtesy of University of Tennessee Medical Center, Knoxville, TN, USA; University of Groningen Medical Center, Groningen, The Netherlands; Keio University Hospital, Keio, Japan.

SIEMENS Healthineers

Imprint

Publisher
Siemens Medical Solutions USA, Inc.
2501 N. Barrington Road
Hoffman Estates, IL 60192-2061
USA
Phone: +1 847-304-7700
siemens-healthineers.com/mi

Editor
Catherine Marcic Joyce
catherine.joyce@siemens-healthineers.com

Journalists
Linda Brookes
Santina Russo
Florian Bayer
Claudette Lew
Sameh Fahmy

Photographers
Jonathan Browning
Scott van Osdol
Raphael Zubler
Gorm Branderup
Steven Bridges
Lars Berg

Illustrations
Joseph Schmidt-Klingenberg
David Hänggi

Text & Photographic Contribution
Primafila AG, Zurich, Switzerland/
Primafila Correspondents
independent Medien-Design, Munich, Germany

Layout
Clint Poy Design, Georgia, USA

Printer
The YGS Group, Pennsylvania, USA

***Imaging Life* is available online:**
siemens-healthineers.com/NMNS

Some of the imaging biomarkers in this publication are not currently recognized by the U.S. Food and Drug Administration (FDA) or other regulatory agencies as being safe and effective, and Siemens does not make any claims regarding their use.

DISCLAIMERS: *Imaging Life*: "The information presented in this magazine is for illustration only and is not intended to be relied upon by the reader for instruction as to the practice of medicine. Healthcare practitioners reading this information are reminded that they must use their own learning, training and expertise in dealing with their individual patients. This material does not substitute for that duty and is not intended by Siemens Healthcare GmbH to be used for any purpose in that regard." Contrast agents: "The drugs and doses mentioned herein are consistent with the approved labeling for uses and/or indications of the drug. The treating physician bears the sole responsibility for the diagnosis and treatment of patients, including drugs and doses prescribed in connection with such use. The operating instructions must always be strictly followed when operating your Siemens system. The source for the technical data is the corresponding data sheets." Trademarks: "All trademarks mentioned in this document are property of their respective owners." Results: "The outcomes achieved by the Siemens customers described herein were achieved in the customer's unique setting. Since there is no "typical" hospital and many variables exist (e.g., hospital size, case mix, level of IT adoption), there can be no guarantee that others will achieve the same results."

SIEMENS Healthineers

HIGHLIGHTS OF PRESCRIBING INFORMATION

These highlights do not include all the information needed to use Fludeoxyglucose F 18 Injection safely and effectively. See full prescribing information for Fludeoxyglucose F 18 Injection.

Fludeoxyglucose F 18 Injection, USP
For intravenous use
Initial U.S. Approval: 2005

INDICATIONS AND USAGE

Fludeoxyglucose F 18 Injection is indicated for positron emission tomography (PET) imaging in the following settings:

- Oncology: For assessment of abnormal glucose metabolism to assist in the evaluation of malignancy in patients with known or suspected abnormalities found by other testing modalities, or in patients with an existing diagnosis of cancer.
- Cardiology: For the identification of left ventricular myocardium with residual glucose metabolism and reversible loss of systolic function in patients with coronary artery disease and left ventricular dysfunction, when used together with myocardial perfusion imaging.
- Neurology: For the identification of regions of abnormal glucose metabolism associated with foci of epileptic seizures (1).

DOSAGE AND ADMINISTRATION

Fludeoxyglucose F 18 Injection emits radiation. Use procedures to minimize radiation exposure. Screen for blood glucose abnormalities.

- In the oncology and neurology settings, instruct patients to fast for 4 to 6 hours prior to the drug's injection. Consider medical therapy and laboratory testing to assure at least two days of normoglycemia prior to the drug's administration (5.2).
- In the cardiology setting, administration of glucose-containing food or liquids (e.g., 50 to 75 grams) prior to the drug's injection facilitates localization of cardiac ischemia (2.3).

Aseptically withdraw Fludeoxyglucose F 18 Injection from its container and administer by intravenous injection (2).

The recommended dose:

- for adults is 5 to 10 mCi (185 to 370 MBq), in all indicated clinical settings (2.1).
- for pediatric patients is 2.6 mCi in the neurology setting (2.2).

Initiate imaging within 40 minutes following drug injection; acquire static emission images 30 to 100 minutes from time of injection (2).

DOSAGE FORMS AND STRENGTHS

Multi-dose 30mL and 50mL glass vial containing 0.74 to 7.40 GBq/mL (20 to 200 mCi/mL) Fludeoxyglucose F 18 Injection and 4.5mg of sodium chloride with 0.1 to 0.5% w/w ethanol as a stabilizer (approximately 15 to 50 mL volume) for intravenous administration (3).

CONTRAINDICATIONS

None.

WARNINGS AND PRECAUTIONS

- Radiation risks: use smallest dose necessary for imaging (5.1).
- Blood glucose adnormalities: may cause suboptimal imaging (5.2).

ADVERSE REACTIONS

Hypersensitivity reactions have occurred; have emergency resuscitation equipment and personnel immediately available (6).

To report SUSPECTED ADVERSE REACTIONS, contact PETNET Solutions, Inc. at 877-473-8638 or FDA at 1-800-FDA-1088 or www.fda.gov/medwatch.

USE IN SPECIFIC POPULATIONS

- Lactation: Temporarily discontinue breastfeeding. A lactating woman should pump and discard breastmilk for 9 hours after Fludeoxyglucose F 18 Injection (8.2).
- Pediatric Use: Safety and effectiveness in pediatric patients have not been established in the oncology and cardiology settings (8.4).

See 17 for PATIENT COUNSELING INFORMATION

Revised: 10/2019

FULL PRESCRIBING INFORMATION: CONTENTS*

* Sections or subsections omitted from the full prescribing information are not listed.

FULL PRESCRIBING INFORMATION

1 INDICATIONS AND USAGE

Fludeoxyglucose F 18 Injection is indicated for positron emission tomography (PET) imaging in the following settings:

1.1 Oncology

For assessment of abnormal glucose metabolism to assist in the evaluation of malignancy in patients with known or suspected abnormalities found by other testing modalities, or in patients with an existing diagnosis of cancer.

1.2 Cardiology

For the identification of left ventricular myocardium with residual glucose metabolism and reversible loss of systolic function in patients with coronary artery disease and left ventricular dysfunction, when used together with myocardial perfusion imaging.

1.3 Neurology

For the identification of regions of abnormal glucose metabolism associated with foci of epileptic seizures.

2 DOSAGE AND ADMINISTRATION

Fludeoxyglucose F 18 Injection emits radiation. Use procedures to minimize radiation exposure. Calculate the final dose from the end of synthesis (EOS) time using proper radioactive decay factors. Assay the final dose in a properly calibrated dose calibrator before administration to the patient *[see Description (11.2)]*.

2.1 Recommended Dose for Adults

Within the oncology, cardiology and neurology settings, the recommended dose for adults is 5 to 10 mCi (185 to 370 MBq) as an intravenous injection.

2.2 Recommended Dose for Pediatric Patients

Within the neurology setting, the recommended dose for pediatric patients is 2.6 mCi, as an intravenous injection. The optimal dose adjustment on the basis of body size or weight has not been determined *[see Use in Special Populations (8.4)]*.

2.3 Patient Preparation

- To minimize the radiation absorbed dose to the bladder, encourage adequate hydration. Encourage the patient to drink water or other fluids (as tolerated) in the 4 hours before their PET study.
- Encourage the patient to void as soon as the imaging study is completed and as often as possible thereafter for at least one hour.
- Screen patients for clinically significant blood glucose abnormalities by obtaining a history and/or laboratory tests *[see Warnings and Precautions (5.2)]*. Prior to Fludeoxyglucose F 18 PET imaging in the oncology and neurology settings, instruct patient to fast for 4 to 6 hours prior to the drug's injection.
- In the cardiology setting, administration of glucose-containing food or liquids (e.g., 50 to 75 grams) prior to Fludeoxyglucose F 18 Injection facilitates localization of cardiac ischemia.

2.4 Radiation Dosimetry

The estimated human absorbed radiation doses (rem/mCi) to a newborn (3.4 kg), 1-year old (9.8 kg), 5-year old (19 kg), 10-year old (32 kg), 15-year old (57 kg), and adult (70 kg) from intravenous administration of Fludeoxyglucose F 18 Injection are shown in Table 1. These estimates were calculated based on human[2] data and using the data published by the International Commission on Radiological Protection[4] for Fludeoxyglucose ^{18}F. The dosimetry data show that there are slight variations in absorbed radiation dose for various organs in each of the age groups. These dissimilarities in absorbed radiation dose are due to developmental age variations (e.g., organ size, location, and overall metabolic rate for each age group). The identified critical organs (in descending order) across all age groups evaluated are the urinary bladder, heart, pancreas, spleen, and lungs.

Table 1. Estimated Absorbed Radiation Doses (rem/mCi) After Intravenous Administration of Fludeoxyglucose F 18 Injection[a]

Organ	Newborn (3.4 kg)	1-year old (9.8 kg)	5-year old (19 kg)	10-year old (32 kg)	15-year old (57 kg)	Adult (70 kg)
Bladder wall[b]	4.3	1.7	0.93	0.60	0.40	0.32
Heart wall	2.4	1.2	0.70	0.44	0.29	0.22
Pancreas	2.2	0.68	0.33	0.25	0.13	0.096
Spleen	2.2	0.84	0.46	0.29	0.19	0.14
Lungs	0.96	0.38	0.20	0.13	0.092	0.064
Kidneys	0.81	0.34	0.19	0.13	0.089	0.074
Ovaries	0.80	0.8	0.19	0.11	0.058	0.053
Uterus	0.79	0.35	0.19	0.12	0.076	0.062
LLI wall *	0.69	0.28	0.15	0.097	0.060	0.051
Liver	0.69	0.31	0.17	0.11	0.076	0.058
Gallbladder wall	0.69	0.26	0.14	0.093	0.059	0.049
Small intestine	0.68	0.29	0.15	0.096	0.060	0.047
ULI wall **	0.67	0.27	0.15	0.090	0.057	0.046
Stomach wall	0.65	0.27	0.14	0.089	0.057	0.047
Adrenals	0.65	0.28	0.15	0.095	0.061	0.048
Testes	0.64	0.27	0.14	0.085	0.052	0.041
Red marrow	0.62	0.26	0.14	0.089	0.057	0.047
Thymus	0.61	0.26	0.14	0.086	0.056	0.044
Thyroid	0.61	0.26	0.13	0.080	0.049	0.039
Muscle	0.58	0.25	0.13	0.078	0.049	0.039
Bone surface	0.57	0.24	0.12	0.079	0.052	0.041
Breast	0.54	0.22	0.11	0.068	0.043	0.034
Skin	0.49	0.20	0.10	0.060	0.037	0.030
Brain	0.29	0.13	0.09	0.078	0.072	0.070
Other tissues	0.59	0.25	0.13	0.083	0.052	0.042

[a] MIRDOSE 2 software was used to calculate the radiation absorbed dose.
[b] The dynamic bladder model with a uniform voiding frequency of 1.5 hours was used.
* LLI = lower large intestine; ** ULI = upper large intestine

2.5 Radiation Safety – Drug Handling

- Use waterproof gloves, effective radiation shielding, and appropriate safety measures when handling Fludeoxyglucose F 18 Injection to avoid unnecessary radiation exposure to the patient, occupational workers, clinical personnel and other persons.
- Radiopharmaceuticals should be used by or under the control of physicians who are qualified by specific training and experience in the safe use and handling of radionuclides, and whose experience and training have been approved by the appropriate governmental agency authorized to license the use of radionuclides.
- Calculate the final dose from the end of synthesis (EOS) time using proper radioactive decay factors. Assay the final dose in a properly calibrated dose calibrator before administration to the patient *[see Description (11.2)]*.
- The dose of Fludeoxyglucose F 18 used in a given patient should be minimized consistent with the objectives of the procedure, and the nature of the radiation detection devices employed.

2.6 Drug Preparation and Administration

- Calculate the necessary volume to administer based on calibration time and dose.
- Aseptically withdraw Fludeoxyglucose F 18 Injection from its container.
- Inspect Fludeoxyglucose F 18 Injection visually for particulate matter and discoloration before administration, whenever solution and container permit.
- Do not administer the drug if it contains particulate matter or discoloration; dispose of these unacceptable or unused preparations in a safe manner, in compliance with applicable regulations.
- Use Fludeoxyglucose F 18 Injection within 12 hours from the EOS.

2.7 Imaging Guidelines

- Initiate imaging within 40 minutes following Fludeoxyglucose F 18 Injection administration.
- Acquire static emission images 30 to 100 minutes from the time of injection.

3 DOSAGE FORMS AND STRENGTHS

Multiple-dose 30 mL and 50 mL glass vial containing 0.74 to 7.40 GBq/mL (20 to 200 mCi/mL) of Fludeoxyglucose F 18 Injection and 4.5 mg of sodium chloride with 0.1 to 0.5% w/w ethanol as a stabilizer (approximately 15 to 50 mL volume) for intravenous administration.

4 CONTRAINDICATIONS

None.

5 WARNINGS AND PRECAUTIONS

5.1 Radiation Risks

Radiation-emitting products, including Fludeoxyglucose F 18 Injection, may increase the risk for cancer, especially in pediatric patients. Use the smallest dose necessary for imaging and ensure safe handling to protect the patient and health care worker *[see Dosage and Administration (2.5)]*.

5.2 Blood Glucose Abnormalities

In the oncology and neurology setting, suboptimal imaging may occur in patients with inadequately regulated blood glucose levels. In these patients, consider medical therapy and laboratory testing to assure at least two days of normoglycemia prior to Fludeoxyglucose F 18 Injection administration.

6 ADVERSE REACTIONS

Hypersensitivity reactions with pruritus, edema and rash have been reported in the post-marketing setting. Have emergency resuscitation equipment and personnel immediately available.

7 DRUG INTERACTIONS

The interactions of Fludeoxyglucose F 18 Injection with other drugs taken by patients undergoing PET imaging has not been studied.

8 USE IN SPECIFIC POPULATIONS

8.1 Pregnancy

Risk Summary

Data from published case series and case reports describe Fludeoxyglucose F 18 Injection crossing the placenta with uptake by the fetus (see Data). All radiopharmaceuticals have the potential to cause fetal harm depending on the fetal stage of development and the magnitude of the radiation dose. However, published studies that describe Fludeoxyglucose F 18 Injection use in pregnant women have not identified a risk of drug-associated major birth defects, miscarriage, or adverse maternal or fetal outcomes. If considering Fludeoxyglucose F 18 Injection administration to a pregnant woman, inform the patient about the potential for adverse pregnancy outcomes based on the radiation dose from Fludeoxyglucose F 18 Injection and the gestational timing of exposure. The estimated background risk of major birth defects and miscarriage for the indicated population is unknown. All pregnancies have a background risk of birth defect, loss, or other adverse outcomes. In the U.S. general population, the estimated background risk of major birth defects and miscarriage in clinically recognized pregnancies are 2-4% and 15-20%, respectively.

Data

Human Data

Data from published case series and case reports describe Fludeoxyglucose F 18 Injection crossing the placental barrier and visualization of radioactivity throughout the body of the fetus. The estimated fetal absorbed radiation dose from the maximum labeled dose (370 MBq) of Fludeoxyglucose F 18 was 10 mGy with first trimester exposure to PET alone and 20 mGy with first trimester exposure to PET/CT scan combination. Long-term adverse radiation effects to a child exposed to Fludeoyxglucose F 18 Injection in utero are unknown. No adverse fetal effects or radiation-related risks have been identified for diagnostic procedures involving less than 50 mGy, which represents less than 20 mGy fetal doses.

8.2 Lactation

Risk Summary

A published case report and case series show the presence of Fludeoxyglucose F 18 Injection in human milk following administration. There are no data on the effects of Fludeoxyglucose F 18 Injection on the breastfed infant or the effects on milk production. Exposure of Fludeoxyglucose F 18 Injection to a breastfed infant can be minimized by temporary discontinuation of breastfeeding (see Clinical Considerations). The developmental and health benefits of breastfeeding should be considered along with the mother's clinical need for Fludeoxyglucose F 18 Injection, any potential adverse effects on the breastfed child from Fludeoxyglucose F 18 Injection or from the underlying maternal condition.

Clinical Considerations

To decrease radiation exposure to the breastfed infant, advise a lactating woman to pump and discard breastmilk and avoid close (breast) contact with the infant for at least 9 hours after the administration of Fludeoxyglucose F 18 Injection.

8.4 Pediatric Use

The safety and effectiveness of Fludeoxyglucose F 18 Injection in pediatric patients with epilepsy is established on the basis of studies in adult and pediatric patients. In pediatric patients with epilepsy, the recommended dose is 2.6 mCi. The optimal dose adjustment on the basis of body size or weight has not been determined. In the oncology or cardiology settings, the safety and effectiveness of Fludeoxyglucose F 18 Injection have not been established in pediatric patients.

11 DESCRIPTION

11.1 Chemical Characteristics

Fludeoxyglucose F 18 Injection is a positron emitting radiopharmaceutical that is used for diagnostic purposes in conjunction with positron emission tomography (PET) imaging. The active ingredient 2-deoxy-2-[^{18}F]fluoro-D-glucose has the molecular formula of $C_6H_{11}{}^{18}FO_5$ with a molecular weight of 181.26, and has the following chemical structure:

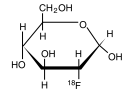

Fludeoxyglucose F 18 Injection is provided as a ready to use sterile, pyrogen free, clear, colorless solution. Each mL contains between 0.740 to 7.40GBq (20.0 to 200 mCi) of 2-deoxy-2-[^{18}F]fluoro-D-glucose at the EOS, 4.5 mg of sodium chloride and 0.1 to 0.5% w/w ethanol as a stabilizer. The pH of the solution is between 4.5 and 7.5. The solution is packaged in a multiple-dose glass vial and does not contain any preservative.

11.2 Physical Characteristics

Fluorine F 18 has a physical half-life of 109.7 minutes and decays to Oxygen O 16 (stable) by positron decay. The principal photons useful for imaging are the dual 511 keV "annihilation" gamma photons, that are produced and emitted simultaneously in opposite direction when the positron interacts with an electron (Table 2).

Table 2. Principal Radiation Emission Data for Fluorine F 18

Radiation/Emission	% Per Disintegration	Mean Energy
Positron (β+)	96.73	249.8 keV
Gamma (±)*	193.46	511.0 keV

*Produced by positron annihilation

From: Kocher, D.C. Radioactive Decay Tables DOE/TIC-I 1026, 89 (1981)

The specific gamma ray constant (point source air kerma coefficient) for fluorine F 18 is 5.7 R/hr/mCi (1.35 x 10^{-6} Gy/hr/kBq) at 1 cm. The half-value layer (HVL) for the 511 keV photons is 4 mm lead (Pb). The range of attenuation coefficients for this radionuclide as a function of lead shield thickness is shown in Table 3. For example, the interposition of an 8 mm thickness of Pb, with a coefficient of attenuation of 0.25, will decrease the external radiation by 75%.

Table 3. Radiation Attenuation of 511 keV Photons by lead (Pb) shielding

Shield thickness (Pb) mm	Coefficient of attenuation
0	0.00
4	0.50
8	0.25
13	0.10
26	0.01
39	0.001
52	0.0001

For use in correcting for physical decay of this radionuclide, the fractions remaining at selected intervals after calibration are shown in Table 4.

Table 4. Physical Decay Chart for Fluorine F 18

Minutes	Fraction Remaining
0*	1.000
15	0.909
30	0.826
60	0.683
110	0.500
220	0.250

*calibration time

12 CLINICAL PHARMACOLOGY

12.1 Mechanism of Action

Fludeoxyglucose F 18 is a glucose analog that concentrates in cells that rely upon glucose as an energy source, or in cells whose dependence on glucose increases under pathophysiological conditions. Fludeoxyglucose F 18 is transported through the cell membrane by facilitative glucose transporter proteins and is phosphorylated within the cell to [^{18}F] FDG-6-phosphate by the enzyme hexokinase. Once phosphorylated it cannot exit until it is dephosphorylated by glucose-6-phosphatase. Therefore, within a given tissue or pathophysiological process, the retention and clearance of Fludeoxyglucose F 18 reflect a balance involving glucose transporter, hexokinase and glucose-6-phosphatase activities. F 18 is used to assess glucose metabolism.

In comparison to background activity of the specific organ or tissue type, regions of decreased or absent uptake of Fludeoxyglucose F 18 reflect the decrease or absence of glucose metabolism. Regions of increased uptake of Fludeoxyglucose F 18 reflect greater than normal rates of glucose metabolism.

12.2 Pharmacodynamics

Fludeoxyglucose F 18 Injection is rapidly distributed to all organs of the body after intravenous administration. After background clearance of Fludeoxyglucose F 18 Injection, optimal PET imaging is generally achieved between 30 to 40 minutes after administration.

In cancer, the cells are generally characterized by enhanced glucose metabolism partially due to (1) an increase in activity of glucose transporters, (2) an increased rate of phosphorylation activity, (3) a reduction of phosphatase activity or, (4) a dynamic alteration in the balance among all these processes. However, glucose metabolism of cancer as reflected by Fludeoxyglucose F 18 accumulation shows considerable variability. Depending on tumor type, stage, and location, Fludeoxyglucose F 18 accumulation may be increased, normal, or decreased. Also, inflammatory cells can have the same variability of uptake of Fludeoxyglucose F 18.

In the heart, under normal aerobic conditions, the myocardium meets the bulk of its energy requirements by oxidizing free fatty acids. Most of the exogenous glucose taken up by the myocyte is converted into glycogen. However, under ischemic conditions, the oxidation of free fatty acids decreases, exogenous glucose becomes the preferred myocardial substrate, glycolysis is stimulated, and glucose taken up by the myocyte is metabolized immediately instead of being converted into glycogen. Under these conditions, phosphorylated Fludeoxyglucose F 18 accumulates in the myocyte and can be detected with PET imaging.

In the brain, cells normally rely on aerobic metabolism. In epilepsy, the glucose metabolism varies. Generally, during a seizure, glucose metabolism increases. Interictally, the seizure focus tends to be hypometabolic.

12.3 Pharmacokinetics

Distribution: In four healthy male volunteers, receiving an intravenous administration of 30 seconds induration, the arterial blood level profile for Fludeoxyglucose F 18 decayed triexponentially. The effective half-life ranges of the three phases were 0.2 to 0.3 minutes, 10 to 13 minutes with a mean and standard deviation (STD) of 11.6 (±) 1.1 min, and 80 to 95 minutes with a mean and STD of 88 (±) 4 min.

Plasma protein binding of Fludeoxyglucose F 18 has not been studied.

Metabolism: Fludeoxyglucose F 18 is transported into cells and phosphorylated to [^{18}F]-FDG-6-phosphate at a rate proportional to the rate of glucose utilization within that tissue. [^{18}F]-FDG-6-phosphate presumably is metabolized to 2-deoxy-2-[^{18}F]fluoro-6-phospho-D-mannose([^{18}F]FDM-6-phosphate).

Fludeoxyglucose F 18 Injection may contain several impurities (e.g., 2-deoxy-2-chloro-D-glucose (ClDG)). Biodistribution and metabolism of ClDG are presumed to be similar to Fludeoxyglucose F 18 and would be expected to result in intracellular formation of 2-deoxy-2-chloro-6-phospho-D-glucose (ClDG-6-phosphate) and 2-deoxy-2-chloro-6-phospho-D-mannose (ClDM-6-phosphate). The phosphorylated deoxyglucose compounds are dephosphorylated and the resulting compounds (FDG, FDM, ClDG, and ClDM) presumably leave cells by passive diffusion. Fludeoxyglucose F 18 and related compounds are cleared from non-cardiac tissues within 3 to 24 hours after administration. Clearance from the cardiac tissue may require more than 96 hours. Fludeoxyglucose F 18 that is not involved in glucose metabolism in any tissue is then excreted in the urine.

Elimination: Fludeoxyglucose F 18 is cleared from most tissues within 24 hours and can be eliminated from the body unchanged in the urine. Within 33 minutes, a mean of 3.9% of the administrated radioactive dose was measured in the urine. The amount of radiation exposure of the urinary bladder at two hours post-administration suggests that 20.6% (mean) of the radioactive dose was present in the bladder.

Special Populations:

The pharmacokinetics of Fludeoxyglucose F 18 Injection have not been studied in renally-impaired, hepatically impaired or pediatric patients. Fludeoxyglucose F 18 is eliminated through the renal system. Avoid excessive radiation exposure to this organ system and adjacent tissues.

The effects of fasting, varying blood sugar levels, conditions of glucose intolerance, and diabetes mellitus on Fludeoxyglucose F 18 distribution in humans have not been ascertained [*see Warnings and Precautions (5.2)*].

13 NONCLINICAL TOXICOLOGY

13.1 Carcinogenesis, Mutagenesis, Impairment of Fertility

Animal studies have not been performed to evaluate the Fludeoxyglucose F 18 Injection carcinogenic potential, mutagenic potential or effects on fertility.

14 CLINICAL STUDIES

14.1 Oncology

The efficacy of Fludeoxyglucose F 18 Injection in positron emission tomography cancer imaging was demonstrated in 16 independent studies. These studies prospectively evaluated the use of Fludeoxyglucose F 18 in patients with suspected or known malignancies, including non-small cell lung cancer, colo-rectal, pancreatic, breast, thyroid, melanoma, Hodgkin's and non-Hodgkin's lymphoma, and various types of metastatic cancers to lung, liver, bone, and axillary nodes. All these studies had at least 50 patients and used pathology as a standard of truth. The Fludeoxyglucose F 18 Injection doses in the studies ranged from 200 MBq to 740 MBq with a median and mean dose of 370 MBq.

In the studies, the diagnostic performance of Fludeoxyglucose F 18 Injection varied with the type of cancer, size of cancer, and other clinical conditions. False negative and false positive scans were observed. Negative Fludeoxyglucose F 18 Injection PET scans do not exclude the diagnosis of cancer. Positive Fludeoxyglucose F 18 Injection PET scans can not replace pathology to establish a diagnosis of cancer. Non-malignant conditions such as fungal infections, inflammatory processes and benign tumors have patterns of increased glucose metabolism that may give rise to false-positive scans. The efficacy of Fludeoxyglucose F 18 Injection PET imaging in cancer screening was not studied.

14.2 Cardiology

The efficacy of Fludeoxyglucose F 18 Injection for cardiac use was demonstrated in ten independent, prospective studies of patients with coronary artery disease and chronic left ventricular systolic dysfunction who were scheduled to undergo coronary revascularization. Before revascularization, patients underwent PET imaging with Fludeoxyglucose F 18 Injection (74 to 370 MBq, 2 to 10 mCi) and perfusion imaging with other diagnostic radiopharmaceuticals. Doses of Fludeoxyglucose F 18 Injection ranged from 74 to 370 MBq (2 to 10 mCi). Segmental, left ventricular, wall-motion assessments of asynergic areas made before revascularization were compared in a blinded manner to assessments made after successful revascularization to identify myocardial segments with functional recovery.

Left ventricular myocardial segments were predicted to have reversible loss of systolic function if they showed Fludeoxyglucose F 18 accumulation and reduced perfusion (i.e., flow-metabolism mismatch). Conversely, myocardial segments were predicted to have irreversible loss of systolic function if they showed reductions in both Fludeoxyglucose F 18 accumulation and perfusion (i.e., matched defects).

Findings of flow-metabolism mismatch in a myocardial segment may suggest that successful revascularization will restore myocardial function in that segment. However, false-positive tests occur regularly, and the decision to have a patient undergo revascularization should not be based on PET findings alone. Similarly, findings of a matched defect in a myocardial segment may suggest that myocardial function will not recover in that segment, even if it is successfully revascularized. However, false-negative tests occur regularly, and the decision to recommend against coronary revascularization, or to recommend a cardiac transplant, should not be based on PET findings alone. The reversibility of segmental dysfunction as predicted with Fludeoxyglucose F 18 PET imaging depends on successful coronary revascularization. Therefore, in patients with a low likelihood of successful revascularization, the diagnostic usefulness of PET imaging with Fludeoxyglucose F 18 Injection is more limited.

14.3 Neurology

In a prospective, open label trial, Fludeoxyglucose F 18 Injection was evaluated in 86 patients with epilepsy. Each patient received a dose of Fludeoxyglucose F 18 Injection in the range of 185 to 370 MBq (5 to 10 mCi). The mean age was 16.4 years (range: 4 months to 58 years; of these, 42 patients were less than 12 years and 16 patients were less than 2 years old). Patients had a known diagnosis of complex partial epilepsy and were under evaluation for surgical treatment of their seizure disorder. Seizure foci had been previously identified on ictal EEGs and sphenoidal EEGs. Fludeoxyglucose F 18 Injection PET imaging confirmed previous diagnostic findings in 16% (14/87) of the patients; in 34% (30/87) of the patients, Fludeoxyglucose F 18 Injection PET images provided new findings. In 32% (27/87), imaging with Fludeoxyglucose F 18 Injection was inconclusive. The impact of these imaging findings on clinical outcomes is not known.

Several other studies comparing imaging with Fludeoxyglucose F 18 Injection results to subsphenoidal EEG, MRI and/or surgical findings supported the concept that the degree of hypometabolism corresponds to areas of confirmed epileptogenic foci. The safety and effectiveness of Fludeoxyglucose F 18 Injection to distinguish idiopathic epileptogenic foci from tumors or other brain lesions that may cause seizures have not been established.

16 HOW SUPPLIED/STORAGE AND DRUG HANDLING

Fludeoxyglucose F 18 Injection is supplied in a multi-dose, capped 30 mL and 50 mL glass vial containing between 0.740 to 7.40 GBq/mL (20 to 200 mCi/mL), of no carrier added 2-deoxy-2-[^{18}F-fluoro-D-glucose, at end of synthesis, in approximately 15 to 50 mL. The contents of each vial are sterile, pyrogen-free and preservative-free.

NDC 40028-511-30; 40028-511-50

Receipt, transfer, handling, possession, or use of this product is subject to the radioactive material regulations and licensing requirements of the U.S. Nuclear Regulatory Commission, Agreement States or Licensing States as appropriate.

Store the Fludeoxyglucose F 18 Injection vial upright in a lead shielded container at 25°C (77°F); excursions permitted to 15-30°C (59-86°F).

Store and dispose of Fludeoxyglucose F 18 Injection in accordance with the regulations and a general license, or its equivalent, of an Agreement State or a Licensing State.

The expiration date and time are provided on the container label. Use Fludeoxyglucose F 18 Injection within 12 hours from the EOS time.

17 PATIENT COUNSELING INFORMATION

Instruct patients in procedures that increase renal clearance of radioactivity. Encourage patients to:

- drink water or other fluids (as tolerated) in the 4 hours before their PET study.
- void as soon as the imaging study is completed and as often as possible thereafter for at least one hour.

Pregnancy: Advise pregnant women of the risk of fetal exposure to radiation with Fludeoxyglucose F 18 Injection [see Use in Specific Populations (8.1)].

Lactation: Advise lactating women that exposure to Fludeoxyglucose F 18 Injection through breast milk can be minimized by pumping and discarding breast milk and avoiding close (breast) contact with the infant for 9 hours after Fludeoxyglucose F 18 Injection [see Use in Specific Populations (8.2)].

Manufactured and distributed by:
PETNET Solutions, Inc.
810 Innovation Drive
Knoxville, TN 37932

PETNET Solutions

Legal information: On account of certain regional limitations of sales rights and service availability, we cannot guarantee that all products included in this publication are available through the Siemens sales organization worldwide. Availability and packaging may vary by country and is subject to change without prior notice. Some/all of the features and products described herein may not be available in the United States.

The information in this document contains general technical descriptions of specifications and options as well as standard and optional features, which do not always have to be present in individual cases.

Siemens reserves the right to modify the design, packaging, specifications, and options described herein without prior notice.

Please contact your local Siemens sales representative for the most current information.

Note: Any technical data contained in this document may vary within defined tolerances. Original images always lose a certain amount of detail when reproduced.

Siemens Healthineers Headquarters
Siemens Healthcare GmbH
Henkestr. 127
91052 Erlangen
Germany
Phone: +49 9131 84-0
siemens-healthineers.com

Published by
Siemens Medical Solutions USA, Inc.
2501 N. Barrington Road
Hoffman Estates, IL 60192-2061
USA
Phone: +1 847-304-7700
siemens-healthineers.com/mi

Order No. A91MI-10542-M1-7600 | Printed in USA | MI-5709.CJ.CP.SNMMI.10K

siemens-healthineers.com/NMNS